

1

Upscaling aquifer storage 2 and recovery (ASR)

3 A northern Ghana multiple case study
4 on small scale agriculture

5 by

6 Frank J. van den Toorn

7 to obtain the degree of Master of Science
8 at the Delft University of Technology,
9 to be defended publicly on .. August .., 2018 at AM.

10 Student number: 4179404
Project duration: September 18, 2017 – August 1, 2018
Thesis committee: Prof. dr. ir. M. Bakker, TU Delft (Chair)
Prof. dr. ir. N.C. van de Giesen, TU Delft
Dr. ir. J.S. Timmermans, TU Delft
Ir. D.A. Brakenhoff, Witteveen+Bos

11 An electronic version of this thesis is available at <http://repository.tudelft.nl/>.



Preface

14 This thesis accommodates the final product in becoming a Master of Science in Watermanagement at the
 15 Delft University of Technology - faculty of Civil Engineering and Geosciences. I would like to acknowledge
 16 all the people who contributed to my graduation. Some however do deserve a special emphasis. First of
 17 all, I would like to thank the entire committee for assessing my thesis. Subsequently I would like to give
 18 a word of gratitude to Witteveen+Bos - Herman Mondeel & Davíd Brakenhoff - for the abundant research
 19 facilities and daily supervision. And last but not least I owe Conservation Alliance - Paa Kofi Osei-Owusu -
 20 a special gratitude. Without the cooperation of CA the fieldwork data collection within the northern Ghana
 21 local communities would not have been possible.

22
23

*Frank J. van den Toorn
Delft, July 2018*



Summary

25 Summary will follow soon

26

27 For now the focus is on the thesis core itself.

28 Chapters do contain sub-conclusions / summaries

Contents

29

30	List of Figures	ix
31	List of Tables	xiii
32	1 Introduction	1
33	1.1 Background	1
34	1.2 Research gap	1
35	1.3 Research purpose	1
36	1.4 Reader's guide	2
37	2 Fieldwork data analysis	5
38	2.1 Parameter derivation methods	6
39	2.1.1 Theoretical model definition	6
40	2.1.2 Techniques in analysis	6
41	2.1.3 Optimization functions	7
42	2.2 From fieldwork data to T & S values	8
43	2.2.1 Location: Bingo	8
44	2.2.2 Location: Nungo	10
45	2.2.3 Location: Nyong Nayili	10
46	2.2.4 Location: Janga (1/2)	11
47	2.2.5 Location: Janga (2/2)	12
48	2.2.6 Location: Ziong (monitoring)	13
49	2.3 Results & conclusions	14
50	3 ASR-system upscaling - Test problem	17
51	3.1 Base model definition	17
52	3.1.1 Soil scenarios	17
53	3.1.2 Well dimensions & pump placement	17
54	3.1.3 Time frame	18
55	3.2 MODFLOW model design	18
56	3.2.1 MODFLOW-NWT	19
57	3.2.2 MODFLOW - GHB	19
58	3.2.3 MODFLOW - MNW2	19
59	3.3 Base model performance	21
60	3.4 Impact of ASR-system upscaling	24
61	3.4.1 Upscaling daily pumping time	24
62	3.4.2 Upscaling borehole cross-sectional dimension	25
63	3.4.3 Upscaling by system cleaning	27
64	3.5 Results & Conclusions	28
65	4 (Financial) yield - upscaling	31
66	4.1 Theory: ASR-system - (financial) yield	31
67	4.1.1 Crops: financial yield	31
68	4.1.2 Water withdrawal: costs	33
69	4.2 Data processing (from water volumes to yield)	34
70	4.2.1 Crop cover area	34
71	4.2.2 Financial yield	34
72	4.3 Results & conclusions	35

73	5 Conclusions	37
74	6 Discussion & Recommendations	39
75	Bibliography	41
76	Appendices	43
77	A Original Borehole Logsheets	45
78	B Fieldwork set-up	51
79	B.1 Equipment	51
80	B.2 General measurement structure	53
81	B.3 Site-specific measurement results	56
82	C Extense report - Fieldwork data analysis	63
83	C.1 Bingo - overview	64
84	C.2 Nungo - overview	66
85	C.3 Nyong Nayili - overview	67
86	C.4 Janga (1/2) - overview	69
87	C.5 Janga (2/2) - overview	71
88	C.6 Ziong - overview	73
89	D MODFLOW radial conversion	75
90	D.1 Test 1: Steady flow to a fully penetrating well in confined aquifer	78
91	D.2 Test 2: Steady flow to a fully penetrating well in unconfined aquifer	80
92	D.3 Test 3: Unsteady flow to a partially penetrating well in unconfined aquifer	82
93	E Extense report - MODFLOW model definition	85
94	E.1 Leakage factor λ	85
95	F Pedrollo - 4" submersible pump - Product specifications	87

List of Figures

96

97	1.1 Example on (a) flood near Weisi, Upper West Region and (b) drought near Nungo, Upper East Region	1
98	1.2 Principle Aquifer Storage & Recovery (ASR) system	2
99	1.3 Schematic: dry season system use	3
100	1.4 Schematic: desired up-scaling in dry season system use	3
102	2.1 Overview of fieldwork locations in northern Ghana	5
103	2.2 Schematic cross-sectional view of (a) generalized northern Ghana soil stratification and sim- plified representations: (b) a single layer system, (c) a double layer system, and (d) a system with two layers and partial penetration of the well	6
104	2.3 Bingo - Simplified models best fit	9
105	2.4 Nyong Nayili - Simplified models best fit	11
106	2.5 Janga first attempt - Simplified models best fit	12
107	2.6 Janga second attempt - Simplified models best fit	13
108	2.7 Ziong - Simplified models best fit	14
109	2.8 T & S bandwidth selection	16
112	3.1 Schematic base model definition	18
113	3.2 Example scenario 3 - base model - Cross-sectional contour head after (a) five days and (b) 122 days of infiltration	21
114	3.3 Example scenario 3 - base model - Head in representative layers after (a) five days and (b) 122 days of infiltration	22
115	3.4 Example scenario 3 - base model - Discharge performance for (a) the first five days and (b) the last five days of dry season	23
116	3.5 Example scenario 3 - base model - Cross-sectional contour head after four hours of pumping on (a) the first day (day 123) and (b) the last day (day 365) of dry season	23
117	3.6 Example scenario 3 - base model - Head in representative layers after four hours of pumping on (a) the first day (day 123) and (b) the last day (day 365) of dry season	23
118	3.7 Schematic upscaling daily pumping time	25
119	3.8 Results of yearly total volumes (in, out, ratio) by upscaling daily pumping time	25
120	3.9 Schematic upscaling borehole cross-sectional dimension	26
121	3.10 Results of yearly total volumes (in, out, ratio) by upscaling well diameter	26
122	3.11 Example scenario 1 - base model - Discharge performance for (a) the first five days and (b) the last five days of dry season	27
123	3.12 Example scenario 1 - 5x base model well diameter - Discharge performance for (a) the first five days and (b) the last five days of dry season	27
124	3.13 Schematic upscaling penetration length due to well cleaning	28
125	3.14 Results of yearly total volumes (in, out, ratio) by upscaling the penetration length due to well cleaning	28
134	4.1 Fictive schematic of crop cover area (C%)	32
135	4.2 Well diameter upscaling dependent results on net agricultural field size, areal groundwater cone of interest and "crop cover ratio"	34
136	4.3 Well diameter upscaling dependent results on net agricultural yield, costs and net returns	34
138	B.1 Comparable example of the fieldwork submersible pump	51
139	B.2 Comparable example of the fieldwork generator	52
140	B.3 Actual fieldwork hose & bucket	52

141	B.4 Comparable examples of Van Essen TD- & Baro-Divers	53
142	B.5 Comparable examples of In-Situ TD- & Baro-Divers	53
143	B.6 Comparable example of the fieldwork water tape	54
144	B.7 Fieldwork (measurement) set-up (a) general, (b) simplified	55
145	B.8 Fieldwork fact-sheet: Bingo	57
146	B.9 Fieldwork fact-sheet: Nungo	58
147	B.10 Fieldwork fact-sheet: Nyong Nayili	59
148	B.11 Fieldwork fact-sheet: Janga (attempt 1)	60
149	B.12 Fieldwork fact-sheet: Jamga (attempt 2)	61
150	B.13 Fieldwork fact-sheet: Ziong (location of monitoring)	62
151	C.1 Bingo single layer fieldwork data analysis by the optimization (a) fmin-RMSE method and (b) TTim calibration method	64
152	C.2 Bingo double layer fieldwork data analysis by the optimization (a) fmin-RMSE method and (b) TTim calibration method	64
153	C.3 Bingo partially penetrating double layer fieldwork data analysis by the optimization (a) fmin- 154 RMSE method and (b) TTim calibration method	64
155	C.4 Bingo - overview determined (Fmin and Cal) optimal parameter values of (??) a single layer 156 system, (??) a double layer system, and (??) a system with two layers and partial penetration of 157 the well	65
158	C.5 Nyong Nayili single layer fieldwork data analysis by the optimization (a) fmin-RMSE method 159 and (b) TTim calibration method	67
160	C.6 Nyong Nayili double layer fieldwork data analysis by the optimization (a) fmin-RMSE method 161 and (b) TTim calibration method	67
162	C.7 Nyong Nayili partially penetrating double layer fieldwork data analysis by the optimization (a) 163 fmin-RMSE method and (b) TTim calibration method	67
164	C.8 Nyong Nayili - overview determined (Fmin and Cal) optimal parameter values of (??) a single 165 layer system, (??) a double layer system, and (??) a system with two layers and partial penetra- 166 tion of the well	68
167	C.9 Janga first attempt single layer fieldwork data analysis by the optimization (a) fmin-RMSE 168 method and (b) TTim calibration method	69
169	C.10 Janga first attempt double layer fieldwork data analysis by the optimization (a) fmin-RMSE 170 method and (b) TTim calibration method	69
171	C.11 Janga first attempt partially penetrating double layer fieldwork data analysis by the optimiza- 172 tion (a) fmin-RMSE method and (b) TTim calibration method	69
173	C.12 Janga first attempt - overview determined (Fmin and Cal) optimal parameter values of (??) a 174 single layer system, (??) a double layer system, and (??) a system with two layers and partial 175 penetration of the well	70
176	C.13 Janga second attempt single layer fieldwork data analysis by the optimization (a) fmin-RMSE 177 method and (b) TTim calibration method	71
178	C.14 Janga second attempt double layer fieldwork data analysis by the optimization (a) fmin-RMSE 179 method and (b) TTim calibration method	71
180	C.15 Janga second attempt partially penetrating double layer fieldwork data analysis by the opti- 181 mization (a) fmin-RMSE method and (b) TTim calibration method	71
182	C.16 Janga second attempt - overview determined (Fmin and Cal) optimal parameter values of (??) 183 a single layer system, (??) a double layer system, and (??) a system with two layers and partial 184 penetration of the well	71
185	C.17 Ziong single layer fieldwork data analysis by the optimization (a) fmin-RMSE method and (b) 186 TTim calibration method	72
187	C.18 Ziong double layer fieldwork data analysis by the optimization (a) fmin-RMSE method and (b) 188 TTim calibration method	73
189	C.19 Ziong partially penetrating double layer fieldwork data analysis by the optimization (a) fmin- 190 RMSE method and (b) TTim calibration method	73
191		73

193	C.20 Ziong - overview determined (Fmin and Cal) optimal parameter values of (??) a single layer	
194	system, (??) a double layer system, and (??) a system with two layers and partial penetration of	
195	the well	74
196	D.1 Schematic of an axially symmetric model (Langevin, 2008)	75
197	D.2 Modflow topview schematisation of a: (a) Rectangular model, (b) Rectangular round model	
198	and (c) Single row model	77
199	D.3 Schematic test 1	78
200	D.4 Results test 1	79
201	D.5 Schematic test 2	80
202	D.6 Results test 2	81
203	D.7 Schematic test 3	82
204	D.8 Results test 3: Cross-section head contour after 1 day of pumping	82
205	D.9 Results test 3: Head after 1 day of pumping at 2.0m (relative to aquifer bottom)	83

List of Tables

206

207	2.1 Bingo - overview best fit parameters	9
208	2.2 Nyong Nayili - overview best fit parameters	11
209	2.3 Janga first attempt - overview best fit parameters	12
210	2.4 Janga second attempt - overview best fit parameters	12
211	2.5 Ziong - overview best fit parameters	13
212	3.1 Base model scenarios - Wet season recharge (m3)	22
213	3.2 Base model scenarios - Dry season discharge (m3)	24
214	3.3 Base model scenarios - Recovery ratio $R\%$	24
215	E.1 Lambda (m) overview per location	85

216

217

Introduction

218 Introduction: work in progress.

219

220 For now the focus is on the thesis core itself.

221 Chapters do contain sub-conclusions / summaries

222

1.1. Background

223

1.2. Research gap

224

ASR systems

blabla



(a)



(b)

Figure 1.1: Example on (a) flood near Weisi, Upper West Region (source: Owusu et al., 2017) and (b) drought near Nungo, Upper East Region

225

226

227

1.3. Research purpose

228

229

PIT & Irrigation purpose

230 PIT application on irrigation (single figure). and the desired upscaling of this system (multiple figure).

231

232

Research question

233

234 How can scaled-up Aquifer Storage and Recovery (ASR) systems be beneficial for the availability and sus-
235 tainable use of groundwater in northern Ghana small-scale agriculture?

236

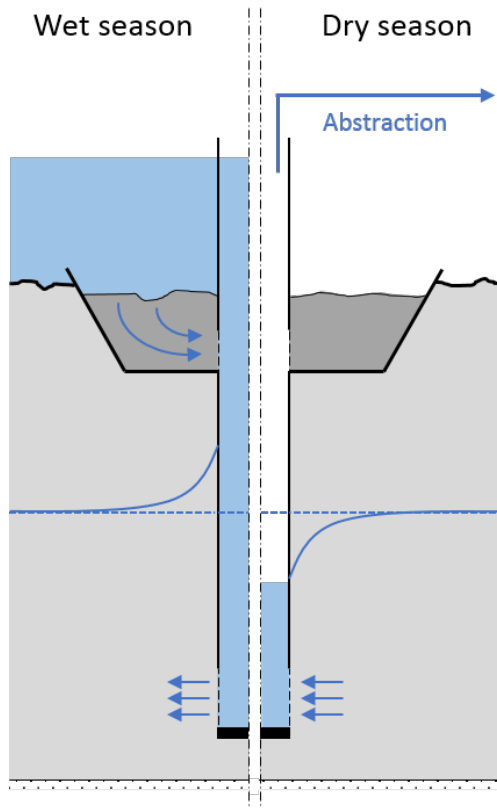


Figure 1.2: Principle Aquifer Storage & Recovery (ASR) system

237 **1.4. Reader's guide**

238 to answer this research question...

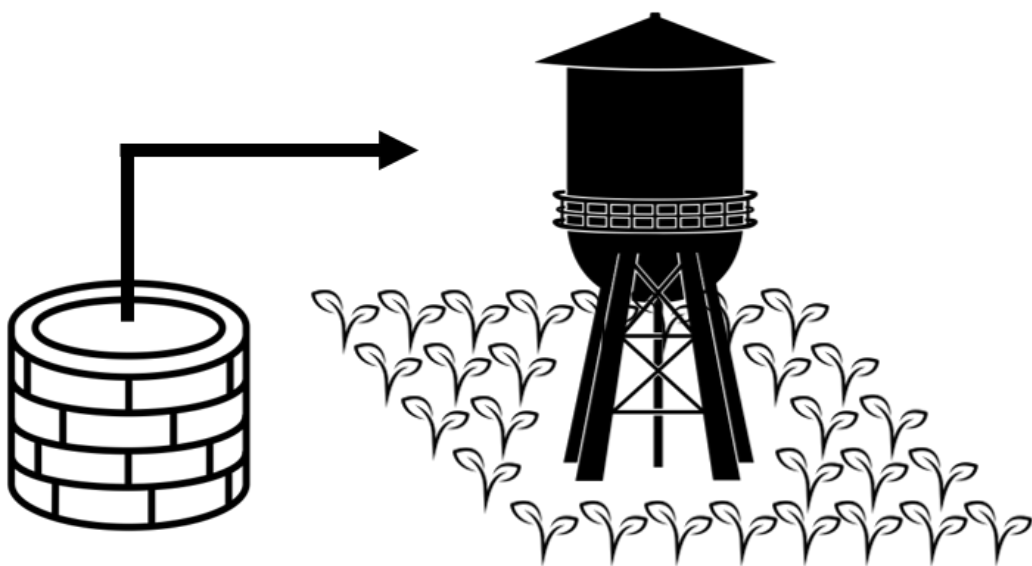


Figure 1.3: Schematic: dry season system use
(visual support by Housin Aziz, Jhun Capaya and Nibras@design from Noun Project - <https://thenounproject.com>)



Figure 1.4: Schematic: desired up-scaling in dry season system use
(visual support by Housin Aziz, Jhun Capaya and Nibras@design from Noun Project - <https://thenounproject.com>)

2

239

240

Fieldwork data analysis

241 Geological conditions are highly heterogeneous in northern Ghana. Subsurface characteristics vary at short
242 mutual distances. Adequate and reliable information about local geohydrological conditions is preferably
243 gathered through site-specific fieldwork. In this research perspective, multiple northern Ghana borehole
244 locations are subjected to groundwater pumping tests.

245 The NGO Conservation Alliance (CA) installed several PIT locations in the summer of 2016, in the Upper
246 East and Northern Region. Pumping tests are performed at four of these boreholes. A fifth PIT borehole (in
247 Ziong) is monitored to study how the ASR system is used by local farmers. The figure below shows a map of
248 the research locations in northern Ghana (Figure 2.1).

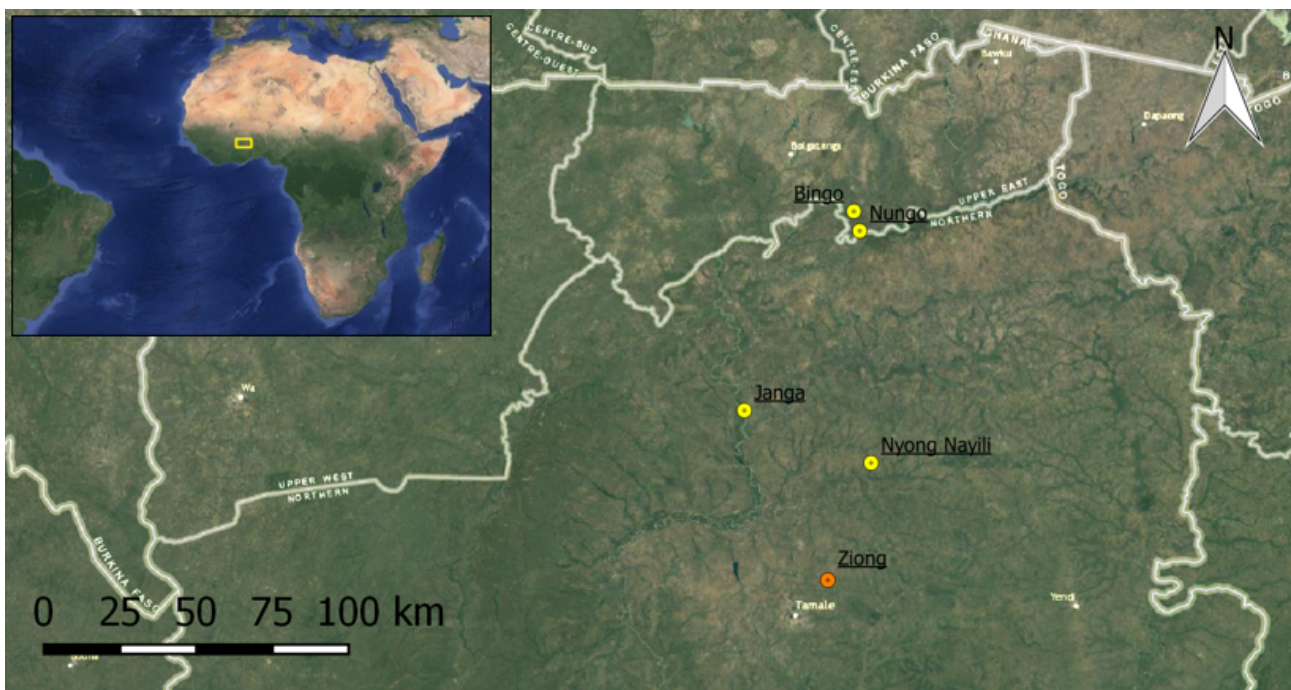


Figure 2.1: Overview of fieldwork locations in northern Ghana

249 Detailed information on the equipment that was used, the set-up of the pumping tests as well as the mon-
250 itoring of an operating ASR system can be found in appendix B. The obtained raw fieldwork data can be
251 found in the site-specific fact-sheets of appendix B.3. The purpose of this fieldwork is to determine geo-
252 hydrological subsurface parameters, transmissivity (T) and storativity (S), which are used as input for further
253 investigation into upscaling these systems.

254 This chapter contains the analysis of gathered fieldwork data. First, the methodology for data analysis,
255 including some theoretical background, is explained (Section 2.1). Section 2.2 contains the derivation of

256 the local geohydrological parameter values: T and S . Finally, the chapter concludes with the determination
 257 of parameter bandwidths (Section ??), which will be used in the subsequent model simulations.

258 2.1. Parameter derivation methods

259 2.1.1. Theoretical model definition

260 In large parts of northern Ghana the geohydrological soil characteristics are unknown. Strong variations at
 261 short mutual distance makes it necessary to obtain more information about local geology. The most reliable
 262 site-specific information was recorded during the drilling of boreholes (2016). The borehole log-sheets
 263 (appendix A) are used as a starting point for the construction of the applied theoretical models in fieldwork
 264 analysis.

265
 266 The site-specific borehole logsheets show similarities in stratification. In each case the upper 50 meters is
 267 divided into two or three layers, consisting of a confining top layer, and below that one or two "aquifers".
 268 Groundwater tables are predominantly positioned in the first aquifer. Based on these observations three
 269 simplified theoretical models for the analysis of fieldwork data are derived, as depicted in Figure 2.2.

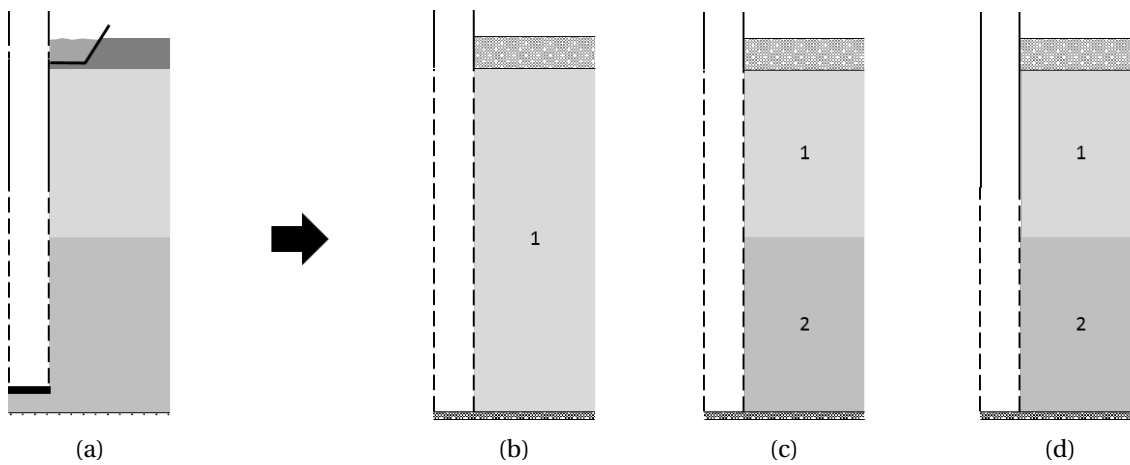


Figure 2.2: Schematic cross-sectional view of (a) generalized northern Ghana soil stratification and simplified representations: (b) a single layer system, (c) a double layer system, and (d) a system with two layers and partial penetration of the well

270 These simplified models (Figure 2.2b - 2.2d) mimic local conditions, making the derivation of representative
 271 hydraulic subsurface characteristics (T and S) possible (Kruseman and de Ridder, 2000). Double layered
 272 models are applied to provide more degrees of freedom, potentially generating more accurate simulations.
 273 A maximum of two soil layers are implemented to limit chances of equifinality, due to an abundance of de-
 274 grees of freedom.

275

276 2.1.2. Techniques in analysis

277 This section contains a description of the (analytical) models and methods used for optimal groundwater
 278 parameter estimation.

279

280 Theis's method

281 Groundwater drawdown due to the withdrawal of water can be determined analytically with Theis's equa-
 282 tion (Equation 2.1). Theis's method is applicable on the situation depicted in 2.2b; a constant rate pumping
 283 test in a fully penetrating well in a confined single layer aquifer (Kruseman and de Ridder, 2000). The ana-
 284 lytical solution is suitable for obtaining a first indication of geohydrological parameters.

$$s = \frac{Q}{4\pi K D} \exp(-u) \quad (2.1)$$

$$u = \frac{r^2 S}{4 K D t} \quad (2.2)$$

285 Where s (m) is the drawdown at distance r (m) from the well, Q (m^3) is the constant well discharge , KD
 286 (m^2/d) is the aquifer transmissivity ($KD = T$), S (-) is the aquifer storativity, t (d) is the time measured from
 287 the start of pumping and $\exp1$ is the exponential integral. The drawdown measurements in this research
 288 are limited to in-well measurements. The distance r in Theis's equation is assumed to be the length of the
 289 well radius (0.0635 m). Theis's method is applicable for the time of pumping as well as the recovery process.
 290 The script below shows the implementation of Theis's method in Python.

```
291
292 def drawdown(t, T, S):
293     s = Qo / (4 * np.pi * T) * exp1(ro ** 2 * S / (4 * T * t))
294     s[t > toff] -= Qo / (4 * np.pi * T) * exp1(ro ** 2 * S / (4 * T * (t[t>toff] -
295                                                 toff)))
296
297     return s
```

299 Analytic Element Modelling in TTIm

300 TTIm is a computer program based on analytic elements and designed for the analysis of transient ground-
 301 water flow in one or more layers. Multiple elements (and types of elements) can be added to specific prede-
 302 fined model layers. The use of TTIm makes it possible to take additional well characteristics into account.
 303 Groundwater heads can be determined inside the well and the model optionally accounts for borehole stor-
 304 age and well skin resistance. Well discharge can be toggled on and off multiple times. This allows simula-
 305 tions of both single pumping and recovery tests and long-term well operations (Bakker, 2013a,b).

306 The analysis of the pumping and recovery tests is performed with the TTIm Model3D configuration. The
 307 inclusion of a single well element is sufficient in this case. Depending on which subsurface model is used
 308 (Figure 2.2) the well (analytic element) is screened in one or more model layers. The top layer is configured
 309 as phreatic layer, meaning the top layer storage coefficient (S) is a phreatic storage coefficient (S_y). This is
 310 based on observed initial groundwater tables, which are located below the bottom of the confining top layer.
 311 Multiplying this value with the aquifer thickness is therefore no longer needed. Each layer in the simplified
 312 model has a thickness of 1 meter. This means derived hydraulic conductivities (k) can be interpreted as
 313 transmissivities (T) and the storage is expressed as the layer storage coefficient (S). This is done to directly
 314 derive T and S values. Additionally, this approach automatically corrects for the unknown thickness of the
 315 deepest soil layer in which the well is screened. There is no information about soil conditions beyond the
 316 bottom of the wells in the borehole log-sheets (Appendix A).

318 MODFLOW

319 The modelling of ASR upscaling scenario's (see Chapter 3) is done with Modular Ground-Water Flow Model
 320 (MODFLOW), a finite difference model for groundwater flow developed by the U.S. Geological Survey (USGS).
 321 MODFLOW is the international standard in groundwater simulation ((Harbaugh, 2005; Niswonger et al.,
 322 2011)). More information on the applied inputs can be found in Chapter 3. In the case of fieldwork data
 323 analysis MODFLOW is not used for the derivation of geohydrological parameters. Optimal parameters de-
 324 rived with TTIm models are implemented in corresponding MODFLOW models to validate obtained TTIm
 325 results.

327 2.1.3. Optimization functions

328 Pumping test data (section ??) is used as input for the derivation of local geohydrological parameter values.
 329 The values of T and S are determined by the method of (curve) fitting the analytical solutions and TTIm
 330 models to the data. In this process two optimization functions are used.

331 Fmin-RMSE optimization

332 Differences between the measured and modelled drawdown curves can be expressed by the Root-Mean-
 333 Square-Error (Equation 2.3). The Fmin function (part of Python's `scipy.optimize` package) is applied to
 334 minimize the difference between modelled and observed drawdowns. This optimization results in optimal
 335 T and S values (and optionally values for borehole storage and well skin resistance) that represent local con-
 336 ditions. An example Python implementation of Fmin optimization is given below. It shows an optimization
 337 of five parameters (T and S values for two model layers and well skin resistance).

339

$$RMSE = \sqrt{\frac{\sum (s_{mod} - s_{field})^2}{N}} \quad (2.3)$$

340 Where s_{mod} is the modelled drawdown (m), s_{field} is the observed drawdown (m) and N is the number of data
341 points.

```
342
343
344 def optimTTim_Qvar(params, t, meas):
345     kaq = np.zeros(2)
346     Saq = np.zeros(2)
347     kaq[0] = params[0]
348     kaq[1] = params[1]
349     Saq[0] = params[2]
350     Saq[1] = params[3]
351     res = params[4]
352     s = drawdownTTim_Qvar(t, kaq, Saq, res)
353     error = np.sqrt(np.mean((s-meas)**2))
354     return error
355
356 xopt = fmin(optimTTim_Qvar, x0=[10, 10, .01, .001, 0.1], args=(to[mask], do[mask]),
357               xtol=1e-4)
```

359 Calibration function

360 TTIm has an in-built calibration function for the derivation of parameter values. Application of this second
361 method improves the research robustness. In the Python script below, an example of the TTIm Calibrate
362 function is given. It is the same example as mentioned in the Fmin optimization above.

```
363
364 cal = Calibrate(mlc)
365 cal.parameter(name='kaq0', layer=0, initial=10, pmin=0)
366 cal.parameter(name='kaq1', layer=1, initial=10, pmin=0)
367 cal.parameter(name='Saq0', layer=0, initial=.01, pmin=0, pmax=0.3)
368 cal.parameter(name='Saq1', layer=1, initial=.001, pmin=0, pmax=0.3)
369 cal.parameter(name='res', par=wc.res, initial=0.1)
370 cal.series(name='obs3', x=ro, y=0, layer=[0,1], t=to[mask], h=do[mask])
371 cal.fit()
```

374 Both optimization methods require an initial estimate for the parameters. More than one suitable solution
375 is possible, which makes the outcome of the optimization dependent on the choice of initial values. Other
376 studies found that T and S values are commonly low in northern Ghana (e.g. Owusu et al., 2017, 2015).
377 Based on these other studies the following initial conditions are applied: k_{aq0} is 10 (m/d), k_{aq1} is 10 (m/d),
378 S_{aq0} is 0.01 (-), S_{aq1} is 0.001 (-) and well resistance is 0.1 (d). The actual well radius is used as the (initial)
379 borehole storage: 0.0635 (m). Boundary conditions are applied to avoid the optimization resulting in phys-
380 ically improbable parameter values, i.e. negative parameter values and unnaturally high storativity values
381 (greater than 0.3 (-)).

382 2.2. From fieldwork data to T & S values

383 The methods and models mentioned in the previous section are applied on the measurements from the
384 five locations: Bingo, Nungo, Nyong Nayili, Janga and Ziong. Measurements results are included in the fact-
385 sheets of Appendix B.3. A complete overview of all optimization simulations (overall 25 per location) can be
386 found in Appendix C. Most important outcomes are discussed below for each of the five locations.

387 2.2.1. Location: Bingo

388 Site inspection

389 The surroundings of Bingo are characterized by a mildly sloping landscape. (Bed)rock appears occasionally
390 at the surface. Site inspection showed an abundance of charred vegetation. The area is exposed to bush
391 fires. As a consequence the agricultural field is not in operation. Map inspection shows the presence of the

392 Volta river within several kilometres from Bingo. However, no indications of surface water (water-bodies
 393 and/or ponds) were observed. Bingo inhabitants label wet season flooding as high. Inundation levels of 1-2
 394 m are common and usually last for several days. Flooding is not always caused by rain, every now and then
 395 a surplus of water accumulates at the surface by "popping up" out of ground. Inspection on the infiltration
 396 technology itself revealed the presence of a steel lid. Above surface level no well screen perforations were
 397 observed. The infiltration bed is an entrance path for the replenishment of groundwater.

398

399 Measurement quality

400 A malfunctioning power converter postponed the pumping test start. Since nightfall was a time limiting
 401 factor, the delay resulted in a shortened total test duration. In-well drawdown observation further down-
 402 graded the measurement quality. Well turbulence (due to pumping) caused the origin of a tangled rope.
 403 Hand measurements became more complicated and unreliable. An even more important consequence of
 404 the tangled rope was the occurrence of an undesirably high position of the deepest pressure sensor installed
 405 (see measurement set-up in Appendix B.2). Direct result is a long-term gap in pumping test drawdown data
 406 (yellow dotted line in Figure 2.3). The exact drawdown at the last moment of pumping is for example miss-
 407 ing. Among other things due to the deliberate choice of a relative long-time recovery measurement the
 408 overall dataset can potentially be of use.

409

410 Fit analysis

411 The long-term absence of adequate data has its effects on the parameter fitting capabilities. As visible in Fig-
 412 ure 2.3, Theis's method encounters difficulties here. Drawdown most definitely exceeded the measurement
 413 limit of 8m. This is not reflected in the parameter outcome of Theis's method. Defective fitting capabili-
 414 ties, due to a gab in data, are clearly less emphatically present in the analysis by the use of TTIm. Optimal
 415 parameter values are found at which drawdown curves exceed the drawdown measurement limit. Taking
 416 borehole storage and/or well resistance in consideration may potentially underlie this. This example shows
 417 it is not by definition required to feature complete drawdown data. By the use of TTIm incomplete time se-
 418 ries can result in adequate optimal parameter values. In order size the values found are low but align initial
 419 conditions. Furthermore it can be appointed that the double-layered transmissivity values found, suggest
 420 the presence of only one preferential layer of groundwater flow.

421

Table 2.1: Bingo - overview best fit parameters

	Method	Stor [m]	Res [d]	T1	T2 [m^2/d]	S1	S2 [-]	RMSE [m]
Analytical	fmin	-	-	10.83	-	2.0e-04	-	0.798
1 lay	fmin	0.0647	5.6e-02	26.23	-	6.6e-03	-	0.163
2 lay	fmin	0.0635	-	2.8e-04	8.25	3.0e-03	2.1e-06	0.107
2 lay (pp)	fmin	0.0597	-	8.6e-04	7.44	7.1e-03	6.3e-06	0.078

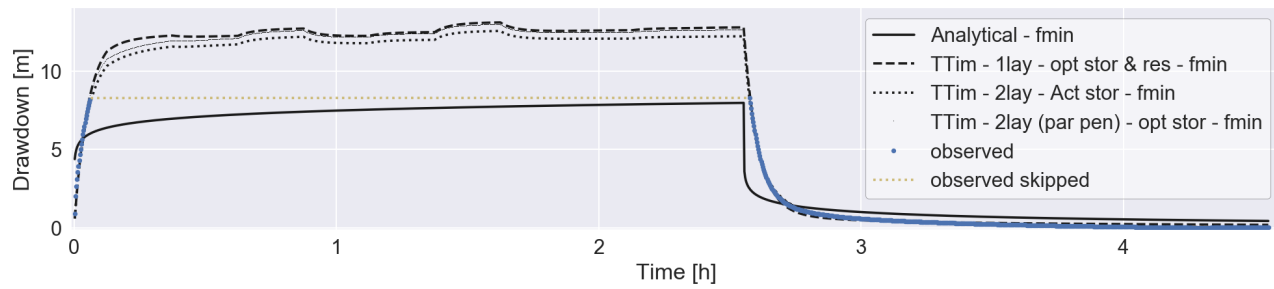


Figure 2.3: Bingo - Simplified models best fit

422

Substantive remark

423 Both parameter optimization functions (Fmin and Calibrate) are able to derive reasonable solutions. Re-
 424 sults of the Calibrate optimization function reveal that an increase in model degrees of freedom not nec-
 425 essary leads to better performance (Appendix C). Also by looking at the TTIm best fit solutions (Figure 2.3)
 426 only minor distinction can be made in performance of the applied simplified models with a single layer,

427 double layer or double layer with a partially penetrating well. Overall model accuracy slightly increases
 428 (Root-Mean-Square-Error slightly decreases) by an increase in complexity. An increase that can not be la-
 429 belled as significant. All three simplistic theoretical models potentially represent nature properly by the in
 430 TTIm found optimal parameters, depicted in Table 2.1.

431 **2.2.2. Location: Nungo**

432 **Site inspection**

433 The remote community of Nungo is located in the Upper East region of Ghana. Access is possible by an un-
 434 prepared road or river cross only. The landscape is mildly sloping till flat. Low afforestation is interspersed
 435 by plains. Adjacent to the community an out of use agricultural field is present. The Volta river looms a
 436 close range (approximately 400m). Wet season flooding occurs due to riverbank over-topping. Inhabitants
 437 label inundation levels as extreme. Water levels of 3m and higher persist for the entire rainy season. The
 438 groundwater infiltration technology is characterized by perforations above surface level. At the moment of
 439 inspection the top was distorted by heat. The closure by the use of a lid was thus excluded.

440

441 **Measurement quality**

442 Installation of the test set-up was heavily influenced by difficulties in pump immersion. From the first mo-
 443 ment of pumping discharge rates were zero by approach. Well inspection revealed the presence of a liquid
 444 consisting of a combination of water, sandy clay and debris. The pumping test was restarted twice with a
 445 raised pump elevation. No improvements in outcomes were encountered.

446

447 **Fit analysis**

448 -

449

450 **Substantive remark**

451 Due to an aborted test no drawdown results perceived. The well is clogged and should be cleaned before
 452 measurements can be done.

453 **2.2.3. Location: Nyong Nayili**

454 **Site inspection**

455 The landscape of Nyong Nayili and her surroundings is typically flat. A mix of bushes, low vegetation and
 456 crop fields is present. During site inspection the agricultural field related to the infiltration technology of in-
 457 terest is not (yet) defined. The local community encounters wet season inundation levels up to 1 m. Within
 458 the season fluctuation occur, and can be explained by its rainfall based origin. During inspection no river
 459 or water flow is observed in the area. A muddy stagnant pond is present at close well range (approximately
 460 40m). It definitely needs to be appointed, the infiltration bed is still inundated (approximately 0.2 m) dur-
 461 ing pumping test application. Well perforations reach above the infiltration bed. The accumulated water
 462 present definitely has its repercussions on the test.

463

464 **Measurement quality**

465 Start of the pumping test was delayed due to the well location search and the initial use of a clogged dis-
 466 charge hose. Since nightfall was a time limiting factor, the delay resulted in a shortened total test duration.
 467 In addition, the inundated infiltration bed heavily affected the pumping test. The first 20 minutes of draw-
 468 down measurements are labelled as useless due to an (unknown) additional inflow (see Appendix B.3). This
 469 period is not taken into account during further analysis. Visual inspection during pumping test application
 470 implies the interference of additional inflow even beyond this 20 minutes data skip. Usability of the data set
 471 (especially during pumping) can therefore be questioned.

472

473 **Fit analysis**

474 Theis's method encounters difficulties in finding adequate parameter values. The optimal solution does
 475 not result in a reasonable curve fit (compared to data-set). Found storativity equals the predefined upper
 476 bound. The solution is unreliable and can be neglected. The use of TTIm has a positive impact on the
 477 outcome in data analysis. Found transmissivity values are not analogous, but potentially represent nature.

478 Storativity values can be interpreted as low. Obtained optimal borehole storage values are strikingly high.
 479 These values potentially reflect the presence of additional inflow. Being a constant value, this reflection only
 480 accounts to a certain extent. Overall curve fitting performances are moderate. The lack in fitting capabilities
 481 can potentially be attributed to the data skip and/or the unknown additional inflow of water over time.
 482

Table 2.2: Nyong Nayili - overview best fit parameters

	Method	Stor [m]	Res [d]	T1	T2 [m²/d]	S1	S2 [-]	RMSE [m]
Analytical	fmin	-	-	6.00	-	3.0e-01	-	0.752
1 lay	cal	0.2419	-	13.35	-	7.8e-05	-	0.457
2 lay	cal	0.2436	-	6.95	6.98	4.6e-06	3.6e-05	0.457
2 lay (pp)	fmin	0.2659	1.7e-02	1.7e-04	28.61	1.1e-02	4.4e-06	0.450

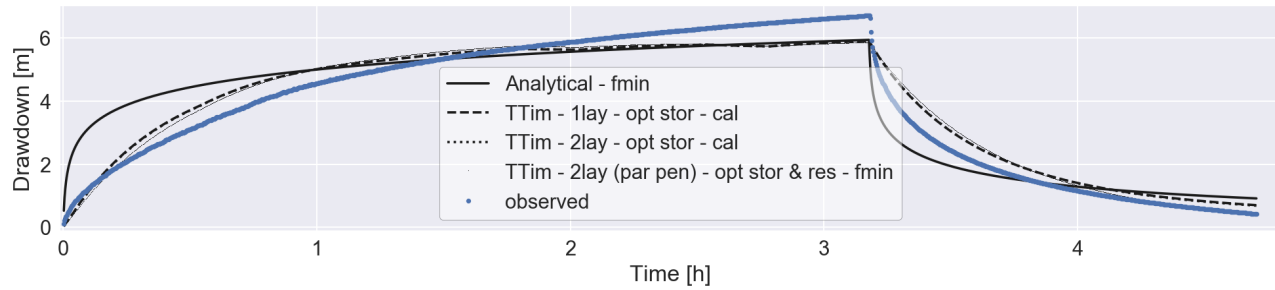


Figure 2.4: Nyong Nayili - Simplified models best fit

483 Substantive remark

484 Deviations in obtained data-set and the different (TTim) modelled optimal simulations are of equal size,
 485 regardless the optimization function applied. An increase in parameter freedom does not necessarily im-
 486 prove model performance. Reverse effects do occur. In all model simulations the Root-Mean-Square-Error
 487 is substantial. The accuracy of the found optimal parameter values can therefore be doubted. Further re-
 488 search on the impact of missing starting data and/or the impact of water inflow during a pumping test is
 489 advised.

490 2.2.4. Location: Janga (1/2)

491 Site inspection

492 The infiltration technology near Janga is potentially located at the bank (edge) of a dry river bed. The Volta
 493 river is located at walking distance (see fact-sheet visualisation, Appendix B.3). A stagnant pond is present
 494 at a distance of approximately 70 m from the well. Wet season flooding is caused by river overflow. The
 495 flooding is labelled as constant, extreme (>4m) and lasts for months. During field visit no agricultural field
 496 is encountered related to the infiltration technology. The pipe segment above surface level accommodates
 497 perforations and is equipped with a plastic/concrete cover.

498

499 Measurement quality

500 Bush fires are abundant in the region. Due to close range appearance the test is aborted just before sunset.
 501 The duration of recovery process monitoring is affected. Noteworthy is the color change in water discharged
 502 during the pumping test. Alternately the water switched color (brownish, grey, white, clear) several times.
 503 No further complications occurred. The gathered data can potentially be of use for analysis.

504

505 Fit analysis

506 Found parameter order size is in line with the data gathered at the other research locations. This does
 507 not apply for the Root-Mean-Square-Error scale size. Large RMSE-values can be attributed to the pump-
 508 ing test drawdown part. Shape of the time series is most definitely worth-mentioning. Regardless which
 509 method and/or model applied, not a single combination is capable of approaching the remarkable draw-
 510 down shape. Analytical Theis method as well as TTIm is not capable of correction for irregular patterns of

511 groundwater tables over time.
 512

Table 2.3: Janga first attempt - overview best fit parameters

	Method	Stor [m]	Res [d]	T1	T2 [m²/d]	S1	S2 [-]	RMSE [m]
Analytical	fmin	-	-	8.84	-	3.0e-01	-	1.339
1 lay	fmin	0.0635	-9.7e-03	9.09	-	1.6e-02	-	1.382
2 lay	fmin	0.1287	-	12.48	1.3e-04	1.9e-02	1.1e-08	1.445
2 lay (pp)	fmin	0.0635	-	9.1e-05	15.19	4.3e-08	3.1e-03	1.530

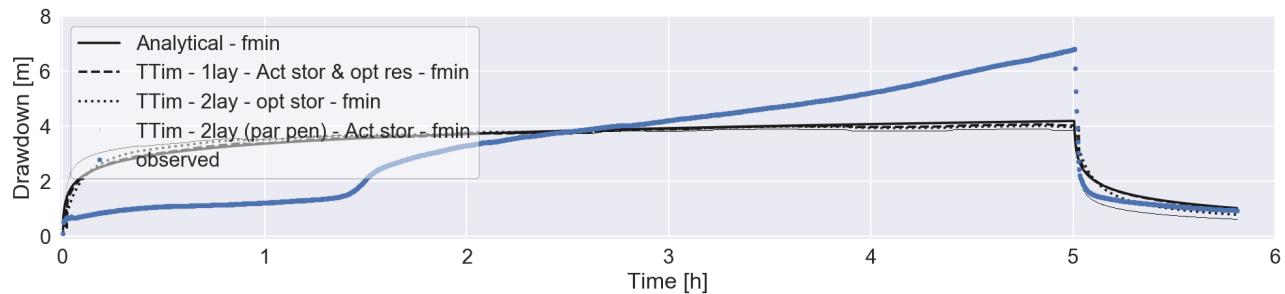


Figure 2.5: Janga first attempt - Simplified models best fit

513 Substantive remark

514 The course of the drawdown curve is most definitely catching the eye. Several details are striking. There is
 515 a sudden increase in drawdown after 90 minutes of pumping. Towards the end of pumping period (four to
 516 five hours) the curve does not show the characteristic behaviour of movement towards a new equilibrium.
 517 And the fluctuations are no longer monitored in the recovery process. As stated by Kruseman and de Ridder
 518 (2000), most of the time there is not a unique theoretical solution for these well-flow problem. Making the
 519 identification of the right (theoretical) system more difficult. Additional fieldwork can provide solutions.
 520 Validation is applied to confirm or disprove the correctness of the data-set. The same ASR system is exposed
 521 to a second pumping test.

522 2.2.5. Location: Janga (2/2)

523 Measurement quality

524 Initial (first two hours) pumping test discharge rates vary slightly (Appendix B.3). The drawdown curve is
 525 potentially affected. Just as in the first attempt, the extracted water changed color several times. Compared
 526 to the previous research a longer monitoring of the recovery process is applied. The collected pumping test
 527 time series data is presumably useful.

528

529 Fit analysis

530 Despite the application of a lower rate pumping test (compared to first attempt) the gathered drawdown
 531 data shows similar behaviour. Lower values in Root-Mean-Square-Error can be assigned to the lower general
 532 drawdown pursued and the increased duration of recovery monitoring. It does not necessarily mean the
 533 obtained parameter values are more reliable. Values as depicted in Table 2.4 are at most useful as a plausible
 534 indication.

Table 2.4: Janga second attempt - overview best fit parameters

	Method	Stor [m]	Res [d]	T1	T2 [m²/d]	S1	S2 [-]	RMSE [m]
Analytical	fmin	-	-	15.97	-	3.0e-01	-	0.571
1 lay	fmin	5.4e-07	-9.7e-03	13.54	-	1.9e-02	-	0.551
2 lay	fmin	0.2228	-2.2e-02	2.05	8.13	2.1e-02	4.1e-04	0.545
2 lay (pp)	fmin	0.2005	-3.1e-02	6.59	0.86	9.4e-05	2.1e-03	0.545

535 Substantive remark

536 The applied validation confirms the correctness in data gathering. Nevertheless the uncertainty in the-

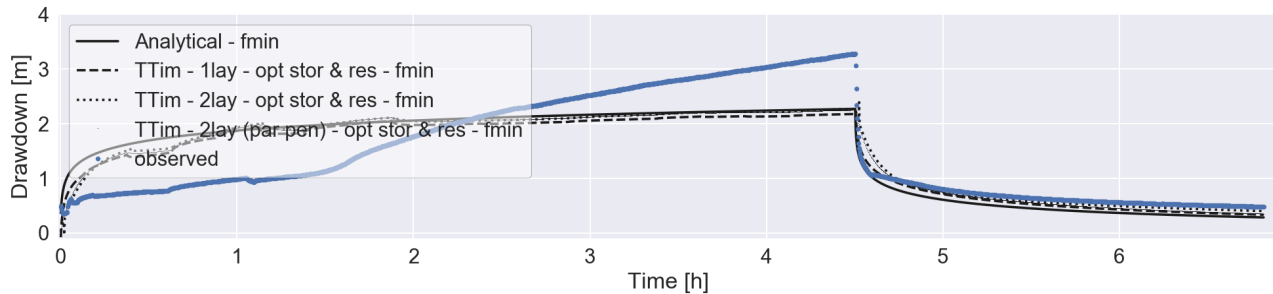


Figure 2.6: Janga second attempt - Simplified models best fit

537 theoretical model selection persist. A conclusion confirmed by Kruseman and de Ridder (2000). Causes of the
 538 authentic drawdown curve can be widespread. One can think of the drying preferential flow-path layers,
 539 distinctive subsurface connections to the river bed, fracture zones and more. Instead of further fieldwork
 540 investigation, it is advisable to gain knowledge in complex drawdown data interpretation.

541 2.2.6. Location: Ziong (monitoring)

542 Site inspection

543 In the local surroundings of Ziong no river, water flow or ponds are perceived. Wet season land inundation
 544 is typically less than 2 m. Day to day variations takes place due to its origin by temporal heavy rain. The
 545 regional landscape is flat. Occasionally (bed)rock is observed at the surface. High grasses and bushes are
 546 present. Nature is supplemented by several agricultural fields. The infiltration technology does not contain
 547 tube perforations above surface level. A steel lid is present to cover the top inlet. Inspection showed the
 548 agricultural field related to the ASR-system is ready for the supply of water.

549

550 Measurement quality

551 During inspection the system was put in daily operation. Instead of a single pumping test, an unique op-
 552 portunity is seized by an improvised monitoring of the system performance over multiple days. Due to the
 553 permanent seasonal pump installation and the limits of diver memory, monitoring divers are positioned in
 554 the borehole by an hanging rope only. The inescapable high positioning of the divers (above lowest encoun-
 555 tered groundwater tables) results in the absence of multiple time-series segments (yellow dotted line in 2.7).
 556 The adopted discharge rate of $20 \text{ m}^3/\text{d}$ is based on multiple time measurements of the present dated vol-
 557 ume meter. In analysis it is assumed to be constant. Operational hours of pumping are not precisely known.
 558 In data analysis it is assumed recovery starts four minutes before the first sign of recovery appears in data.
 559 Despite these defects the collected data can be used for further analysis.

560

561 Fit analysis

562 Given the measurements nature no parameter definition is applied by the use of the analytical Theis method.
 563 Analysis by the use of TTim show reasonable results. Curve fit simulation shows thorough overlap with the
 564 measured time-series. This example shows the wide deployment of TTim. Although above areal prevailing,
 565 storativity values are plausible. Obtained transmissivity values are extremely low, but generally consistent.

566

Table 2.5: Ziong - overview best fit parameters

	Method	Stor [m]	Res [d]	T1	T2 [m^2/d]	S1	S2 [-]	RMSE [m]
1 lay	fmin	0.0382	-	1.76	-	1.1e-03	-	0.255
2 lay	fmin	0.0635	-0.05	0.38	1.05	2.9e-02	1.2e-03	0.240
2 lay (pp)	fmin	0.0147	-0.08	0.23	0.78	2.6e-02	1.3e-03	0.243

567 Substantive remark

568 Both optimization functions (Fmin and Calibrate) can be used for the generation of reasonable parameter
 569 outcome. When applying a simplified model with an increased number of degrees of freedom, the Fmin
 570 optimization function tends to score slightly better on values for the Root-Mean-Square-Error (Appendix

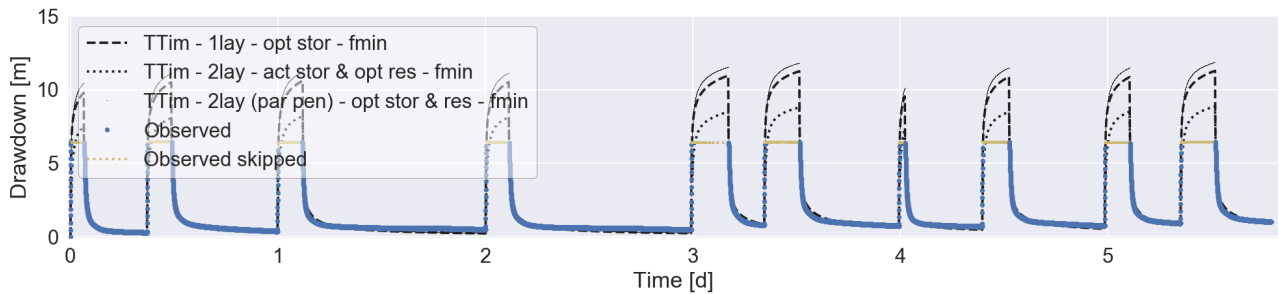


Figure 2.7: Ziong - Simplified models best fit

571 C). This however concerns a single measurement analysis, with a single set of predefined initial parameter.
 572 Moreover no other objective functions are taken into account. Regarding the optimisation functions no ad-
 573 dditional conclusions can be drawn. Looking at the performance of the different simplified models no line
 574 of improvement is discovered. Models with an increased number of degrees of freedom do not necessarily
 575 represent nature better. Sometimes reverse effects are even effective. By the use of the right optimal param-
 576 eter set all three simplified theoretical models are capable to represent the local nature of Ziong to a certain
 577 extend.

578 2.3. Results & conclusions

579 A brief elaboration on key findings regarding the applied fieldwork pumping tests and data analysis is stated
 580 below. The section concludes with parameters definition, applicable on subsequent research.

581

582 ASR-system performance

- 583 • ASR-system cleaning

584 The ASR-systems of interest are exposed to natural forces. Only one year after construction (2016)
 585 the penetration depth of all five boreholes has shrunk. The order of impact differs per location. Most
 586 striking example is the borehole at location Nungo. Be aware of the relative fast system degra-
 587 dation. Measures should be taken to prevent the occurrence of clogging. It is advisable to provide each
 588 borehole with a plastic/concrete lid. Tube penetrations above the infiltration bed should be sealed
 589 permanently to avoid inflow of undesired particles. In addition, annual based preventive cleaning of
 590 borehole and infiltration bed is desirable.

- 591 • Complementary research

592 Obtained pumping test drawdown data is potentially plausible. Nevertheless, uncertainty in the
 593 derivation of parameters and the selection of a (simplified) model consists. As stated by Kruseman
 594 and de Ridder (2000), additional fieldwork does not necessarily solve these uncertainties. No new
 595 comparable pumping tests at the same borehole locations are needed at short term. Gaining knowl-
 596 edge on the interpretation of data can possibly offer solutions. Complementary research on how to
 597 deal with gaps in pumping test data and/or irregularities in drawdown time-series is advisable. More-
 598 over, future research can be pointed at the impact of (time-dependent) inflow of water during pump-
 599 ing test application.

- 600 • Future test applications

601 If applied, additional pumping tests should be targeted at the impact of ASR-systems on its surround-
 602 ings. Pumping tests should be applied in combination with at least one (preferably more) piëzometer
 603 at a certain known distance from the well (Kruseman and de Ridder, 2000). These tests potentially
 604 generate insight in well skin behaviour (degree of resistance). The year round installation of one or
 605 more divers is an option if complete ASR-system understanding is desirable. This can provides more
 606 accurate or new system interpretations. To succeed, it is advisable to set up a measurement plan in
 607 advance. Generated data can be used for a more optimal system use.

608 Applicability of methods & models

609 • Functionality (analytical) methods; Theis & TTIm

610 Compared to the conventional pumping test Theis's method, TTIm offers many more model options
 611 (borehole storage, well skin resistance, multiple layers) in drawdown data analysis (Bakker, 2013a,b).
 612 In this research TTIm unsurprisingly outperforms Theis's method. Yet, the attendance of irregular
 613 drawdown time-series shows that TTIm (e.g. analytical element modelling) also encounters limita-
 614 tions.

615 • Functionality optimization functions; Fmin & Calibrate

616 Obtained geohydrological parameters represent local nature to a certain extend. This is confirmed by
 617 the Root-Mean-Square-Error values (objective function). Application of the two optimization func-
 618 tions generates outcomes. The results of corresponding optimizations can differ in parameter size,
 619 but accuracies (RMSE) are comparable (some exceptions). It can be concluded that both optimiza-
 620 tion functions (Fmin and Calibrate) are potentially usable for the determination of suitable T and S
 621 values.

622 • Functionality simplified models

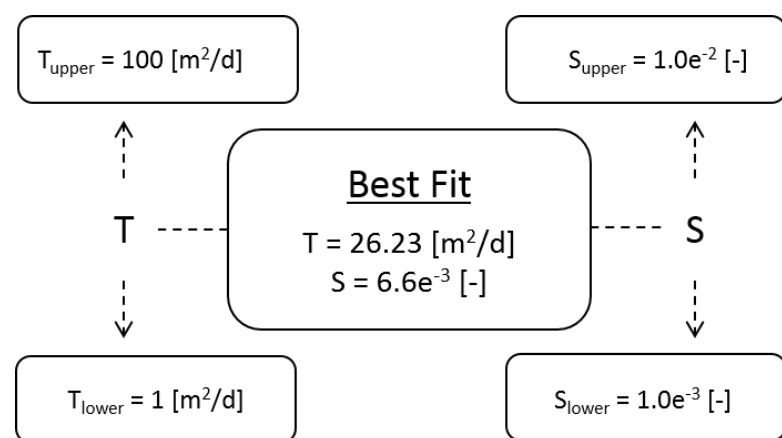
623 Representation of local nature is pursued by the use of three simplistic system: a single layer system,
 624 a double layer system and a system with two layers and partial penetration of the well (Figure 2.2b
 625 - 2.2d). Based on the Root-Mean-Square-Error objective function none of these systems sticks out
 626 positively or negatively. Therefore, subsequent parts of this research are carried out by the use of the
 627 (most simplistic) single layer system. This puts the emphasis on the main goal of this research; effects
 628 of ASR-system upscaling.

629 ***T & S value definition***

630 Drawdown measurements are performed within the extraction well. A set-up which deviates from the de-
 631 sired common standard (Kruseman and de Ridder, 2000). It should be kept in mind the correctness of data
 632 can be questioned. From the perspective of robustness two optimization functions (Fmin & Calibrate)
 633 are applied in data analysis. Comparative system optimizations obtain parameters of different size, while
 634 Root-Mean-Square-Error values are similar (some exceptions). Moreover, local nature can be represented
 635 equally good by a diversity of (single and/or double layered) simplistic systems. For each individual location
 636 there is more than one representative parameter-set available. In short, by the analysis of fieldwork data an
 637 abundance of uncertainties in parameter definition are present.

638 A bandwidth is defined to deal with these uncertainties. Upper and lower T and S values are stated around
 639 the single layer "best" fit solution (Bingo). A visualization of the bandwidth can be found in Figure 2.8.
 640 Transmissivity extremes are based on the combination of obtained values in data analysis and a factor of
 641 safety. Definition of the outer storativity values needed a different approach. Found values in data analy-
 642 sis more than once approached the predefined boundaries conditions (0 and 0.3 (-)) (Appendix C). These
 643 physically improbable parameters are ignored. Outer parameters are preferably based on more common
 644 applied values. The chosen lower limit storativity (S_{lower}) corresponds with the situation of a confined
 645 aquifer, while the upper limit (S_{upper}) is more related to the specific yield of a phreatic storage (bron:
 646 geo1) (Fitts, 2012; Strack, 1989).

647 The defined scope can not be interpreted as a generalization of the different locations. Not a single combi-
 649 nation of the upper and lower parameter boundaries is the one on one representation of a specific location.
 650 The bandwidth predominantly acts as an input for scenario modelling in the subsequent parts of this re-
 651 search. Outcome of these scenarios can only be interpreted as indication of the ASR-system possibilities
 652 within northern Ghana.

Figure 2.8: T & S bandwidth selection

3

654

655

ASR-system upscaling - Test problem

656 General aim of research is pointed at the provision of larger water quantities during northern Ghana's dry
657 seasons. The research investigates to what extent Aquifer Storage and Recovery systems (ASR-systems) can
658 contribute to water availability. The water is in the essence used for local small-scale agriculture.

659

660 A single test problem is selected to explore and access the capabilities in ASR-system upscaling. The test
661 problem consists of a single layer aquifer which is partially penetrated by a well. In accordance with Houghton
662 Mifflin (2016), upscaling can be defined as "*The raise to an higher level; an upgrade*". Free interpretation
663 learn, multiple directions of upscaling are applicable. The single test problem is exposed to three types of
664 ASR-system upscaling; (1) upscaling in dry season daily pumping time, (2) upscaling the borehole cross-
665 sectional dimension and (3) upscaling by ASR-system cleaning.

666

667 The hypothetical northern Ghana test problem will be outlined first. It concerns both the natural (Section
668 3.1) as well as the model-based description (Section 3.2). As a follow-up, the unimproved (base) model
669 performance is described (Section 3.3). The section can be used as reference material for the different types
670 of system upscaling (Section 3.4). The chapter concludes with a discussion on the (ASR-system upscaling)
671 results obtained (Section 3.5).

672 3.1. Base model definition

673 The test problem contains a fictive, simplistic ASR-system in northern Ghana. Year-round well performance
674 due to water infiltration and extraction is modelled. Applied conditions are based on local fieldwork mea-
675 surements. Model results do not apply to a single research location (depicted in Figure 2.1). Obtained results
676 should only be interpreted as indicative (upscale) options in northern Ghana ASR-system application.

677 3.1.1. Soil scenarios

678 Interaction between the ASR-system and the upper 50 m of subsurface is simulated. Model top is bounded
679 by a 3m-thick poor permeable soil layer. Well penetration occurs in the underlying 47m-thick aquifer. With
680 an elevation of -6 m the initial groundwater table (GWT) is positioned just under the aquifer top (uncon-
681 fined). The aquifer is homogeneous and horizontally isotropic, while a vertical anisotropy of 1/4 (-) is as-
682 sumed. The bandwidth of transmissivity and storativity values (derivatives from fieldwork data analysis
683 (Chapter 2)), is used for the definition of five aquifer scenarios. An overview of the applied scenarios can be
684 found in Figure 3.1). These conditions are the base for the simulation of unsteady state flow in the radial
685 and vertical direction.

686 3.1.2. Well dimensions & pump placement

687 Base model design (not subjected to upscaling) accommodates a single well with a radius of 0.0635 m (2.5
688 inch). Water displacement between well and aquifer is possible through a partially penetrating screen. Well
689 skin perforation are present from 20 to 47m below model top. It is assumed the, in total 27 m, screen is clean.
690 Due to the tiny nature of wall perforations (and constructional soil improvement around the borehole) a

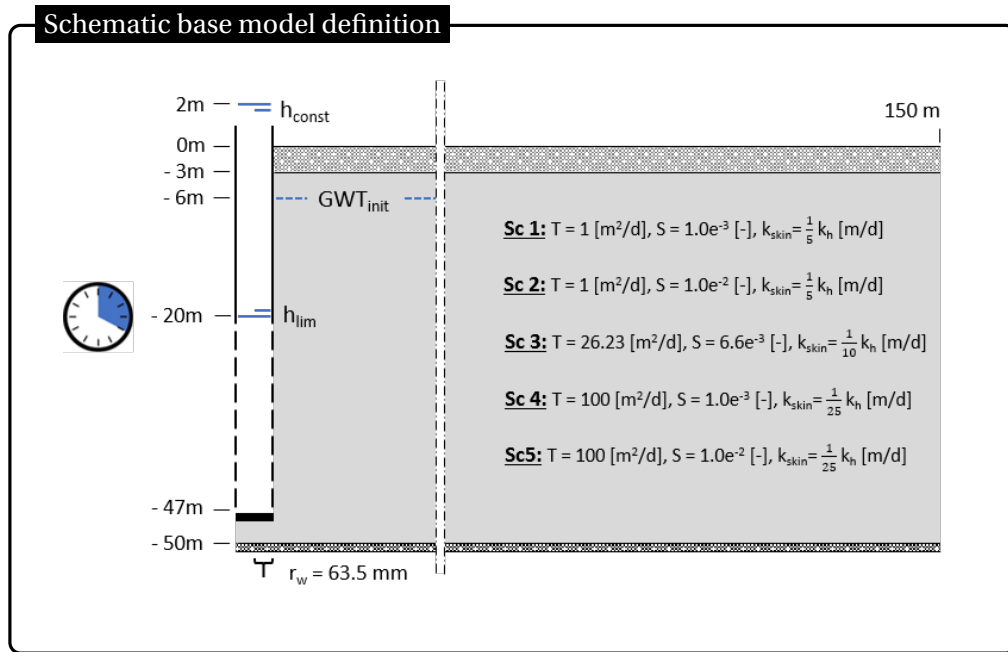


Figure 3.1: Schematic base model definition

well skin resistance is taken into account. More information on skin resistance is included in Section 3.2. Dry season groundwater withdrawal is possible through the installation of a pump. The model contains a pump at an elevation of -30 m. A drop in GWT is preferable limited to an elevation of -20 m (14 m drawdown relative to initial conditions). In this way the occurrence of well screen dry-out and pump malfunctioning is prevented.

3.1.3. Time frame

ASR-systems can theoretically add value to groundwater availability constantly. Seasonal system behaviour is simulated by a year-round (long term) temporal model resolution. For a duration of four months, starting on June 1st, gravity based infiltration simulates wet season flooding. A constant (122 days) 2 m inundation level (on top of well) is assumed (Figure 3.1). In the subsequent eight months of dry season no flooding or rainfall is accounted. Dry season water withdrawal takes place by four hours of pumping daily (243 days). Intermediate day time offers time-space for GWT recovery.

Applied conditions serve research purposes. Assumptions made, are not by definition realistic. Actual wet season inundation levels are expected to fluctuate over time. And groundwater withdrawal needs day-specific tuning with respect to agricultural needs. Aspects advisable to take into account in further research.

3.2. MODFLOW model design

For the ASR-system simulation MODFLOW is used. A finite difference model, written by US Geological Survey (USGS). It is stated to be the worldwide most convenient (open source) computer program for the simulation of groundwater flow. MODFLOW has a modular structure. A variety of aquifer features can be simulated by the introduction of (free available) packages. In this research, input files (needed by MODFLOW) are created by the use of Python and the FloPy package ((Harbaugh, 2005; Niswonger et al., 2011)).

Unmodified versions of MODFLOW uses Cartesian geometry. Simulations are standard performed in a (single or multi layer) rectangular grid model. These models can simulate the three-dimensional ASR-system performance accurately. However, it requires disadvantageous large computational power. In this particular case the single well simulation is approached axially symmetric. As prescribed by Langevin (2008), the rectangular model structure is radially scaled by the adjustment of several input parameter. Results are advantageous on model precision and run times. A detailed description of this radial scaled MODFLOW model can be found in Appendix D.

721
722 Due to the applied MODFLOW radial scaling the defined grid consist of a single row (1 m width) and mul-
723 tiple columns. The well is located in the first cell (column 0, row 0). Column width increases (grouped)
724 stepwise, based on the (radial) distance between the specific column and the well. By the use of the cell
725 sizes 0.0635 m (40x), 0.1 m (25x), 0.5 m (20x), 1.0 m (25x), 2.0 m (30x) and 5.0 m (10x) a total (radial) length
726 of 150 m is simulated. An extent assumed to be sufficient for the purposes of this research (Appendix E.1).
727 The vertical (third) dimension is added to the model by a total of 50 layers (thickness of 1.0 m each).

728
729 Model timespan (one year) is devised into an abundance of logarithmic time frames. Higher temporal res-
730 olutions is added to the moments at which fluctuation in head are expected. The design of four months
731 infiltration contains a single logarithmic time frame of 200 steps. Every single day in dry season (243 days)
732 contains a 4 hour logarithmic time frame for pumping (8 steps) and a subsequent 20 hour logarithmic time
733 frame for recovery (10 steps). This puts the year-round total number of time steps on 4574.

734 3.2.1. MODFLOW-NWT

735 Due to initial conditions and expected strong temporal variations in GWT cells may fall dry and become
736 wet again over time. Model simulation is therefore performed through the use of MODFLOW-NWT: The
737 Newton-Raphson formulation for the (more convenient) MODFLOW-2005 program. As stated by Niswonger
738 et al. (2011), MODFLOW-NWT is intended for solving problems involving drying and re-wetting non-linearities
739 of the unconfined groundwater-flow equation. MODFLOW-NWT requirs a combined use with the Upstream
740 Weighting (UPW) package for calculation conductances between cells (instead of the BCF, LPF or HUF
741 package applicable with MODFLOW-2005). The UPW package keeps dry cells active, while water outflow
742 of the cell is not allowed. Moreover, if applicable inflow to a dry cell automatically flows further down to
743 the adjacent (non-dry) cell in the layer below (Niswonger et al., 2011). In correspondence with the use of
744 MODFLOW-NWT the (own) NWT solver is used for model simulation (instead of the convenient PCG solver).

745 3.2.2. MODFLOW - GHB

746 Wet season infiltration is included by the use of the General Head Boundary (GHB) package. For as long
747 as the wet season (stress periods), GHB cells are specified through stress period data. General Head
748 Boundaries are added to the well cells (row 0, column 0) in the predefined layers of penetration (layer 20-
749 46). The GHB stress period data requires an additional definition of stage and cond (conductance)
750 (Harbaugh et al., 2000). The stage equals the constant flood inundation level ($h^* = 2$ m). For the purposes of
751 this research conductances are aligned with the CWC (Cell-to-Well hydraulic conductance). More informa-
752 tion on the CWC can be found in Section 3.2.3.

753 3.2.3. MODFLOW - MNW2

754 The ASR-system of interest contains a well which is partially penetrating the aquifer. In simulation the
755 aquifer consisting of multiple model layers. A set-up causing the convenient Well package to be insuffi-
756 cient. For a solid simulation the more extended Multi-Node-Well2 (MNW2) package is used. MNW2 houses
757 several additional well options (e.g. bounded drawdown, addition of well skin resistances and pump re-
758 lated adjustments in discharge). Thence, definition of an abundant list of parameters is required (within
759 node data and stress period data)(Konikow et al., 2009).

760 Many parameters are default correct, some however need specification. The well penetration interval (screen)
761 is recorded by the definition of ztop and zbotm. MNW2 assigns the well screen to model nodes (well cells in
762 the corresponding layers). In-well GWT preferable does not drop below the elevation of -20 m. Hlim defini-
763 tion guarantees this desire. The flag of qlimit is 1 activates the definition of Hlim. Moments (stress-periods)
764 of pump operation are set by ITMP is 1, all other moments (stress-periods) ITMP is set 0. Furthermore,
765 MNW2 requires the input of a desired discharge (qdes and specification of Cell-to-Well hydraulic con-
766 ductance (CWC), topics highlighted below.

768 769 Desired discharge (qdes)

770 Based on a predefined desired discharge the MNW2 determines a (model) layer dependent discharge itera-

tively. As long as the head bound (H_{lim}) is not restrictive, summed layer discharges equal (approximately) the desired discharge. Desired discharges are based on the analytical Thiem method (Kruseman and de Ridder, 2000); confined steady state flow equation 3.1:

$$Q_{Thiem} = \frac{2\pi K D (s_{well} - s_2)}{\ln(r_2/r_{well})} \quad (3.1)$$

where Q_{Thiem} (m^3/d) is the confined steady state well discharge, K (m/d) is the aquifer hydraulic conductivity, D (m) is aquifer height, s_{well} (m) the in-well drawdown, s_2 (m) is the drawdown at a known second location, r_2 (m) is the distance between the second location and the well and r_{well} (m) equals the well radius.

In this particular case thickness D is interpreted as being the well screen height. And the in-well drawdown is set in correspondence with the desired limit in GWT; s_{well} equals 14 m. Due to different horizontal hydraulic conductivities K , obtained desired discharges are scenario dependent. Note, upscaling by borehole cleaning (Section 3.4.3) will result in a variation of desired discharges due to the change in screen height (D).

`FloPy` is used for reading MODFLOW binary output files. In other words, the actual simulated discharges (and recharges) are obtained by reading the `binaryfile.CellBudgetFile`.

Cell-to-Well hydraulic conductance (CWC)

Due to MNW2 application the occurrence of a difference between the head in the well and the head in the model (well)cell is inevitable. Multiple model elements contribute to a difference in head. Total head difference is dependent on the expression of Cell-to-Well hydraulic conductance (CWC), depicted in Equation 3.2 (Konikow et al., 2009).

$$CWC_n = [A + B + CQ_n^{(P-1)}]^{-1} \quad (3.2)$$

Where CWC_n (m^2/d) is the $n^t h$ Cell-to-Well hydraulic conductance, A is the linear aquifer-loss coefficient resulting from the well having a smaller radius than the horizontal dimensions of the cell in which it is located, B is the linear well-loss coefficient accounting for head losses that occur adjacent to and within the borehole and well screen (skin effects) and $CQ_n^{(P)}$ accounts for non-linear head losses due to turbulent flow near the well (Konikow et al., 2009).

$$A = \frac{\ln(r_o/r_w)}{2\pi b \sqrt{K_x K_y}} \quad (3.3)$$

$$r_o = 0.14 \sqrt{\Delta x^2 + \Delta y^2} \quad (3.4)$$

$$B = \frac{SKIN}{2\pi b \sqrt{K_x K_y}} \quad (3.5)$$

$$SKIN = \left(\frac{b K_h}{b_w K_{SKIN}} - 1 \right) \ln \left(\frac{r_{skin}}{r_w} \right) \quad (3.6)$$

Where r_o (m) is the effective external radius of a rectangular finite-difference cell for isotropic porous media, r_w (m) is the well radius, r_{skin} (m) is the well radius plus the thickness of improved soil around the well, b (m) is the saturated thickness of the cell(layer), b_w (m) is the saturated (active) length of the borehole in the cell(layer) (in the purposes of this research equal to b (1m)), K_h (m/d) is the horizontal (non-radial scaled) hydraulic conductivity (equals K_x and K_y due to the assumption of horizontal anisotropy), Δx (m) is the grid spacing in the x-(column-)direction and Δy (m) is the grid spacing in the y-(row-)direction (Konikow et al., 2009).

As stated, the aquifer-loss coefficient (A) accounts for the difference in dimensions between the well (cross-section) and the (well)cell. Perfectly understandable in the case of an unmodified (Cartesian geometry)

rectangular grid MODFLOW model. Simulation in this research is however performed in a radial scaled model, according to the principles as stated by Langevin (2008). Well cell width perfectly aligns the radius of the well. Therefore it is assumed the A term is negligible. In addition, laminar (non-turbulent) flow is expected near the well (ignorance of $CQ_n^{(P)}$ term). Further research should substantiate or refute these assumptions.

What left, is a CWC dependent on the well-loss coefficient B. In the SKIN term (part of coefficient B) the parameters r_{skin} and K_{skin} need additional information. r_{skin} , equals r_w plus a unknown radius of improved soil around the well. As stated by (Bot, 2016), for proper installation a minimum length of 0,125 m (measured from well radius) is required. This length is therefore implemented in research. K_{skin} accounts for both; a higher resistance due to the well screen tiny perforations and at the same time a reduction in resistance due to the improved soil around the well. Further research should be applied to get deeper understanding of the exact parameter magnitude. K_{skin} is typically expected to be lower than the K_h (Konikow et al., 2009). Dependent on the scenarios three different values are assumed in research, as depicted in Figure 3.1. Resulting CWC values used in the different base models are; 0.031 m²/d (sc1&2), 0.358 m²/d (sc3) and 0.512 m²/d (sc4&5). Note, upscaling the borehole cross-sectional dimension (Section 3.4.2) will result in variation of CWC values due to the change in r_w and thus r_{skin} .

3.3. Base model performance

On the base of the different soil scenarios (Figure 3.1) the performances of five base models are taken into account. In terms of time (within the model year) a division can be made between the wet and dry season. Wet season ASR-system behaviour is characterized by the inflow of water. Analysis is pointed at the volumes recharged and the impact of these volumes on GWT. In the subsequent eight months of drought, the system works in reverse. In this time of year, maximum pump operation and the accompanied impact on GWT is of key interest. As supplement the mutual relation between in- and outflow is considered. This is done by the introduction of the recovery ratio (Equation 4.2). Through this term the system impact on nature is discussed.

$$R\% = \frac{V_{out,tot}}{V_{in,tot}} \quad (3.7)$$

Where R% is the year-round recovery ratio (-), $V_{in,tot}$ (m³) is the wet season total volume recharged and $V_{out,tot}$ (m³) is the dry season total volume discharged. R% values smaller than 1 (-) suggests a sustainable system interaction with nature.

Wet season behaviour

Recharge due to flooding has a slightly above average start. After a few days the inflow reaches an equilibrium. From this moment onwards water accumulates in the aquifer at an approximately constant rate. This course takes place in all scenarios. Order of volume do differ and increases in correspondence with the scenarios. The example scenario 3 cross-sectional contour (Figure 3.2), visualizes the system behaviour at the begin (day 5) and absolute end of wet season (day 122).

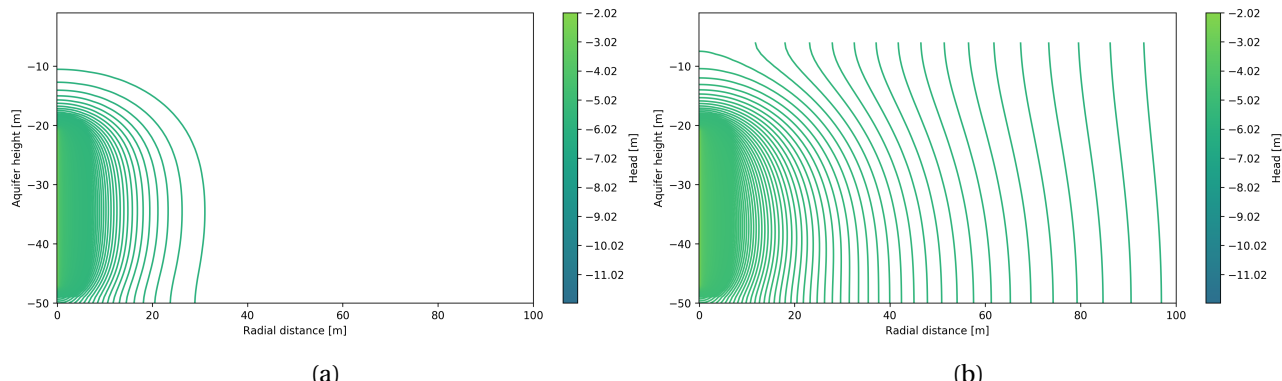


Figure 3.2: Example scenario 3 - base model - Cross-sectional contour head after (a) five days and (b) 122 days of infiltration

Impacts on the groundwater table are also dominant at simulation front. At close well range relative large increases in groundwater heads are encountered in the first days. These heads do not reach the predefined flood level, not even at the end of wet season. A development justifiable by the implemented well skin resistances. Figure 3.3 illustrates the precise impact of flood based ASR-system infiltration on groundwater heads in several representative (model) layers of soil scenario 3. Worth mentioning, groundwater level increase is already limited at a relative short radial distance (steep groundwater cone). Even after 122 days of infiltration the head increase at a radial distances of about 60-80 m is not quite substantial, unregarded the scenario.

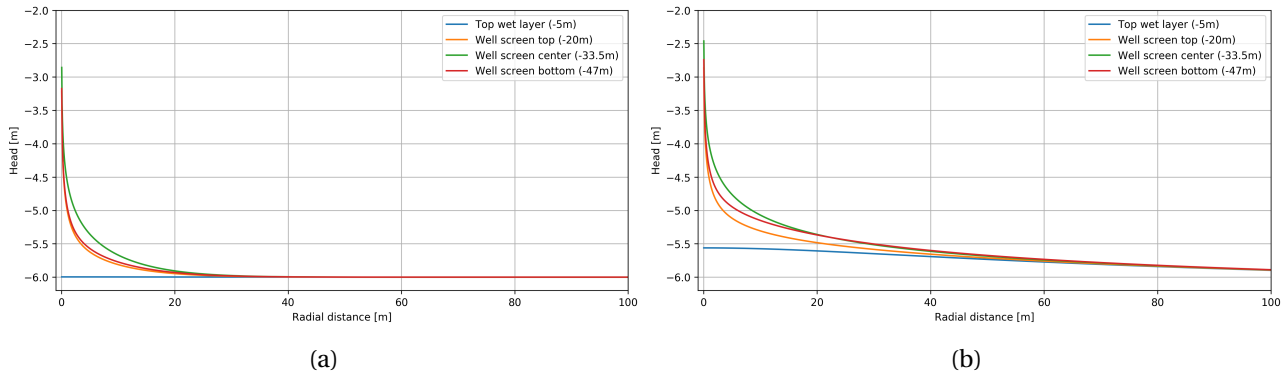


Figure 3.3: Example scenario 3 - base model - Head in representative layers after (a) five days and (b) 122 days of infiltration

Scenario dependent results on total wet season volume inflow are included in Table 3.1. Differences between scenario 1 and 2 as well as scenario 4 and 5 are small. These scenarios only differ from each other in applied storativity (S). Bandwidth defined variance in storativity appears to have only a limited influence on the inflow of water. Most definitely during the application of higher transmisivities these differences in storativity are negligible.

Table 3.1: Base model scenarios - Wet season recharge (m³)

	Sc 1	Sc 2	Sc 3	Sc 4	Sc 5
Volume in (m ³)	306.83	309.28	5373.03	10483.17	10483.86

857 Dry season behaviour

Model well discharge originates by a predefined desired discharge (Q_{thiem}). In all base model scenarios the desired discharge is not reached (visualized for scenario 3 in Figure 3.4). The development can be attributed to the specification of a bound in drawdown. Discharge rates are limited by the head bound (-20 m). At pump operation start, the drop in head reached the bound almost instantaneously. In the subsequent hours of pumping (within day) the head bound keeps decisive. The simulation compensates by a decrease in discharge over time. In practice pumping takes place at a more or less constant rate. It suggests model outcome overestimates the discharged volumes slightly. Mutual comparison between the days shows a difference in total discharge between the first and all other days of pumping. The first day of pumping generates somewhat higher volumes. In the subsequent days discharge is by approximation equal.

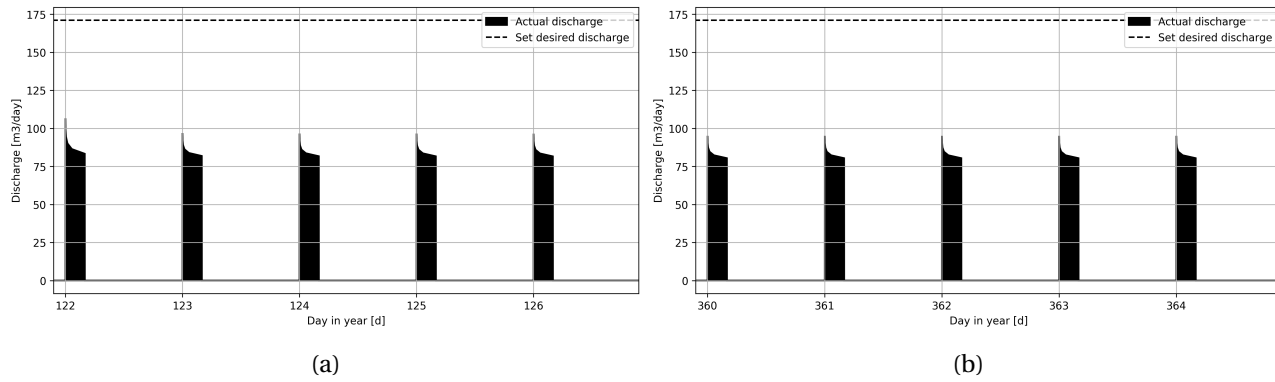


Figure 3.4: Example scenario 3 - base model - Discharge performance for (a) the first five days and (b) the last five days of dry season

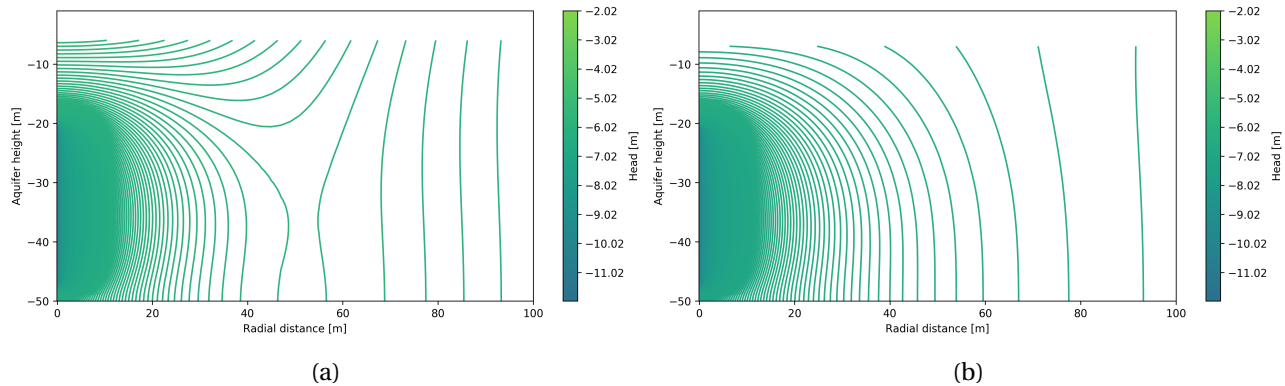


Figure 3.5: Example scenario 3 - base model - Cross-sectional contour head after four hours of pumping on (a) the first day (day 123) and (b) the last day (day 365) of dry season

The impact of well discharge is visualized for scenario 3 in both, a cross sectional contour plot (Figure 3.5) and a figure of groundwater heads in representative model layers over radial distance (Figure 3.6). After the first day of pumping the transition from wet (recharge) to dry season (discharge) is still of influence. Most definitely in the higher model layers (close to surface) the increased heads (due to wet season recharge) remain active for some time. Towards the end of dry season this impact is no longer present. Over the entire dry season the predefined bound in head (-20 m) is not reflected in the visualized heads. This can be justified by the presence of a well skin resistance. Bounded drawdown is only reached within the well. As a result, the consequences on nature (groundwater) are less distinct.

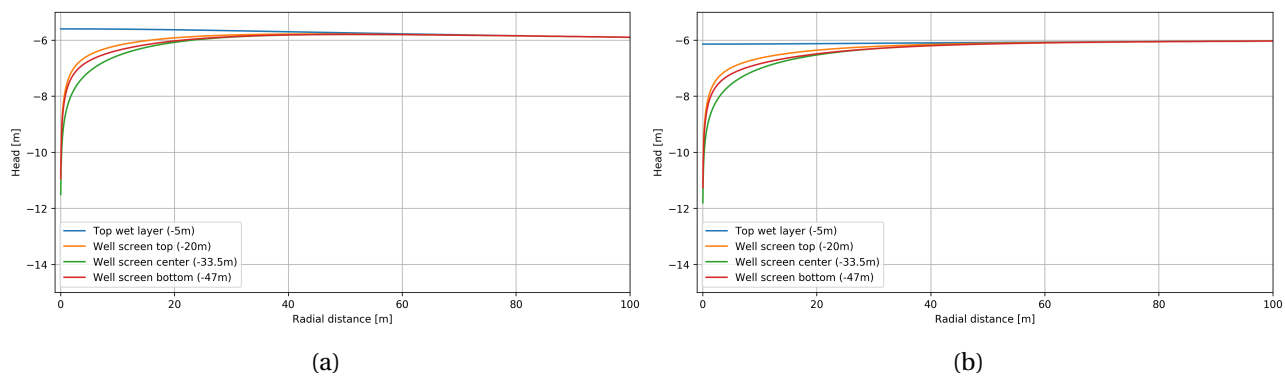


Figure 3.6: Example scenario 3 - base model - Head in representative layers after four hours of pumping on (a) the first day (day 123) and (b) the last day (day 365) of dry season

Unlike the outcomes in recharge (wet season) the soil scenarios show distinctive results in total volumes discharged. It can be suggested the variation in storativity is more pronounced for discharge (after a certain

878 time of recharge). However the differences in total volumes withdrawn are still in the same order of size for
 879 the scenarios 1 and 2 as well as the scenarios 4 and 5.

Table 3.2: Base model scenarios - Dry season discharge (m³)

	Sc 1	Sc 2	Sc 3	Sc 4	Sc 5
Volume out (m ³)	199.25	218.13	3310.17	6161.15	6232.08

880 **Year-round recovery ratio $R\%$**

881 Recovery ratios are for all base models scenarios in the same order of size (Table 3.3. Mutual differences
 882 can potentially be attributed to the varying behaviour of storativity (in combination with different trans-
 883 missivity values). The ratios are however also affected by the (scenario dependent) well skin resistances. As
 884 a consequence, no distinctive conclusions on scenario comparison can be drawn.
 885

Table 3.3: Base model scenarios - Recovery ratio $R\%$

	Sc 1	Sc 2	Sc 3	Sc 4	Sc 5
$R\% (-)$	0.649	0.705	0.616	0.588	0.594

886 In all base scenarios the recovery ratio stays well below 1. In eight months of daily (4 hours) pump operation
 887 it is not possible to fully recover the volumes infiltrated due to four months of constant inundation (2 meter)
 888 on top of a well. Under the defined conditions of system composition and use, the found recovery ratios
 889 suggest a sustainable system impact on nature.

890 **3.4. Impact of ASR-system upscaling**

891 This section elaborates on the impact of ASR-system upscaling. One-by-one the different types of upscaling
 892 (pumping time, dimension and cleaning) are taken into account. Performances are tested and compared to
 893 the base model by the known parameters: total recharge, total discharge and the recovery ratio ($R\%$).

894 **3.4.1. Upscaling daily pumping time**

895 ASR-system upscaling by an extent in (dry season) daily pump operation is easily applicable. Except from
 896 additional fuel and possibly temporal storage requirements (poly tanks), no further modifications are re-
 897 quired. Base model pump operation is set to be four hours daily (243 days, dry season). This study is pointed
 898 at a maximum time-scope of 12 hours daily. A four-steps distinction is made in upscaling (6h, 8h, 10h and
 899 12h), as mentioned in Figure 3.7.

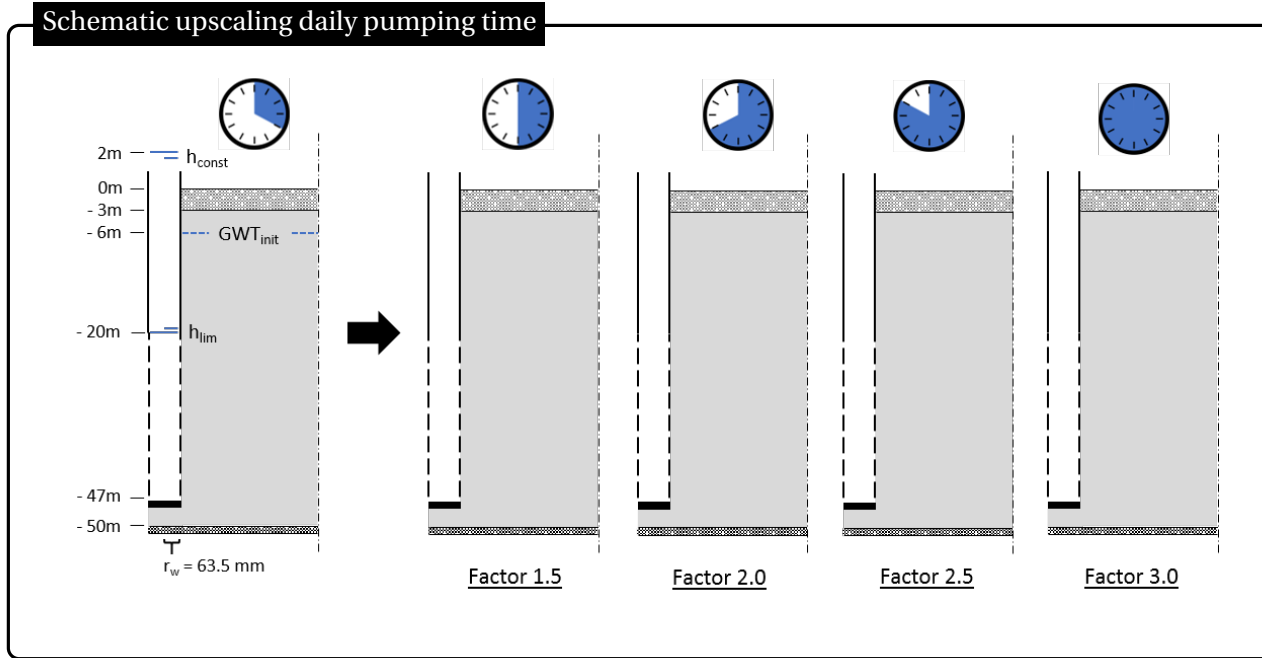


Figure 3.7: Schematic upscaling daily pumping time

Deviations in wet season recharge are not applicable to upscaling by pump duration. Pump operation is in effect during dry season only. As visible in Figure 3.8, discharged volumes are most definitely affected by daily pump duration. An approximately linear relation is encountered in all scenarios. The relation can be justified by the daily discharge performance as depicted for the base model in Figure 3.11. After four hours of pumping a more or less equilibrium discharge rate is encountered. Expansion by adding active hours of pumping daily will not make any significant change in discharge rates. Moreover, the discharge pattern is repeated daily. Mutual differences between the days of pump operation are absent.

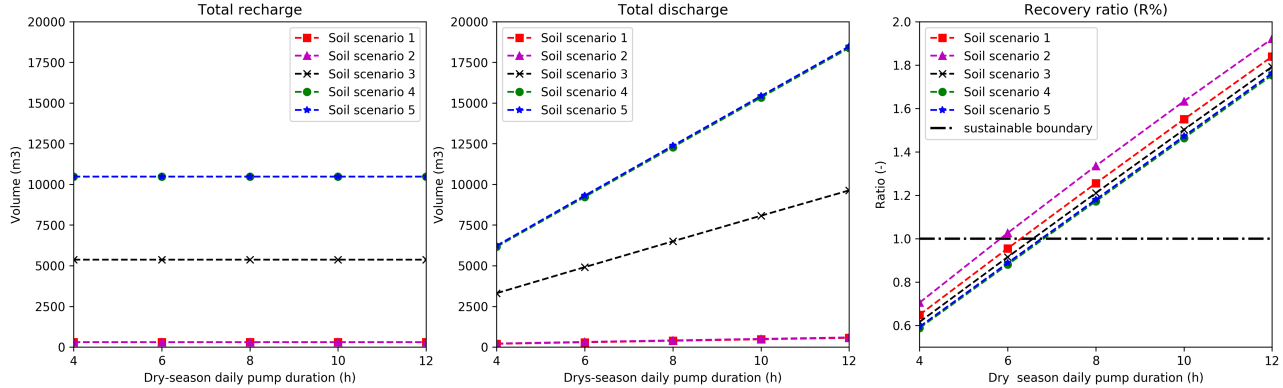


Figure 3.8: Results of yearly total volumes (in, out, ratio) by upscaling daily pumping time

Discharge volumes obtained by upscaling daily pump duration for the total eight months of dry season exceed the four months (gravity based) recharge volumes. under the applied conditions of maximum upscaling (12u daily; total pumping time equals duration wet season) recovery ratio close to two are reached. By scaled-up pump duration the potential negative effects on nature (unsustainable system use) should be considered.

3.4.2. Upscaling borehole cross-sectional dimension

ASR-system upscaling by an increase in borehole dimension is a rigorous approach. An adjustment that can not be applied on existing systems. If the appropriate equipment is present (e.g. drilling machinery), new construction of enlarged ASR-systems can be applied. To take implementation in consideration it is of extra interest to gain knowledge on potential effects. Simulation is executed by stepwise (4 steps) doubling the

918 original borehole radius (Figure 3.9).

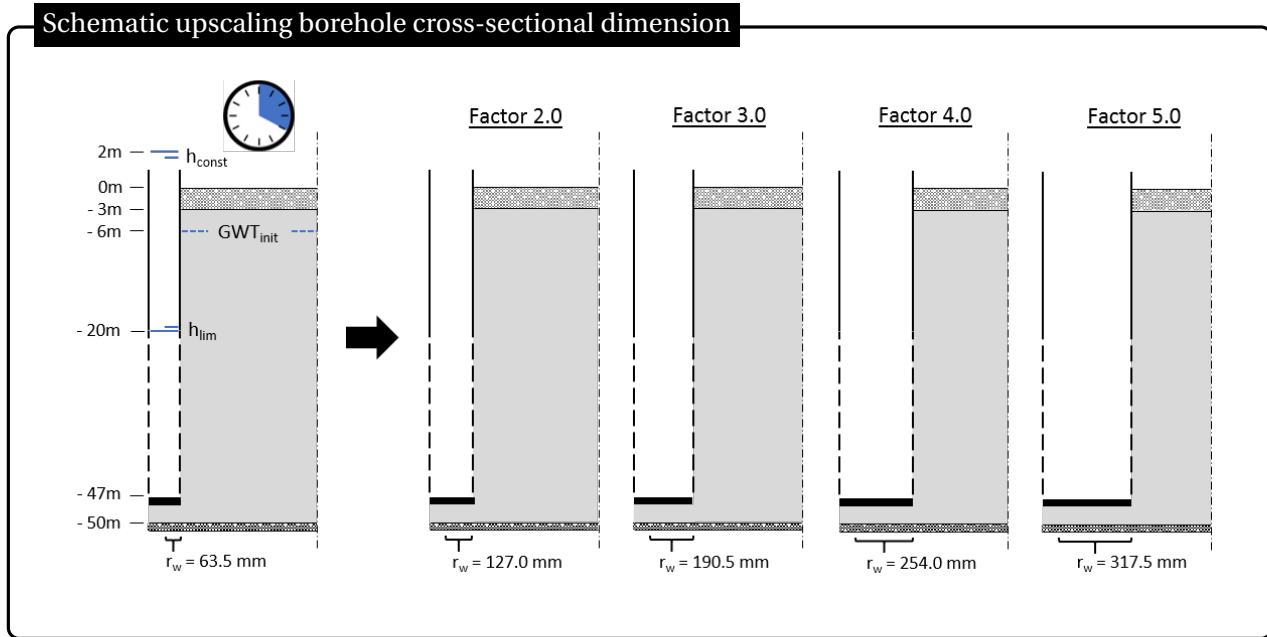


Figure 3.9: Schematic upscaling borehole cross-sectional dimension

919 Magnification of the borehole diameter is beneficial for both groundwater recharge and discharge. Results
920 show a non-linear relation between total season in- and outflow. Well-size upscaling has an increasingly
921 less positive effect on the total volumes obtained. A further magnification has its limits.

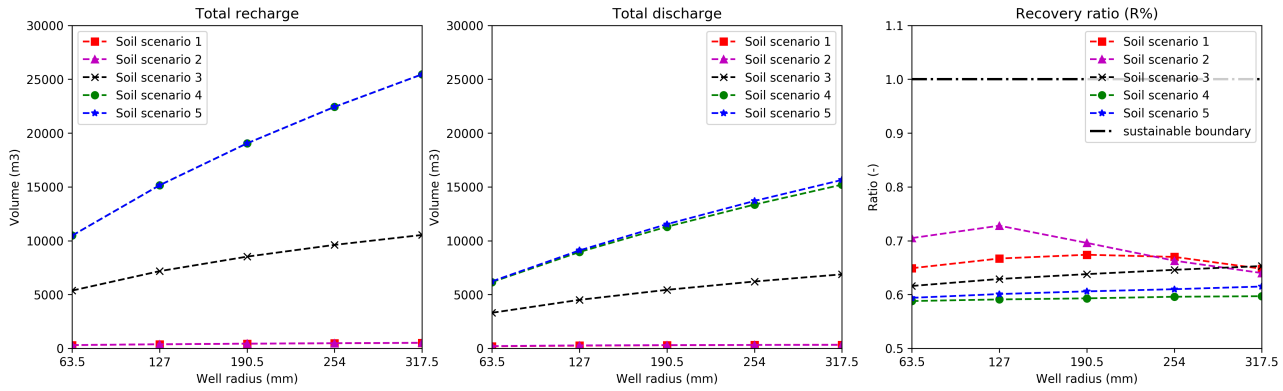


Figure 3.10: Results of yearly total volumes (in, out, ratio) by upscaling well diameter

922 Unforeseen performances are obtained in the recovery ratios of scaled-up simulation in scenarios 1 and
923 2. After solid ratio increase, further system upscaling suddenly causes a decline in recovery performance.
924 Closer inspection exposed the cause. Recharge volumes continue to follow an upward trend, while total
925 discharge volumes stay at the same level. The predefined desired discharge (Q_{thiem}) are reached in these
926 scaled-up scenarios. Impact becomes transparent by the comparison of discharge performances of the
927 (soil) scenario 1 base model versus the model simulation with a (5 times) increased well radius (Figure 3.11
928 & 3.12). In these scenarios further well magnification results in a "release" of the head bound. Demands are
929 met, while GWT is still in range.

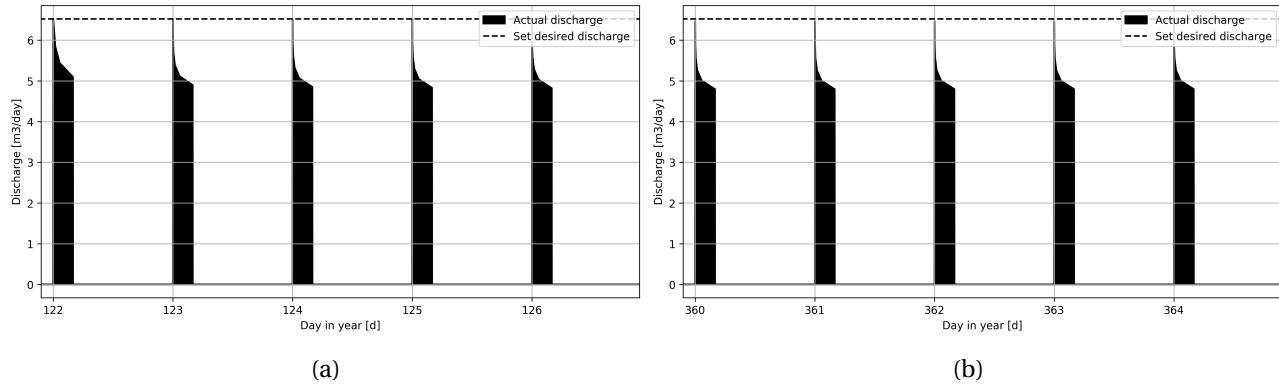


Figure 3.11: Example scenario 1 - base model - Discharge performance for (a) the first five days and (b) the last five days of dry season

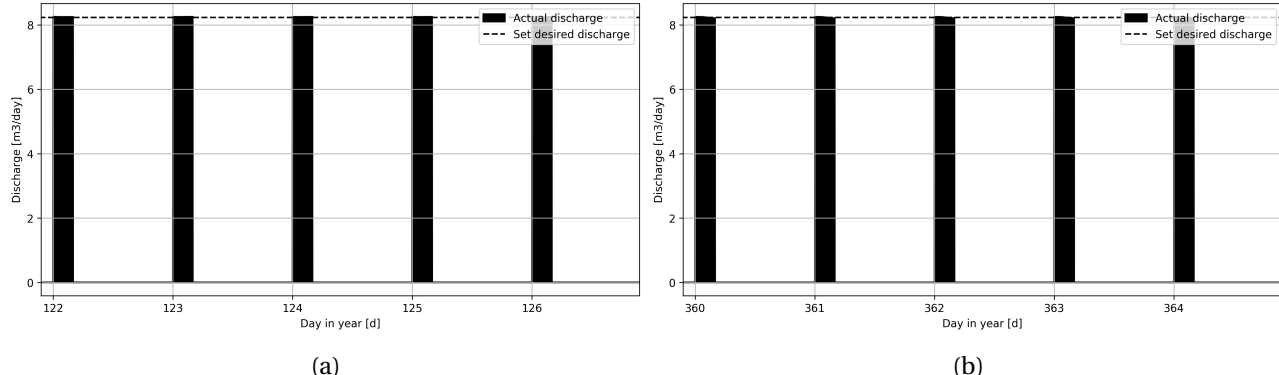


Figure 3.12: Example scenario 1 - 5x base model well diameter - Discharge performance for (a) the first five days and (b) the last five days of dry season

930 3.4.3. Upscaling by system cleaning

931 Unlike the previous forms of upscaling, upscaling by system cleaning does not use the base model sce-
 932 narios as reference start. All prior simulations are based on the assumption of a clean system. Fieldwork
 933 inspection showed clean systems are absent in nature. Debris accumulates at the borehole bottom. Direct
 934 consequence is a decrease in well penetration length. By the approach of a stepwise increase (5 steps) in
 935 borehole depth, the cleaning of a clogged borehole is simulated (3.13).

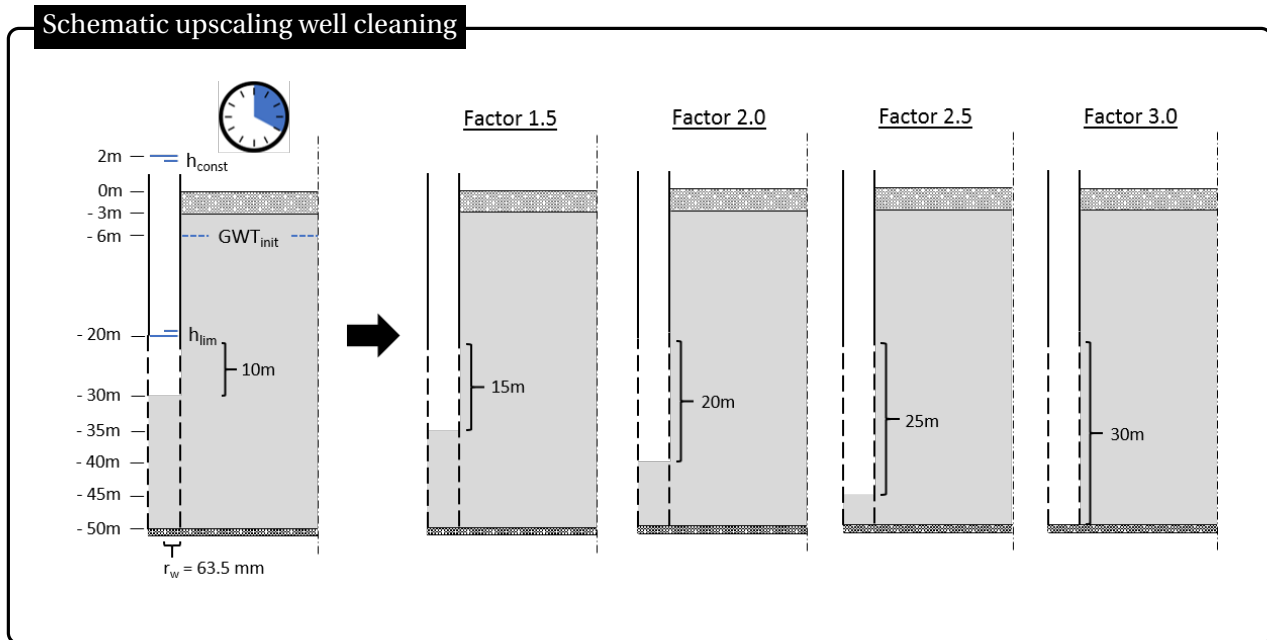


Figure 3.13: Schematic upscaling penetration length due to well cleaning

936 System cleaning has a positive impact on both the wet season recharge and dry season discharge. Total
 937 volumes infiltrated and withdrawn are approximately linear dependent on the (clean) well screen length.
 938 Effects of non-uniform flow (partially aguifer penetration) are not of significance for the simulation condi-
 939 tions applied in this study.

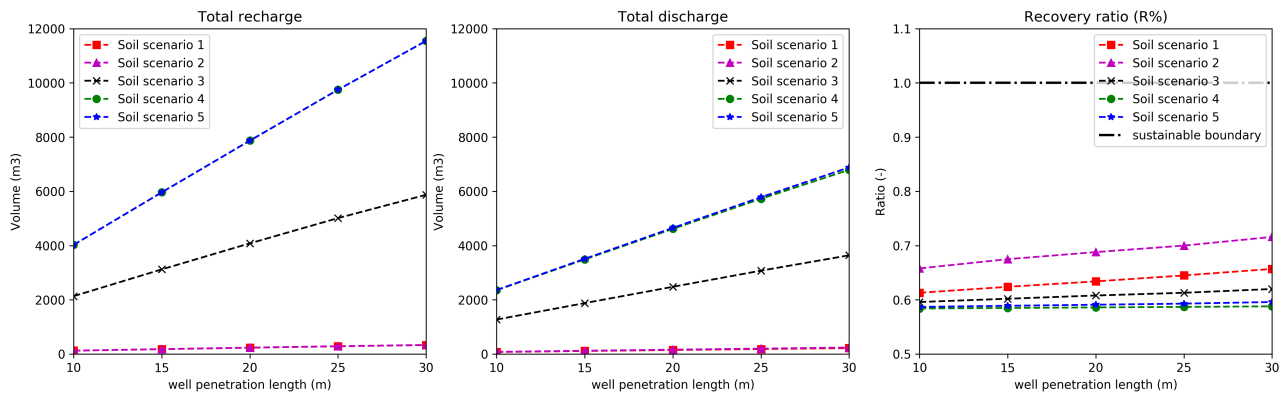


Figure 3.14: Results of yearly total volumes (in, out, ratio) by upscaling the penetration length due to well cleaning

940 System cleaning ensures a increase in recovery ratios (for all soil scenarios). In an absolute sense the total
 941 volumes discharged are slightly more affected by cleaning compared to recharged volumes. In general re-
 942 covery ratio increase is not significant. Moreover the ratios stay within the range of sustainable use. Deepen-
 943 ing the borehole (to its original length) improves system operation. Cleaning of (partially) clogged systems
 944 is advisable.

945 3.5. Results & Conclusions

946 brief conclusion on model simulation ASR-system performances are stated below:

- 947 • Base model scenarios

948 In eight months of daily (4 hours) pump operation it is not possible to fully recover the volumes in-
 949 filtrated due to four months of constant inundation (2 meter) on top of a well. Under the defined
 950 conditions of system composition and use, recovery ratios suggest a sustainable system impact on
 951 nature.

952 • Upscaling daily pumping time

953 Discharge volumes obtained by upscaling daily pump duration for the total eight months of dry sea-
954 son exceed the four months (gravity based) recharge volumes. Potential negative effects on nature
955 (unsustainable system use) should be considered.

956 • Upscaling borehole cross-sectional dimension

957 Magnification of the borehole diameter is beneficial for both groundwater recharge and discharge.
958 Due to the non-linear relation, there is an upper limit in performance by further well enlargement.

959 • Upscaling by system cleaning

960 Deepening the borehole (to its original length) improves system operation. Cleaning of (partially)
961 clogged systems is advisable.

962 Further research can be pointed at a variety of topics:

963 • MNW2 skin resistance

964 Little is known about the exact order of skin resistances (well conductance). A topic that can fill an
965 entire individual research. It is for example unknown how to interpret the CWC in relation to a radial
966 scaled MODFLOW model. Moreover, research can also be performed by the inclusion of a labora-
967 tory or fieldwork set-up. When fieldwork is done, a combination with infiltration bed resistances is
968 possible.

969 • additional options in ASR-system research

970 Simulation are done by a constant flood bound of 2 m for four months. It would be interesting to
971 investigate the ASR-system behaviour under the conditions of temporal flooding (rain-based inunda-
972 tion).

973 • focus from water to crop

974 crop required water withdrawel (potentially in combination with temporal storage in poly tank(s)).

975 • sensitivity analysis

976 A control sample should be applied on the model assumptions made. One can think of a sensitiviy
977 analysis regarding variation in constant head due to flooding, initial groundwater conditions, well
978 skin resistances and/or set drawdown limitations.

4

979

980

(Financial) yield - upscaling

981 Performances of Aquifer Storage and Recovery systems (ASR-systems) are so far expressed in water volumes.
982 The volumetric results are desirable, but it is hard to get a good picture of it. Simplistic transformations make
983 it possible to express the obtained volumes in (financial) yields. Moreover, the transformation houses the
984 transition from volumes of water to actual sizes of agricultural fields. This part of research offers a glimpse
985 in system (financial) feasibility and potential of system spatial multiplication.

986

987 First, an explanation on applied theories in transition from water volumes to agricultural field-sizes and fi-
988 nancial yields (Section 4.1). Subsequently the previously obtained water volumes are exposed to the trans-
989 formation (Section 4.2). This part of research ends with a conclusive remark on ASR-system yields and
990 possibilities in spatial multiplication (Section 4.3).

991 **4.1. Theory: ASR-system - (financial) yield**

992 **4.1.1. Crops: financial yield**

993 Some crops need more water than others. Some crops thrive better in northern Ghana climate than other.
994 Some crops are financially more beneficial than others. And so, many more elements are decisive in the pro-
995 cess of crop type determination. This research is not about crop type decisions. Keeping northern Ghana
996 applicability in mind a selection of crops is made. The crops (mentioned below) are purely included in the
997 study to gain knowledge on hand-on possibilities in the agricultural use of ASR-systems.

998

999 **Crops of interest**

- 1000 • **Groundnut**

1001 Groundnut is an above average profitable crop grown in Ghana. Production is often the responsibility
1002 of small holder farmers in the North. Almost the complete Ghana groundnut production originates
1003 here (Ghana-made, 2018). Growth season length is dependent on the varieties (sequential or alter-
1004 nately). In general harvesting can take place after a period of 90 to 140 days. It is assumed two con-
1005 secutive growth period fit the (243 days) modelled dry season. For a proper single season production
1006 (rain-fed) crops require a water footprint of about 500 to 700 mm. The latter is adapted as normative
1007 in this research. Crop yields diverge strongly. Good rain-fed crops can produce average yields of 2-3
1008 ton/ha unshelled nuts. By the introduction of irrigation these values even reach 3.5-4.5 ton/ha (FAO,
1009 2018a). For the subsequent parts of research 2016 Ghana average is used. An agricultural yield of
1010 1.25 ton/ha unshelled groundnut is accounted (FAO, 2018b). Financial yields are highly fluctuating
1011 over time. Market forces are dominant in actual returns. The march 2018 Ghana average unshelled
1012 groundnut wholesale price is set at a value ranging from 247.50 to 282.50 GHS for a 82 kg bag (Modern
1013 Ghana, 2018). For the purposes of this research the highest average value is applied and interpreted
1014 as the unshelled groundnut price: 3.445 GHS/kg.

- 1015 • **Other options**

1016 if desirable the same can be done for crops as: Maize, chilli pepper, onion, cucumber, tomatoes,
1017 carrots.

1018 As visible assumptions are abundant in size and quantity. Obtained (financial) yields should solely be interpreted
 1019 as indicative. In other words, "All rights reserved".
 1020

1021 Irrigation efficiency

1022 Dry season agriculture is purely dependent on water supply by irrigation. Different types of irrigation are
 1023 suitable in northern Ghana. One can think of border strip/furrow irrigation; simplistic but inefficient.
 1024 Higher degrees of efficiency can be achieved by the use of sprinkler irrigation. In the particular case of
 1025 ASR-system use, minimum water losses are pursued. High efficiency drip irrigation is applied. Systems are
 1026 standard paired with facilities as poly-tank(s), pipes and drip hoses. Distances between extraction and irri-
 1027 gation are small, resulting in limited losses. However, water losses are present due to pipe connections
 1028 and potential evaporation. All-encompassing a irrigation system efficiency of 0.8 (-) is considered. 80% of
 1029 all water withdrawn is assumed as net usable for crop growth. Note, this efficiency number also accounts
 1030 for the in practice required schedule in irrigation water amounts. Over the growth season required water
 1031 volumes are assumed to be daily equal ??.

1032

1033 Cover area (crop specific)

1034 Water volumes obtained in previous research sections are basic input for the determination of agricultural
 1035 field sizes. Net withdrawn (dry season) total volumes are divided by the crop specific water footprint. The
 1036 areal outcome is halved to correct for the double (consecutive) growth periods in a single dry season.

$$A = \frac{V_{out,tot} * Waterfootprint_{crop}}{2 * \eta_{irrigation}} \quad (4.1)$$

1037 Where, A (m^2) is the agricultural field area, $V_{out,tot}$ (m^3) is the dry season total volume discharged, $\eta_{irrigation}$
 1038 (-) is the irrigation efficiency and Wfp_{crop} is the crop specific water footprint.

1039

1040 The extraction of water leaves marks on nature. Pump operation causes a groundwater cone of depression.
 1041 Close range (and most definitely in-well) drawdown is significant. At an increased radial distance impact
 1042 losses magnitude. For system spatial multiplication it is of interest to define a maximum circular area in-
 1043 which groundwater is affected. The groundwater cone of influence (G) is defined as the area corresponding
 1044 with the maximum radius from well at which the groundwater drawdown is labelled as significant. In this
 1045 study, significance is assumed to be bounded by a drawdown of 1.0 m at any moment in year.

1046

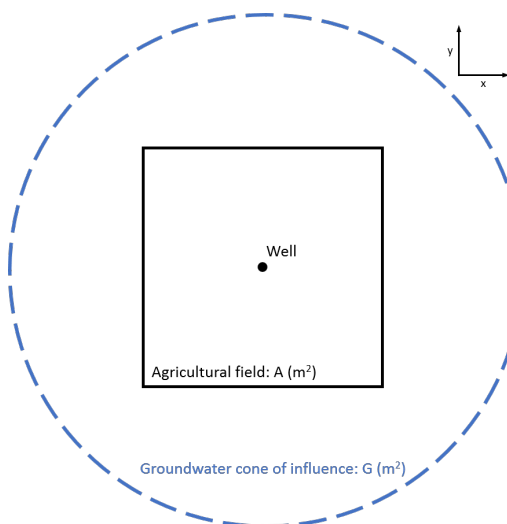


Figure 4.1: Fictive schematic of crop cover area (C%)

1047 The A over G ratio ($C\%$) shows top-view perspectives of spatially concatenated multiplication of agricultural
 1048 fields, as visualized in Figure (4.1). High $C\%$ values (close to one) suggest the implementation of agricultural
 1049 fields is possible at close mutual distance.

1050

$$C\% = \frac{A}{G} \quad (4.2)$$

1051 Where $C\%$ is the crop cover ratio (-), A (m^2) is the crop specific agricultural field size and G (m^2) is the areal
1052 groundwater cone of influence.

1053

1054 Financial yield

1055 Based on the known agricultural field size and (average) agricultural yield (unshelled groundnut 1.25 ton/ha)
1056 yield expression in weight is possible. Moreover weighted crop prices are also known. Because of this the
1057 first known water withdrawal volumes can be expressed in financial returns. From consistence considera-
1058 tions it is chosen to express the financial returns in US dollars. As a last step the The July 7th Bloomberg
1059 financial exchange rate is applied: 0.2081 USD/GHS (Bloomberg, 2018).

1060

1061 4.1.2. Water withdrawal: costs

1062 Profits are accompanied by costs. For this research all Capital Expenditures(CAPEX) are unknown and ig-
1063 nored. The same applies for large parts of the Operating Expenses (OPEX), e.g. farmer wage and fertilizer
1064 costs. The only costs accounted are related to the energy (diesel) consumption. Outcomes therefore purely
1065 focusses on the daily system usability. An impression is generated, whether or not regular ASR-system op-
1066 eration on its own is profitable.

1067

1068 Energy Consumption

1069 First of all the available groundwater has to be lifted to the surface. Depends on the desired discharge, the
1070 lifting action requires a certain magnitude of power (Equation 4.3). Volumes of withdrawal (4 hours daily,
1071 243 days) are known from the model simulation in the previous study section. For water displacement
1072 the difference between pump position and surface level (30m) is retained. An extra lift of 5 m is added to
1073 account for friction losses and the higher position (above surface) of the poly tank(s). A total head lift of 35
1074 m is applied.

$$N_{net} = g * Q * \Delta H \quad (4.3)$$

1075 Where N_{net} (kW) is the net power required, g (m/s^2) is the gravitational acceleration ($9.81 m/s^2$), Q (m^3/s)
1076 is the discharge (total extracted volume of water over the yearly sum of pumping time (in seconds)) and ΔH
1077 (m) is the net head (total lift) required. In this equation it is assumed the water has a density of $1000 kg/m^3$.
1078 In general, the use of power gets accompanied by losses (for example due to friction and turbulence). Ever
1079 single power-related equipment works at a certain level of efficiency. The power generator applied in field-
1080 work (Appendix B) is used before. Because of datedness a generator efficiency of 70% is estimated. The effi-
1081 ciency of the Pedrollo pump is dependent on discharge rate and/or head lift. An overview of the efficiency
1082 curve is present in Appendix F. In this study it is assumed the pump can work on maximum efficiency (58%)
1083 all time. Besides equipment losses, energy get lost due to mutual transmission. An extra efficiency value of
1084 90% is accounted (van de Giesen, 2013). Result is a total (constant) ASR-system efficiency of 36.5 (%).

$$\eta_{total} = \eta_{generator} * \eta_{transmission} * \eta_{pump} \quad (4.4)$$

1085 Where η_{total} (-) is the overall power efficiency, $\eta_{generator}$ (-) is the generator power efficiency, $\eta_{transmission}$
1086 (-) is the transmission power efficiency and η_{pump} (-) is the pump power efficiency.

1087

1088 The combination of total ASR-system efficiency and net required power provides the gross power required.
1089 It is this power what should be delivered by the generator to gain the desired volumes of water at the agri-
1090 cultural fields. Multiplying the gross power required by the total hours of pump operation returns the total
1091 energy consumption (kWh).

$$N_{gross} = \frac{N_{net}}{\eta_{total}} \quad (4.5)$$

Where N_{gross} (kW) is the gross power required, N_{net} (kW) is the net power required and η_{total} (-) is the overall power efficiency.

Energy costs

The Kipor power generator (Appendix B) contains a 15 litre diesel tank. On a full tank the generator can operate for 6.5 hours. A fuel consumption of 2.31 l/h is taken into account. During operation the generator delivers a continuous power capacity of 4.5 kW (TS24, 2018). Ghana diesel price of 5.03 GHS/l (begin of July) is adopted as normative (GlobalPetrolPrices, 2018). To make a good comparison with the agricultural yield, the Bloomberg financial exchange rate (0.2081 USD/GHS) is also applied on the fuel costs (Bloomberg, 2018).

$$Cost_{fuel} = \frac{consumption_{generator} * price_{fuel} * rate_{exchange}}{power_{generator}} \quad (4.6)$$

Where $Cost_{fuel}$ (USD/kWh) is the price of fuel, $consumption_{generator}$ (l/h) is the generator fuel consumption, $price_{fuel}$ (GHS/l) is the fuel price in Ghana, $rate_{exchange}$ (USD/GHS) is the Bloomberg financial currency rate and $power_{generator}$ (kW) is the generator continuous power capacity.

4.2. Data processing (from water volumes to yield)

4.2.1. Crop cover area

In Figure 4.2 an example of outcome. More to follow after first round of feedback graduation committee.

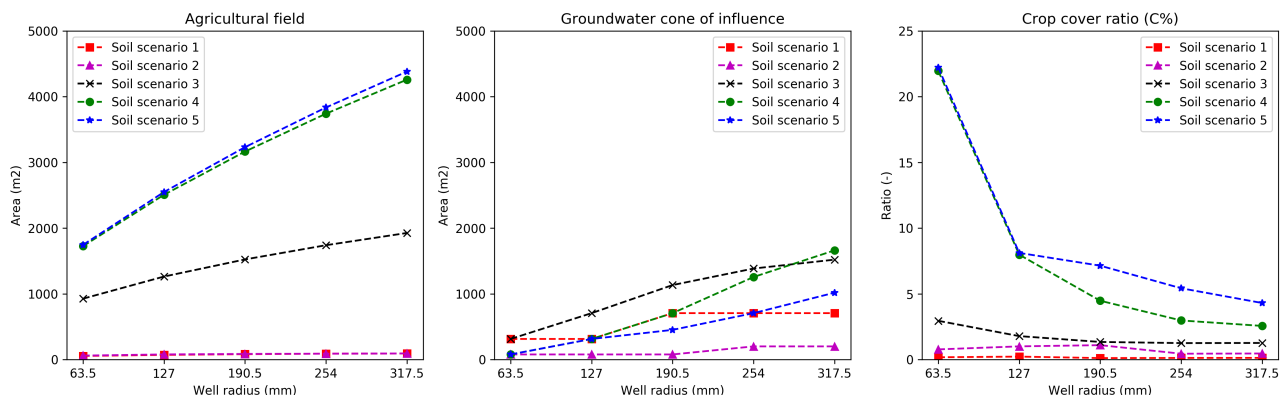


Figure 4.2: Well diameter upscaling dependent results on net agricultural field size, areal groundwater cone of interest and "crop cover ratio"

4.2.2. Financial yield

In Figure 4.3 an example of outcome. More to follow after first round of feedback graduation committee.

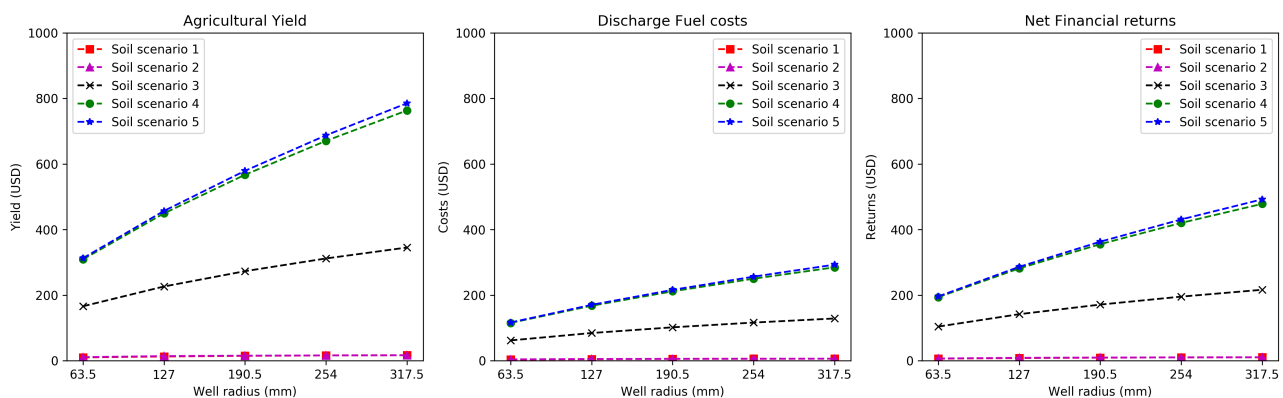


Figure 4.3: Well diameter upscaling dependent results on net agricultural yield, costs and net returns

4.3. Results & conclusions

The preference to receive feedback before conclusions on this part are drawn. Moreover conclusions can
and will be drawn after:

- 1. proper definition for head bound cone of influence
- 2. pump-efficiency construction dependent on discharge
- 3. optionally: the same can also be applied on different types of upscaling (time and cleaning). Added value: for example interesting to see what happens with fuel costs due to time increase
- 4. optionally: agricultural yields dependent on field-size
- 5. optionally: take more OPEX or even CAPEX into account

5

1119

1120

Conclusions

1121 Final conclusion will follow soon

1122

1123 Final conclusions can only be made if the thesis core in terms of content is fixed.

1124 Chapters do contain sub-conclusions / summaries

1125

1126 **Research question**

1127

1128 How can scaled-up Aquifer Storage and Recovery (ASR) systems be beneficial for the availability and sus-
1129 tainable use of groundwater in northern Ghana small-scale agriculture?

1130

6

1131

1132

Discussion & Recommendations

1133 good, bad, advice further research

1134 This part will follow soon

1135 Chapters do contain sub-conclusions / summaries / recommendations

1136

Bibliography

1137

- 1138 Bakker, M. (2013a). Analytical Modeling of Transient Multilayer Flow. In Mishra, P. K. and Kuhlman, K. L.,
1139 editors, *Advances in Hydrogeology*, volume 9781461464, chapter Chapter 5, pages 95–114. Springer Sci-
1140 ence+Business Media, New York, NY.
- 1141 Bakker, M. (2013b). Semi-analytic modeling of transient multi-layer flow with TTim. *Hydrogeology Journal*,
1142 21(4):935–943.
- 1143 Bakker, M. and Anderson, E. I. (2011). Mechanics of Groundwater Flow. In Wilderer, P., editor, *Treatise on*
1144 *Water Science*, pages 115–134. Academic Press, Oxford, United Kingdom, vol. 2 edition.
- 1145 Bloomberg (2018). GHS-USD Cross rate currency.
- 1146 Bot, B. (2016). *Grondwaterzakboekje Gwz2016*. Bot Raadgevend Ingenieur, Rotterdam.
- 1147 FAO (2018a). Crop information - Groundnut.
- 1148 FAO (2018b). FAOSTAT - download data - crops.
- 1149 Fitts, C. R. (2012). *Groundwater Science*. Academic Press, Oxford, United Kingdom, scond edit edition.
- 1150 Ghana-made (2018). Groundnut.
- 1151 GlobalPetrolPrices (2018). Ghana diesel price (litre).
- 1152 Harbaugh, A. W. (2005). MODFLOW-2005 , The U . S . Geological Survey Modular Ground-Water Model —
1153 the Ground-Water Flow Process. *U.S. Geological Survey Techniques and Methods*, page 253.
- 1154 Harbaugh, B. A. W., Banta, E. R., Hill, M. C., and McDonald, M. G. (2000). MODFLOW-2000 , The U . S
1155 . Geological Survey modular graound-water model — User guide to modularization concepts and the
1156 ground-water flow process. *U.S. Geological Survey*, page 130.
- 1157 Houghton Mifflin (2016). *American Heritage Dictionary of the English Language*. Houghton Mifflin, Boston,
1158 MA, United States, fifth edition.
- 1159 Konikow, L. F, Hornberger, G. Z., Halford, K. J., and Hanson, R. T. (2009). Revised Multi-Node Well (MNW2
1160) Package for MODFLOW Ground-Water Flow Model Techniques and Methods 6 – A30. *Methods*, page 80.
- 1161 Kruseman, G. and de Ridder, N. (2000). *Analysis and evaluation of pumping test data*. International Institute
1162 for Land Reclanation and Improvement (ILRI), Wageningen, The Netherlands, second edi edition.
- 1163 Langevin, C. D. (2008). Modeling axisymmetric flow and transport. *Ground Water*, 46(4):579–590.
- 1164 Modern Ghana (2018). Esoko market.
- 1165 Niswonger, R. G., Panday, S., and Motomu, I. (2011). MODFLOW-NWT , A Newton Formulation for
1166 MODFLOW-2005. *USGS reports*.
- 1167 Owusu, S., Cofie, O. O., Osei-Owusu, P. K., Awotwe-Pratt, V., and Mul, M. L. (2017). Adapting aquifer storage
1168 and recovery technology to the flood-prone areas of northern Ghana for dry-season irrigation. *Working*
1169 *Paper 176*.
- 1170 Owusu, S., Mul, M., Ghansah, B., Awotwe-pratt, V., and Osei, P. K. (2015). Technical Report: Identification
1171 and selection of suitable sites for Bhungroo and Pave Irrigation Technologies. pages 1–61.

- 1172 Strack, O. D. L. (1989). *Groundwater Mechanics*. Prentice Hall, Englewood Cliffs, New Jersey.
- 1173 TS24 (2018). KIPOR KDE6700T DIESEL GENERATOR.
- 1174 van de Giesen, N. (2013). Dictaat CTB2120 Waterbeheer. Technical report, Delft University of Technology,
1175 Delft.

Appendices

A

1177

1178

Original Borehole Logsheets

1179 In the first half of the year 2016 Conservation Alliance (CA) commissioned the construction of multiple
1180 boreholes in northern Ghana. The boreholes subjected in this research (five locations, visualized in 2.1) are
1181 all part of this operation. Valuable information is gained with respect to local soil stratification, during
1182 borehole construction. Information is preserved in the original borehole log-sheets, which can be found
1183 in this appendix. Besides the local soil stratification, these log-sheets contain information on individual
1184 applied well structures. A depth dependent distinction is made in plain versus screened well skin. In terms
1185 of content these borehole log-sheets are used as a starting point in the theoretical model determination
1186 (section 2.1).

		CONSERVATION ALLIANCE- THE PAVE PROJECT				BH status:	Successful	✓		
						Dry				
		BOREHOLE LOG SHEET								
Community		Bingo	District	Talensi	Borehole ID	BH B1				
Coordinates - Latitude (N) :		Longitude (W)								
Drilling contractor		Drill rig		Method		ROTARY AIR				
Drilling start date		6-8-2016	Compl. date	6-8-2016	Operator					
TEST PUMPING		Date:			Conductivity	us/cm	Top of screen *	0 m		
Dynamic WL *		m	Pump type	Total Iron		mg/l	Static WL *	m		
Static WL *		m	Pumping rate (Q)	m³/h		Manganese	mg/l	Potential drawdown	m	
Drawdown (s)		m	Duration	h		Nitrate	mg/l	Potential yield	25 l/min	
* Levels to ground level datum		Specific capacity (Q/s)		m³/h/m		Fluoride	mg/l	Depth of borehole *	48 m	
BIT SIZE & TYPE	Temporary Casing	SCALE	PROFILE		TIME/DEPTH M/MIN	WATER ZONES CUMULATIVE Q (l/min)	WELL DIAGRAM			
10"			Light brown clay							
Clay cutter										
6.5" hammer bit			Highly weathered light brown sandstone mixed with shaly materials							
			5						3m PVC Screen	5
			10						12m PVC Plain	10
			15						3m PVC Screen	15
			20						42m Gravel pack	20
			25						6m PVC Plain	25
			30						24m PVC Screen	30
			35							40
			40							45
			45							50
Moderately weathered brownish sandstone					15					
					55					
Gravel for gravel pack		48	LM	Remarks and stoppages:						
Screen Length		30	LM							
Casing length		18	LM							
Installation of grout seal		M	M							
Cleaning & development		2	HRS	Prepared by:						
Centralisers fitted		No								
Safety cap fitted		/	No	Approved:						
Backfill aband. BH			/							
Cement for grout			KG							
Platform construction date										
Distance from last BH			KM							

		CONSERVATION ALLIANCE- THE PAVE PROJECT				BH status:	Successful	Dry	✓			
		BOREHOLE LOG SHEET										
Community	Nungo	District	Talensi	Borehole ID		BH N100						
Coordinates - Latitude (N) :		Longitude (W)										
Drilling contractor		Drill rig		Method		ROTARY AIR						
Drilling start date	6-8-2016	Compl. date	6-8-2016	Operator		Kwaku						
TEST PUMPING		Date:		Conductivity	us/cm	Top of screen *	0	m				
Dynamic WL *	m	Pump type		Total Iron	mg/l	Static WL *		m				
Static WL *	m	Pumping rate (Q)	m³/h	Manganese	mg/l	Potential drawdown		m				
Drawdown (s)	m	Duration	h	Nitrate	mg/l	Potential yield	80 l/min					
* Levels to ground level datum		Specific capacity (Q/s)	m³/h/m	Fluoride	mg/l	Depth of borehole *	42	m				
BIT SIZE & TYPE	Temporary CASING	SCALE	PROFILE	TIME/ DEPTH M/MIN	WATER ZONES CUMULATIVE Q (l/min)	WELL DIAGRAM						
10"	Clay cutter	5	Highly weathered light brown sandstone									
6.5"	hammer bit	10	<p>Moderately weathered light grey sandstone mixed with shaly materials (at 18m, 21-24m)</p> <p>Light grey sandstone</p>			15						
		20										
		25										
		30										
		35										
		40										
		45										
		50										
Gravel for gravel pack		42				LM	Remarks and stoppages:					
Screen Length		36				LM						
Casing length		6				LM						
Installation of grout seal		M				M						
Cleaning & development		2				HRS	Prepared by:					
Centralisers fitted		No										
Safety cap fitted		/				No	Approved:					
Backfill aband. BH			/									
Cement for grout			KG									
Platform construction date			KM									
Distance from last BH												

		CONSERVATION ALLIANCE- THE PAVE PROJECT				BH status:	Successful	✓
						Dry		
BOREHOLE LOG SHEET								
Community	Nyong Nayili	District	Karaga	Borehole ID	BH NN1			
Coordinates - Latitude (N) : Longitude (W)								
Drilling contractor		Drill rig		Method	ROTARY AIR			
Drilling start date	31/05/2016	Compl. date	31/05/2016	Operator	Kwaku			
TEST PUMPING		Date:		Conductivity	us/cm	Top of screen *	0	m
Dynamic WL *	m	Pump type		Total Iron	mg/l	Static WL *		m
Static WL *	m	Pumping rate (Q)		m³/h	Manganese	mg/l	Potential drawdown	m
Drawdown (s)	m	Duration		h	Nitrate	mg/l	Potential yield	
* Levels to ground level datum		Specific capacity (Q/s)		m³/h/m	Fluoride	mg/l	Depth of borehole *	54 m
BIT SIZE & TYPE	Temporary Casing	PROFILE SCALE	TIME/DEPTH M/MIN	WATER ZONES CUMULATIVE Q (l/min)	WELL DIAGRAM			
10"								
Clay cutter		Clay						
		5						
		10						
		15						
		20						
		25						
		30						
		35						
		40						
		45						
		50						
		55						
Gravel for gravel pack	Yes	54	LM	Remarks and stoppages:				
Screen Length		33	LM					
Casing length		21	LM					
Installation of grout seal		M	M					
Cleaning & development		2	HRS	Prepared by:				
Centralisers fitted		No						
Safety cap fitted		/	No	Approved:				
Backfill aband. BH	Yes	/						
Cement for grout		KG						
Platform construction date								
Distance from last BH		KM						

		CONSERVATION ALLIANCE- THE PAVE PROJECT				BH status:	Successful	✓	
						Dry			
BOREHOLE LOG SHEET									
Community		Janga 1	District	West Mamprusi	Borehole ID	BH J1			
Coordinates - Latitude (N) :		0°iu	Longitude (W)						
Drilling contractor			Drill rig		Method	ROTARY AIR			
Drilling start date		6-3-2016	Compl. date	6-3-2016	Operator	Kwaku			
TEST PUMPING		Date:		Conductivity	us/cm	Top of screen *	0	m	
Dynamic WL *		m	Pump type	Total Iron	mg/l	Static WL *		m	
Static WL *		m	Pumping rate (Q)	m³/h	Manganese	mg/l	Potential drawdown	m	
Drawdown (s)		m	Duration	h	Nitrate	mg/l	Potential yield	35 l/min	
* Levels to ground level datum			Specific capacity (Q/s)	m³/h/m	Fluoride	mg/l	Depth of borehole *	48 m	
BIT SIZE & TYPE	Temporary Casing	SCALE	PROFILE	TIME/DEPTH M/MIN	WATER ZONES CUMULATIVE Q (l/min)	WELL DIAGRAM			
10" Clay cutter	6.5" hammer bit		Highly weathered light brown sandstone (Very loose formation) Moderately weathered grey shale		15 35				
						5			
						10			
						15			
						20			
						25			
						30			
						35			
						40			
						45			
50									
Gravel for gravel pack		Yes	48	LM	Remarks and stoppages:				
Screen Length			48	LM					
Casing length				LM					
Installation of grout seal				M					
Cleaning & development			2	HRS	Prepared by:				
Centralisers fitted				No					
Safety cap fitted			/	No	Approved:				
Backfill aband. BH				/					
Cement for grout				KG					
Platform construction date									
Distance from last BH			KM						

		CONSERVATION ALLIANCE- THE PAVE PROJECT				BH status:	Successful	✓		
						Dry				
BOREHOLE LOG SHEET										
Community	Ziong	District	Savelugu Nanton	Borehole ID	BH Z1					
Coordinates - Latitude (N) : Longitude (W)										
Drilling contractor		Drill rig		Method	ROTARY AIR					
Drilling start date	27/05/2016	Compl. date	27/05/2016	Operator						
TEST PUMPING		Date:		Conductivity	us/cm	Top of screen *	0	m		
Dynamic WL *	m	Pump type		Total Iron	mg/l	Static WL *		m		
Static WL *	m	Pumping rate (Q)		m³/h	Manganese	mg/l	Potential drawdown	m		
Drawdown (s)	m	Duration		h	Nitrate	mg/l	Potential yield	25 l/min		
* Levels to ground level datum		Specific capacity (Q/s)		m³/h/m	Fluoride	mg/l	Depth of borehole *	48 m		
BIT SIZE & TYPE	Temporary Casing	PROFILE SCALE	TIME/DEPTH M/MIN	WATER ZONES CUMULATIVE Q (l/min)	WELL DIAGRAM					
10"										
Clay cutter										
6.5" hammer bit		Reddish brown laterite								
		5								
		10								
		15								
		20								
		25								
		30								
		35								
		40								
		45								
50										
Highly weathered light brown sandstone mixed with shaly materials										
Moderately weathered brownish sandstone										
15										
25										
3m PVC Screen										
12m PVC Plain										
48m Gravel pack										
33m PVC Screen										
1m Bail Plug										
50										
Gravel for gravel pack	Yes	48	LM	Remarks and stoppages:						
Screen Length		36	LM							
Casing length		12	LM							
Installation of grout seal		M	M							
Cleaning & development		2	HRS	Prepared by:						
Centralisers fitted			No							
Safety cap fitted		/	No	Approved:						
Backfill aband. BH		Yes	/							
Cement for grout			KG							
Platform construction date			KM							
Distance from last BH										

B

1192

1193

Fieldwork set-up

1194 The northern Ghana in-field geohydrological data collection would not have been possible without the in-
1195 terference of Conservation Alliance (CA). Spread over the Upper East and Northern Region the NGO holds
1196 multiple PIT locations. Five locations, visible in figure 2.1, are appointed as measurement locations for the
1197 purposes of this research. Besides the research locations, CA provided transport, an interpreter and pump-
1198 ing test equipment. The section below contains detailed information on the equipment applied. Moreover,
1199 it describes the general fieldwork pumping test / monitoring set-up. The section concludes with fieldwork
1200 fact-sheets, containing the collected data for each individual location.

1201 **B.1. Equipment**

1202 The applied in-field pumping tests are executed with a same set of equipment. The paragraph below con-
1203 tains a detailed description of the most important tools. In this case a distinction has been made between
1204 the equipment for the pumping tests and the actual groundwater measurements. Moreover small equip-
1205 ment as pliers, screwdrivers, gloves and robes are ignored. Purposes and use of these tools are taken for
1206 granted.

1207

1208 **Pumping test**

- 1209 • Pump: Pedrollo 4" submersible pump; Type 4SR4/18

1210 A 2 HP pump, for example usable for the supply of water to irrigation fields. While pumping the water
1211 should preferably not exceed 35 °C and should not contain too many particles; no more than 150
1212 g/m³. The pump can be submerged in water up to 100 meters. Installed in the right way, the pump
1213 can deliver 20-100 l/min with an head difference of 112-45 m. More specific information regarding
1214 the pump can be found on the Pedrollo webpage.



Figure B.1: Comparable example of the fieldwork submersible pump
(source: <https://www.pedrollo.com/en/4sr-4-submersible-pumps/150>)

1215 • Generator & power converter: Kipor diesel generator - 5 kVA

1216 A mobile generator has been used as a pump power source. The Kipor generator is a relatively small
 1217 model, easy to handle and meets the pump requirements by the use of the 230 V connection. A power
 1218 converter is placed between generator and pump to manually switch on and off the pump. To facili-
 1219 tate a flawless transfer between generator and pump one should be aware the cables and connections
 1220 towards the pump should be waterproof. Moreover these power cables should be of a decent length
 1221 to allow the pump to submerge.



Figure B.2: Comparable example of the fieldwork generator

(source: <https://www.kipor-power.eu/winkel/kipor-kde6700t-diesel-generator-5-kva/>)

1222 • Hose:

1223 As a transport line towards the location of discharge a flexible water hose has been attached to the
 1224 pump. The hose has been manufactured in Polyethylene, has an external diameter of $1\frac{1}{4}$ " and is
 1225 approximately 100 m long.



Figure B.3: Actual fieldwork hose & bucket

1226 • Bucket:

1227 As a rough estimation for discharge an plastic bucket has been used. This oversized measuring cup
 1228 stores volumes up to 50 l and contains 5 l level indicators.

1229 **GWT measurements**

1230 • Pressure sensor data loggers:

1231 - Van Essen; TD-Diver Type DI801 (2x) & Baro-Diver Type DI800 (1x):

1232 TD- and Baro-Divers are applied for the measuring and recording of time dependent fluctuations in
 1233 (ground)water levels, atmospheric pressures and temperatures. The TD-Divers can record a water
 1234 column up to 10 m. Baro-Divers can be used to measure atmospheric pressures and shallow water
 1235 levels, approximately up to a range of 0.9 m. Based on the internal memory these devices can store

1236 up to 72.000 measurements per parameter. Measurement logging can be programmed by the use
 1237 of a USB-Unit and the Diver-Office software. With a battery life of 10 years, long and/or short term
 1238 measurements can be applied with a sample interval of 0.5 seconds to 99 hours. Moreover the sample
 1239 interval can be linear or logarithmic.



Figure B.4: Comparable examples of Van Essen TD- & Baro-Divers
 (source: <https://www.vanessen.com/images/PDFs/TD-Diver-DI8xx-ProductManual-nl.pdf>)

1240 - In-Situ; RuggedTROLL100 (2x) & BaroTROLL (1x):

1241 Rugged TROLL 100 and BaroTROLL divers are applied for the measuring and recording of time depen-
 1242 dent fluctuations in (ground)water levels, atmospheric pressures and temperatures. The RuggedTROLL100
 1243 divers function in a pressure range up to 9 m water column. BaroTROLL divers can be used for the
 1244 measurement of atmospheric pressures, up to 1 bar. The internal memory of 2.0 MB accommodates
 1245 the storage of 120.000 data records. A record contains a set of three items; date & time, pressure and
 1246 temperature. The internal battery has a lifetime of approximately 10 years. By the use of the Rugged
 1247 TROLL docking-station and the Win-Situ 5 software, linear logging can be programmed. Fastest log-
 1248 ging rate is 1 log per second for the Rugged TROLL 100 divers and 1 log per minute for the BaroTROLL
 1249 divers. Optionally it is possible to display the pressure in units of Psi, Bar, Pascal or mH₂O.



Figure B.5: Comparable examples of In-Situ TD- & Baro-Divers
 (source: <https://in-situ.com/product-category/water-level-monitoring/level-temp-data-loggers/>)

1250 • Hand measurement device: Heron water tape

1251 The water tape is applied to hand measure static water levels and verify drawdown water levels during
 1252 the pumping tests. The water tape has a length of 300 ft (100 m). A water level sensing probe is
 1253 attached to the tail of the tape. Probe water contact results in an instant auditory signal, after which
 1254 the depth can be determined by eye. Product specifications can be found on the Heron webpage.

1255 **B.2. General measurement structure**

1256 This section accommodates multiple key aspects in the test set-up. By the implementation of this thought-
 1257 out pumping test and measurement set-up an optimal test result is pursued. Moreover it accommodates



Figure B.6: Comparable example of the fieldwork water tape
(source: <https://envirotechonline.com/water-level-interface-meters/the-heron-water-tape.html>)

1258 information on fieldwork reproduction.

1259 **Pump installation**

1260 Based on the log sheets the original (2016) site-specific borehole depths are known in advance. Due to the
1261 accumulation of sedimentation the borehole depth decreases over time. To prevent pump damage and
1262 make sure proper functioning is maintained, the actual borehole depths are measured before the pumping
1263 tests. Outcome of the measurements are taken into account for each individual test set-up. To prevent
1264 excessive spread of soil particles the submersible pump is positioned at least 5 meters above the measured
1265 bottom. In practice this resulted in a pump suction depth of approximately 35 m for every individual pumping
1266 test.

1267 **Discharge (measurement)**

1268 A single 100 m hose is directly connected to the outlet of the submersible pump. Based on the pump position
1269 (deep inside borehole), a length of circa 60 m is still present for the horizontal displacement of water.
1270 At this distance (relative to the borehole) water is discharged on the surface.
1271 The head of the hose is equipped with a nozzle to roughly regulate the discharge rate. By the use of this nozzle,
1272 discharge rates in the range of 50-75 m³/d are obtained during the pumping tests. Rates are measured
1273 by the use of a 50 l bucket. Starting at the moment of pump operation, the duration of filling is measured
1274 twice every 15 minutes. The average is used to calculate the time dependent discharge rates. More detailed
1275 discharge information can be found in the site-specific fact-sheets below.

1276 **GWT measurement**

1277 Drawdowns due to pumping tests are preferably measured in multiple piezometers located at a certain
1278 known horizontal distance from the discharge well (Kruseman and de Ridder, 2000). In the northern Ghana
1279 surroundings, close range monitoring options are absent. Due to a lack of time and/or resources these facilities
1280 cannot be arranged either. Moreover, the implementation of such facilities do not match research
1281 nature. Aim of this research is to collect fieldwork data by the use of minimal resources. The local absence of
1282 abundant measurement options strengthens this approach. In this research pumping test GWT drawdowns
1283 are measured in the discharge well only.

1284 A water tape (hand equipment) is used, first of all to determine the initial (static) GWT. Subsequently the device
1285 is applied as a real time indicator of drawdown. During the pumping test multiple hand measurements
1286 are applied at randomly picked moments to monitor test progress. Gathered data functions as verification
1287 and back-up of the pressure sensors, which are normative.

1288 Two types of divers (different brands) are used as basic GWT measurement devices. Specifications show
1289 these divers can respectively measure pressures up to 10 m (Van Essen) and 9 m (In-Situ) water column
1290 (bron.). The northern Ghana regional subsurface is characterized as highly heterogeneous. The pumping
1291 test GWT drawdown order of magnitude is therefore unpredictable. To prevent the occurrence of missing

1292 drawdown data, the single borehole accommodates multiple divers at ascending depths. The water column
 1293 between the initial static water table and pump position is preferably filled with about four divers, with a
 1294 mutual distance that meets the divers range specifications. To make sure the divers stay in position they are
 1295 leashed to a rope which runs from well top to pump. This measurement set-up forms a robust network for
 1296 the collection of drawdown data.

1297 Practical circumstance can however cause the application of a more simplified set-up. One can think of a
 1298 situation in which the pump is already installed and/or will not be removed at the end of the pumping test.
 1299 Rope attachment of the divers to the pump is in this case no longer possible. Adverse effect of the sim-
 1300 plified set-up is a data collection which is more vulnerable. To prevent the occurrence of undesired diver
 1301 movement a minimum distance of 5-10 m between pump and lowest diver is implemented in the simplified
 1302 set-up. A complete overview of the borehole measurement set-up (desired and simplified) can be found in
 1303 figure B.7.

1304

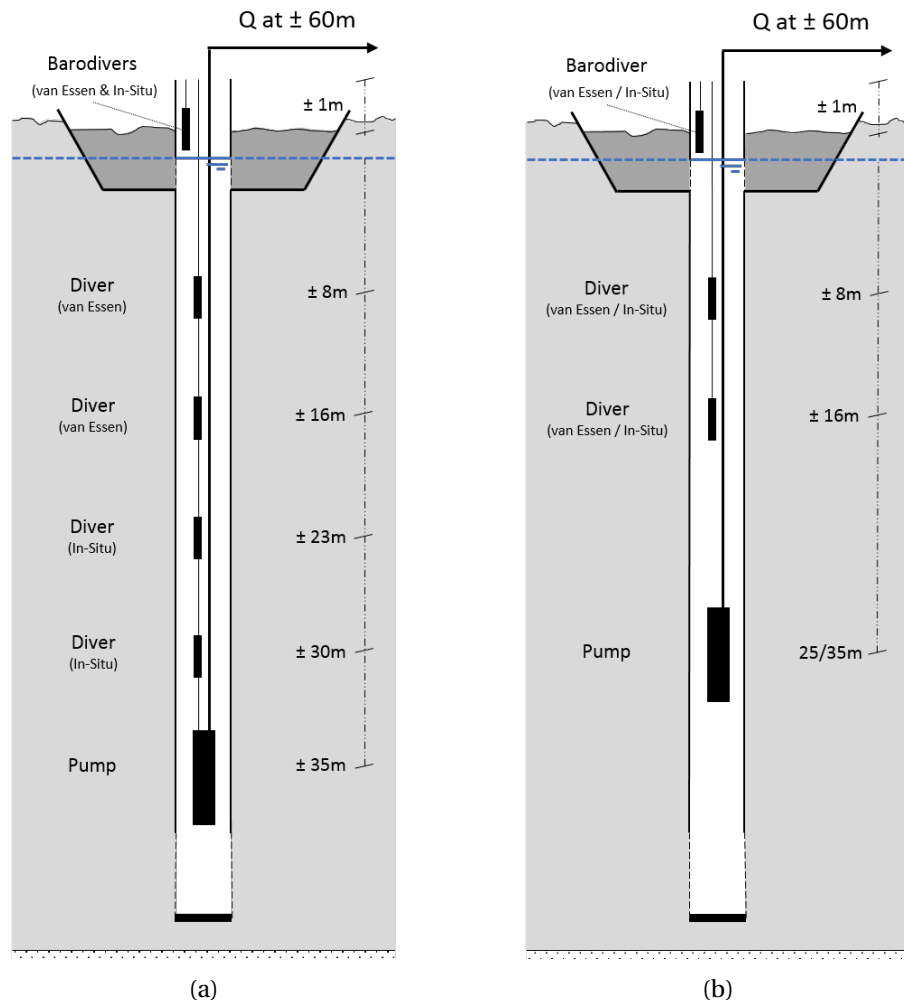


Figure B.7: Fieldwork (measurement) set-up (a) general, (b) simplified

1305 Besides the divers the measurement set-up also accommodates two Baro-divers (van Essen & In-Situ), po-
 1306 sitioned in the borehole top section. Drawdown is by definition expressed as time dependent GWT reduc-
 1307 tions relative to the initial status. Short term atmospheric fluctuations in pressure are compared to the water
 1308 pressures negligible small. Nonetheless these minor atmospheric influences are also included in the data
 1309 collection. The inclusion of these Baro-diver measurements increases measurement accuracy, especially
 1310 with respect to the multi-day system monitoring.

1311 The exact start of pump operation could not be determined in advance. To avoid unnecessary risks in miss-
 1312 ing out on the collection of drawdown data, all pressure sensors are programmed to start logging well in
 1313 time (08:00:00, local time, at pumping test days). All divers are set to log with a similar linear interval of

1314 10 seconds. Only exception is the In-Situ BaroTROLL, which is programmed to linear log at its minimum
1315 sample interval; once a minute.

1316 **B.3. Site-specific measurement results**

1317 In consultation with Conservation Alliance (CA), a total of five pumping tests are applied in boreholes lo-
1318 cated at Bingo, Nungo, Nyong Nayili and Janga. By the use of a fifth borehole, location Ziong, the day-to-day
1319 PIT system-use is monitored for a week. All tests are applied in November-December 2017, shortly after the
1320 transition from wet to dry season. Geohydrological data is gathered by the application of the general pump-
1321 ing test set-up (as described above) at the location Nungo, Nyong Nayili and Janga. The simplified set-up is
1322 applied at the location Bingo and Ziong. Outcome of the tests are widespread. Detailed site-specific results
1323 are displayed in the fact-sheet figures below (Figures B.8 - B.13).

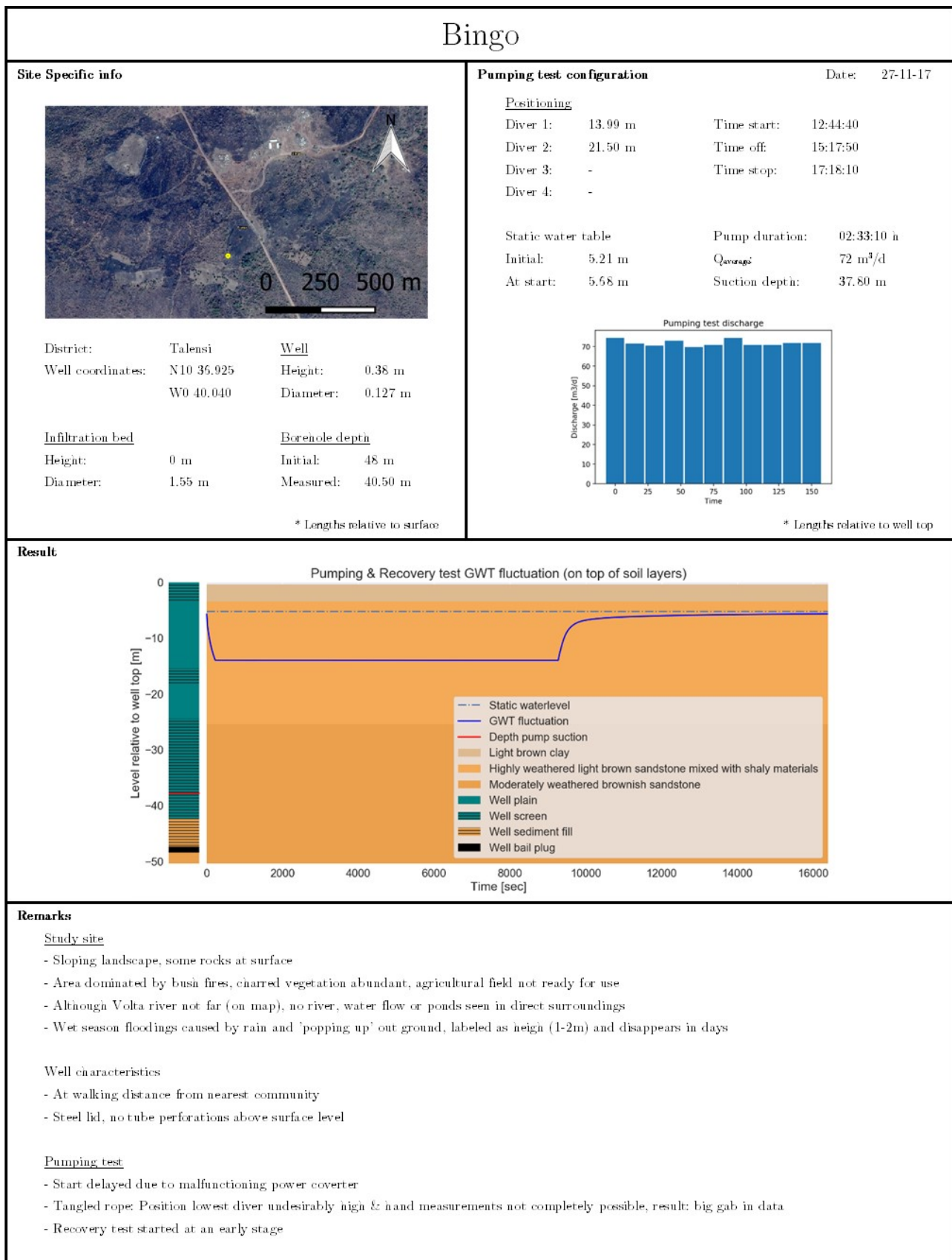


Figure B.8: Fieldwork fact-sheet: Bingo

Nungo		
Site Specific info	Pumping test configuration	Date: 28-11-17
 <p>District: Tafensi Well</p> <p>Well coordinates: N10 33.419 Height: 0.51 m W0 38.990 Diameter: 0.127 m</p>	<u>Positioning</u> Diver 1: 9.05 m Time start: 09:45:00 Diver 2: 17.90 m Time off: 11:00:00 Diver 3: 26.05 m Time stop: 11:15:00 Diver 4: -	
	<u>Static water table</u> Initial: 3.02 m Pump duration: 01:15:00 h At start: 3.00 m Q _{average} : < 5 m ³ /d Suction depth: 31.20 m	
		Pumping test aborted
<u>Infiltration bed</u> Height: -0.35 m Initial: 42 m Diameter: 1.50 m Measured: 9.80 m		
		* Lengths relative to surface
		* Lengths relative to well top
Result -		
		Pumping test aborted
Remarks		
<u>Study site</u> - Mildly sloped till flat landscape - Vegetation abundant, agricultural field present but not ready for use - Volta river in close range (approximately 400 m) - Wet season floodings caused by riverbank overtopping; labeled as extreme (>3m) and constant; duration as long as wetseason		
<u>Well characteristics</u> - At short walking distance from nearest community - No lid, and tube perforations present above surface level		
<u>Pumping test</u> - Pump hard to descend in well; well clogged due to combination of clay, sand and water - Discharge rates very low during test - To improve discharge, test multiple times applied with increased position of pump suction - No drawdowns perceived, pumping test aborted		

Figure B.9: Fieldwork fact-sheet: Nungo

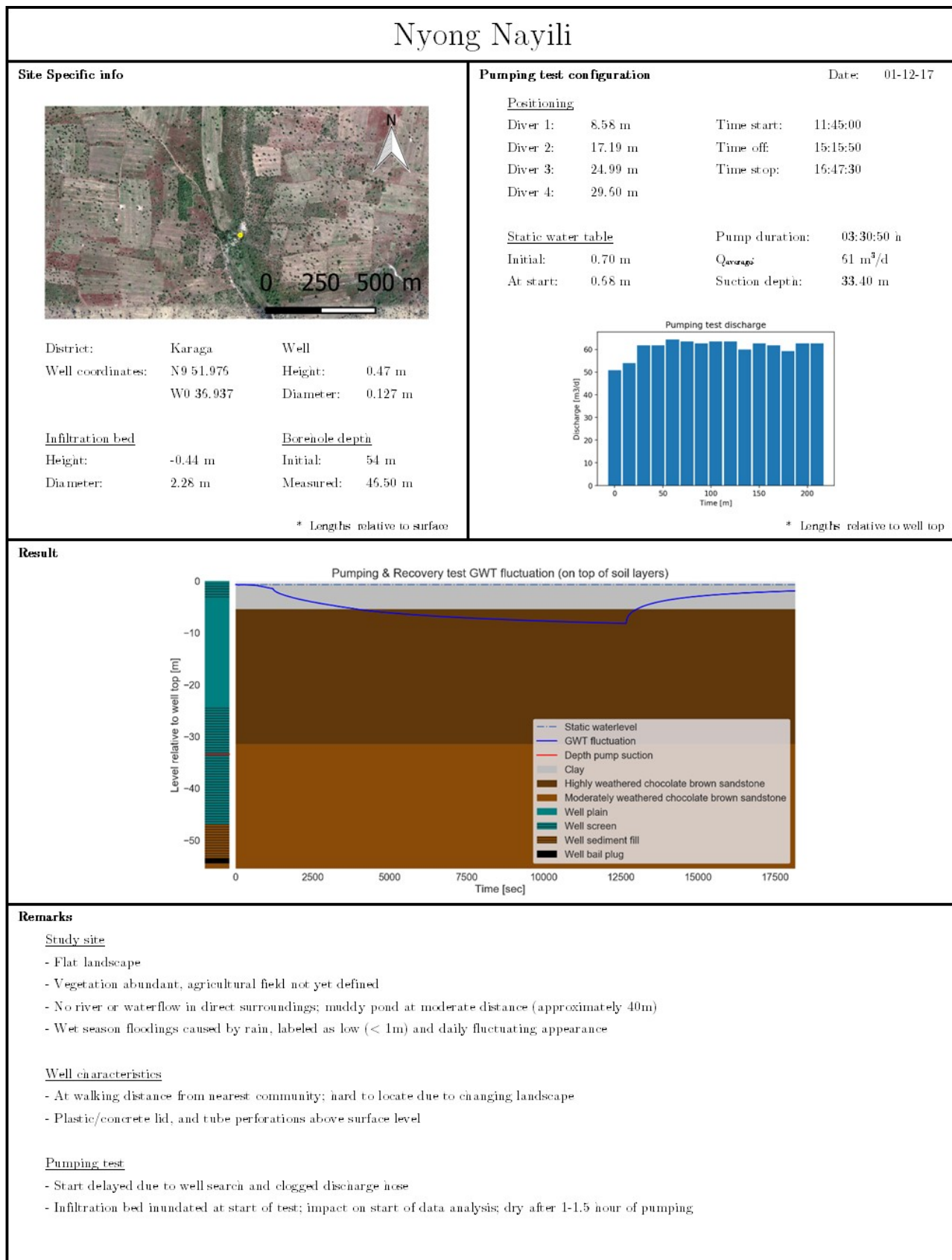


Figure B.10: Fieldwork fact-sheet: Nyong Nayili

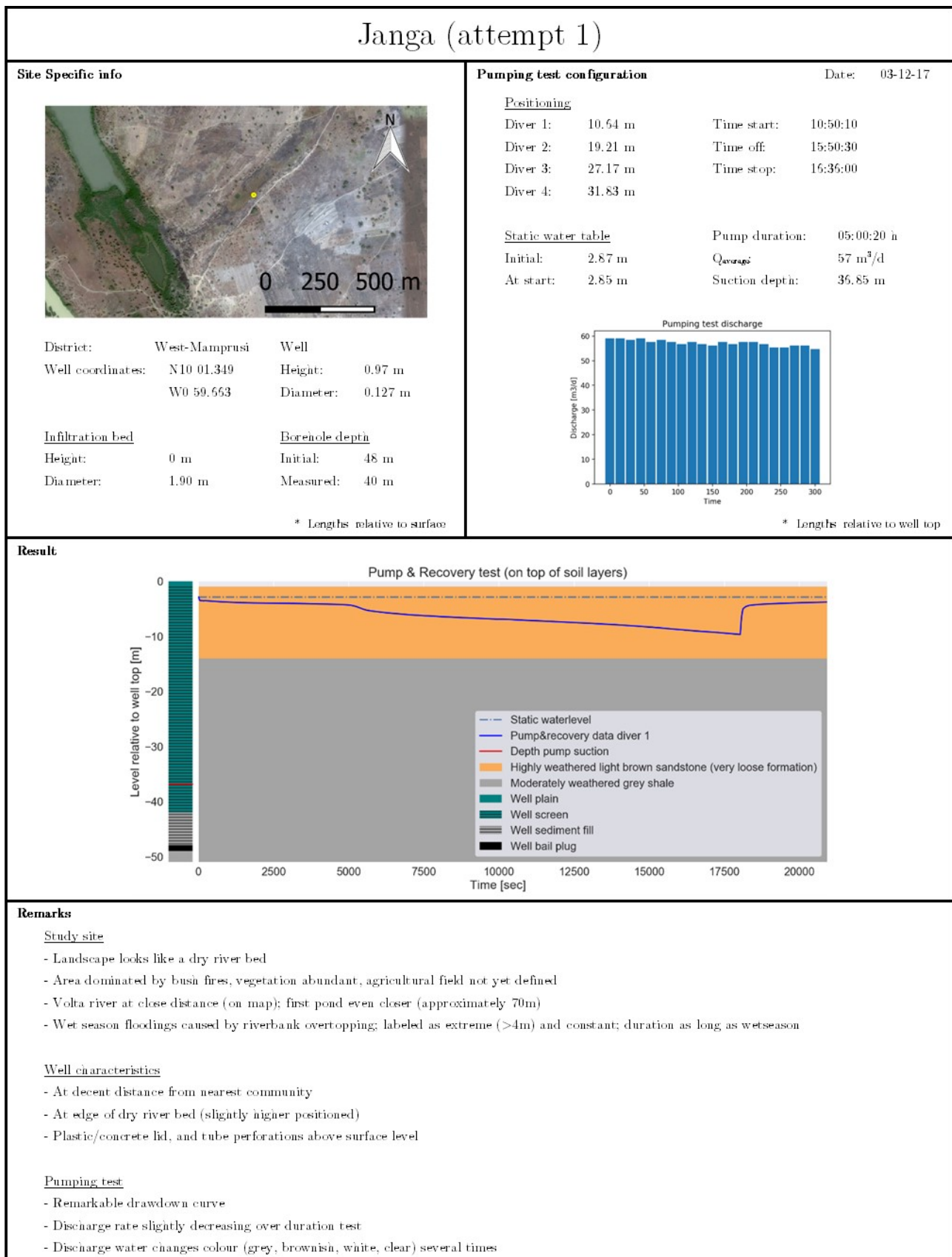


Figure B.11: Fieldwork fact-sheet: Janga (attempt 1)

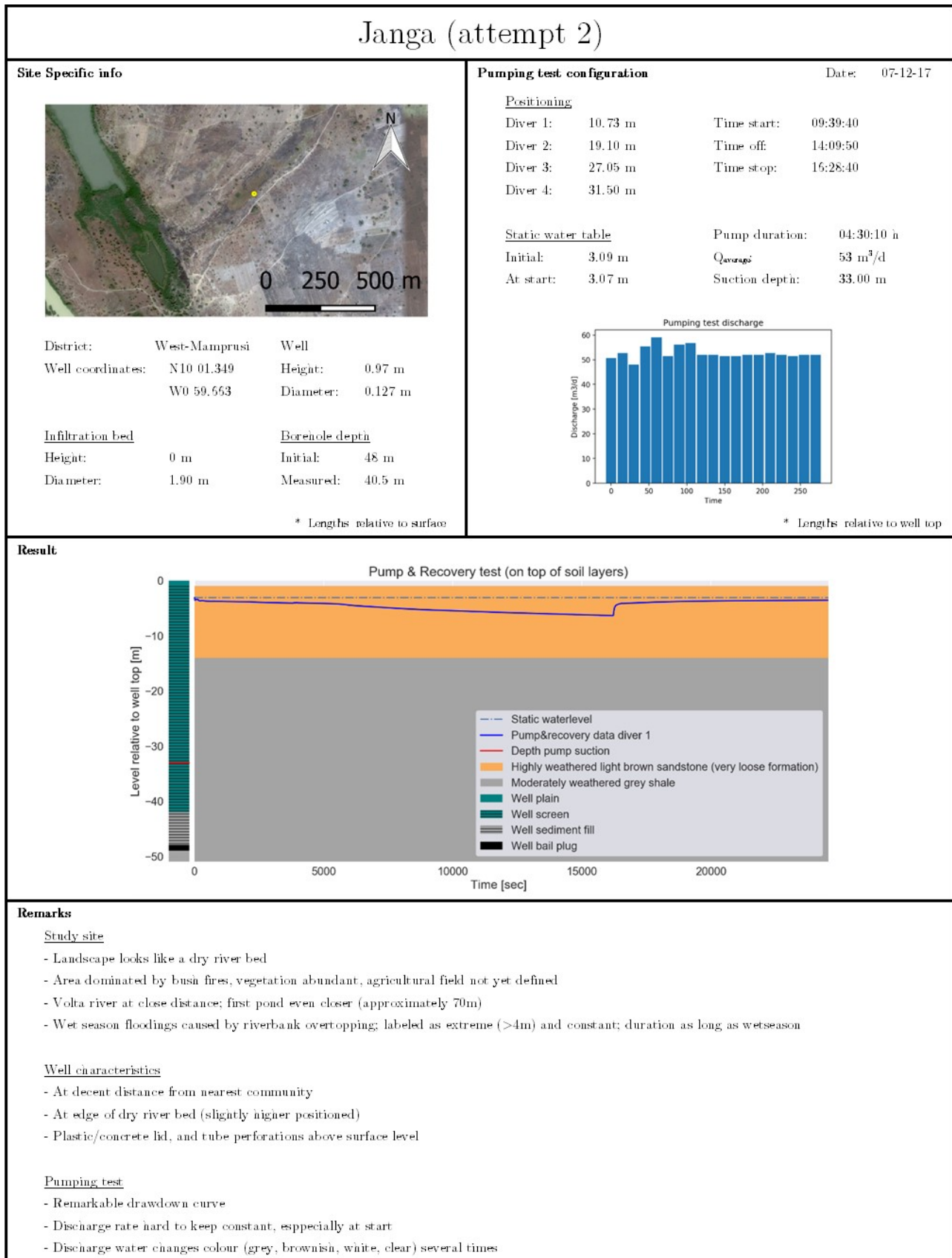


Figure B.12: Fieldwork fact-sheet: Jamga (attempt 2)

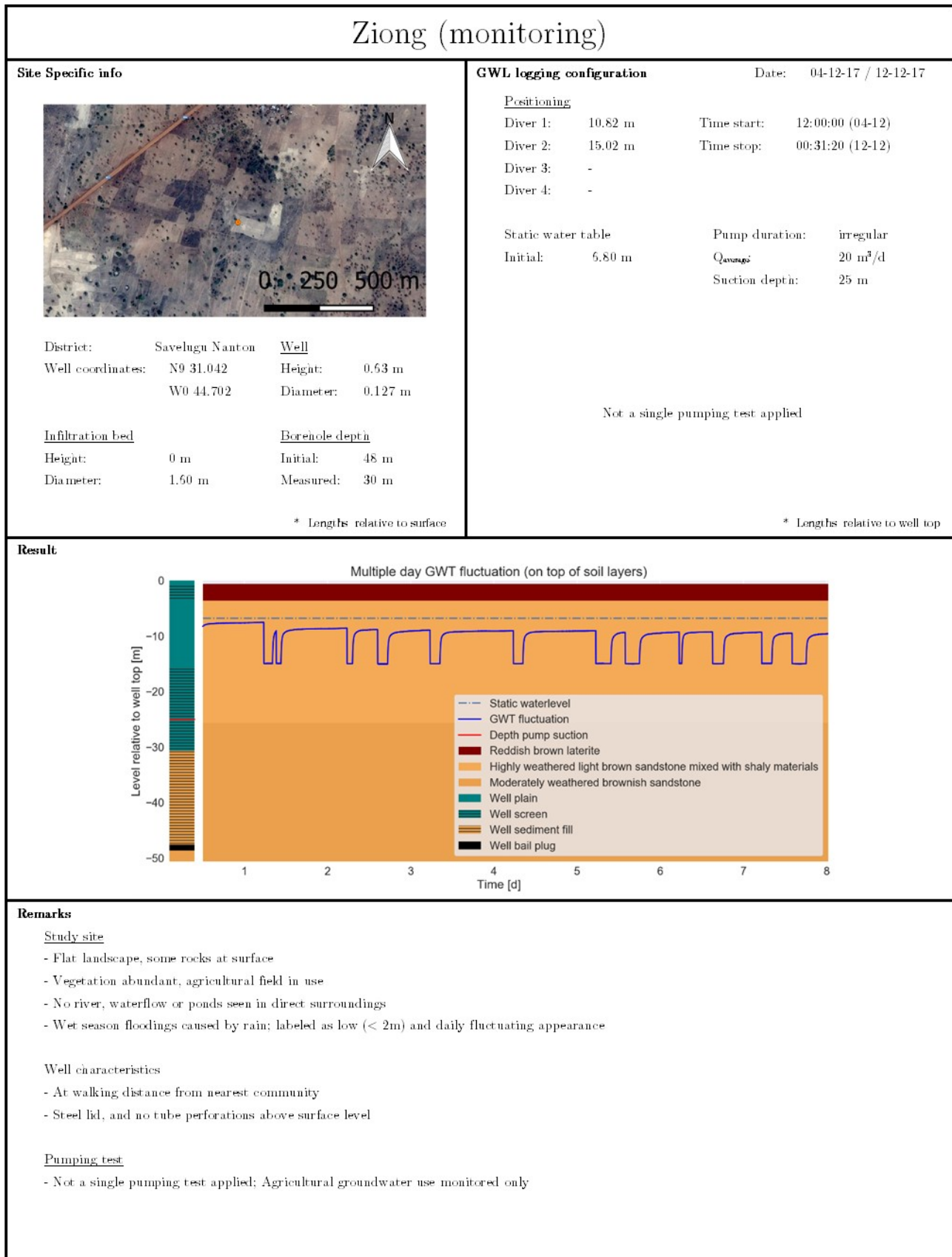


Figure B.13: Fieldwork fact-sheet: Ziong (location of monitoring)

C

1324

1325

Extense report - Fieldwork data analysis

1326 This appendix accommodates a complete overview in fieldwork data analysis. Each location specific dataset
1327 is analysed by a distinction in method (analytical Theis's method (single layer), Fmin and TTim Calibrate))
1328 and theoretical model (single layer, double layer, partially penetrating double layer). In the TTim analysis
1329 an additional distinction is made between analysis by the use of (a) actual borehole storage and no well
1330 resistance, (b) optimal borehole storage and no well resistance, (c) actual borehole storage and optimal well
1331 resistance, (d) optimal borehole storage and optimal well resistance. Result is the location specific dataset
1332 analysis subjected to 25 different approaches; analytical (1x), Fmin-RMSE (4x3 = 12x) and TTim Calibrate
1333 (4x3 = 12x). Outcomes in geohydrological parameter values can be found in the tables and figures below.

1334 C.1. Bingo - overview

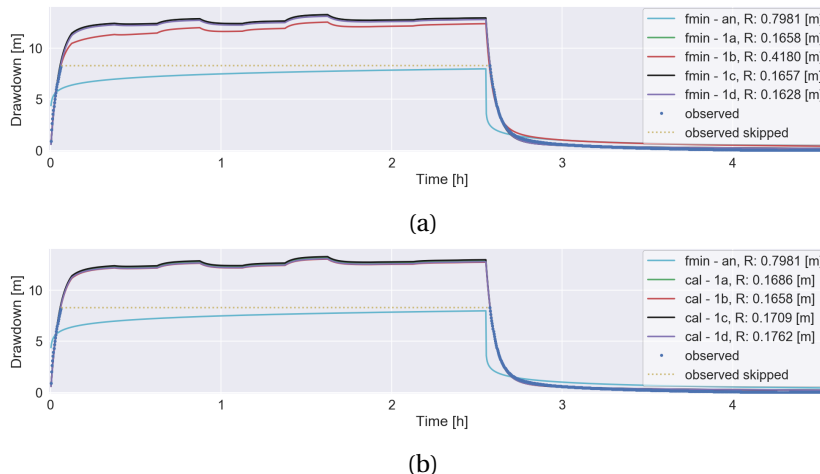


Figure C.1: Bingo single layer fieldwork data analysis by the optimization (a) fmin-RMSE method and (b) TTIm calibration method

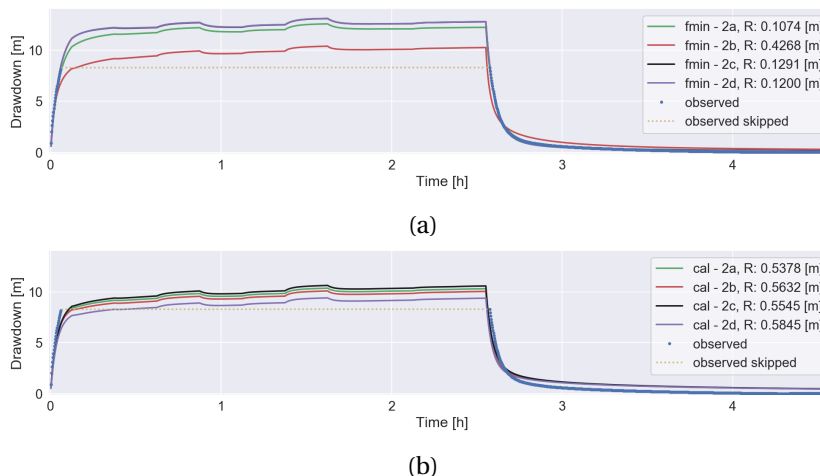


Figure C.2: Bingo double layer fieldwork data analysis by the optimization (a) fmin-RMSE method and (b) TTIm calibration method

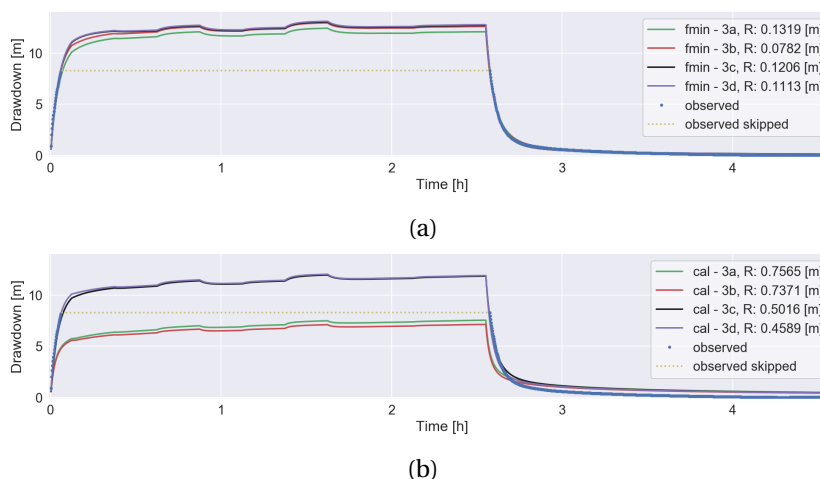


Figure C.3: Bingo partially penetrating double layer fieldwork data analysis by the optimization (a) fmin-RMSE method and (b) TTIm calibration method

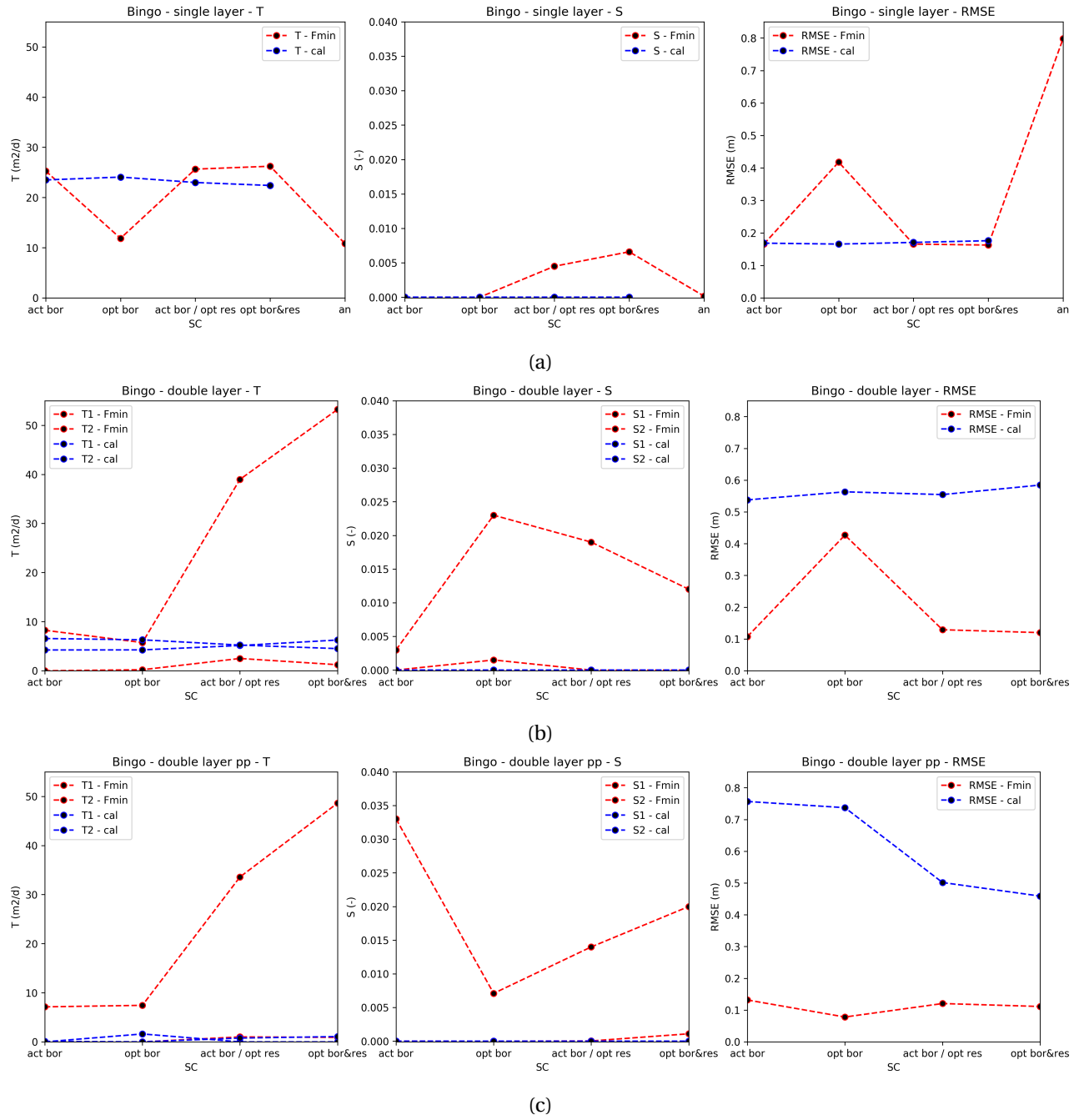


Figure C.4: Bingo - overview determined (Fmin and Cal) optimal parameter values of (??) a single layer system, (??) a double layer system, and (??) a system with two layers and partial penetration of the well

C.2. Nungo - overview

1335
1336 bigskip Gained fieldwork data at the location Nungo not sufficient for the analysis of geohydrological pa-
1337 rameter values.

1338 C.3. Nyong Nayili - overview

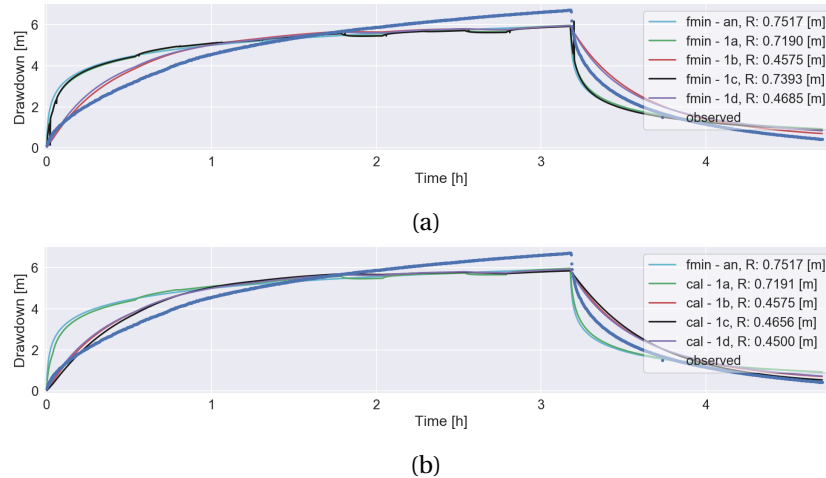


Figure C.5: Nyong Nayili single layer fieldwork data analysis by the optimization (a) fmin-RMSE method and (b) TTIm calibration method

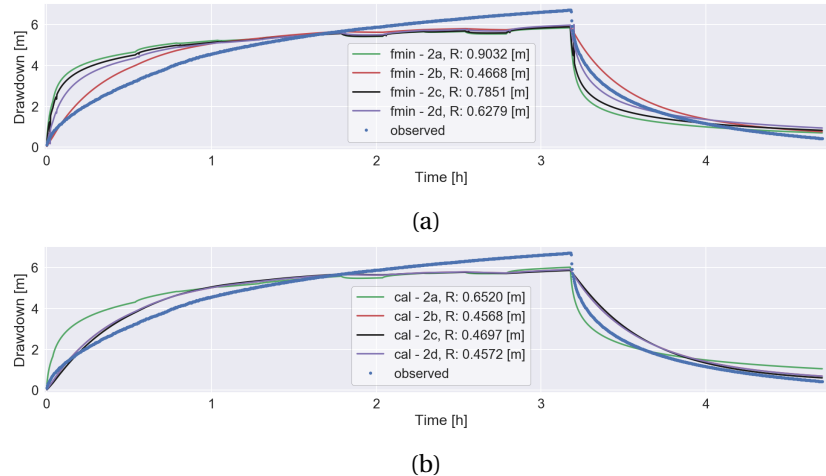


Figure C.6: Nyong Nayili double layer fieldwork data analysis by the optimization (a) fmin-RMSE method and (b) TTIm calibration method

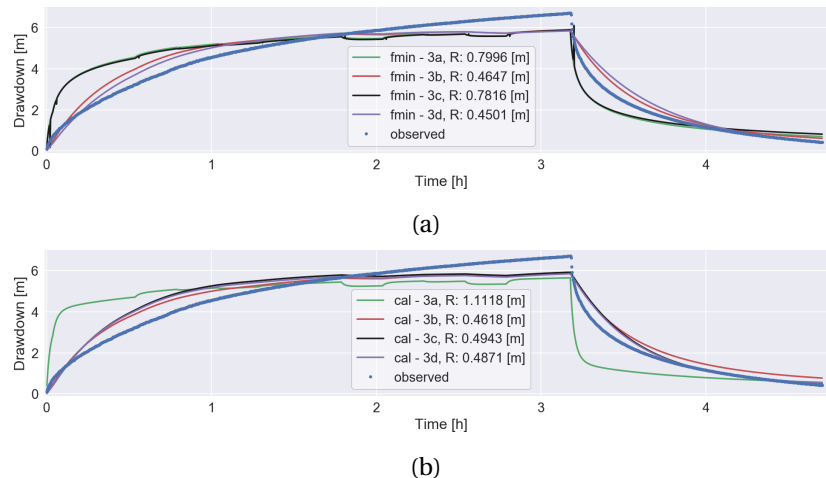


Figure C.7: Nyong Nayili partially penetrating double layer fieldwork data analysis by the optimization (a) fmin-RMSE method and (b) TTIm calibration method

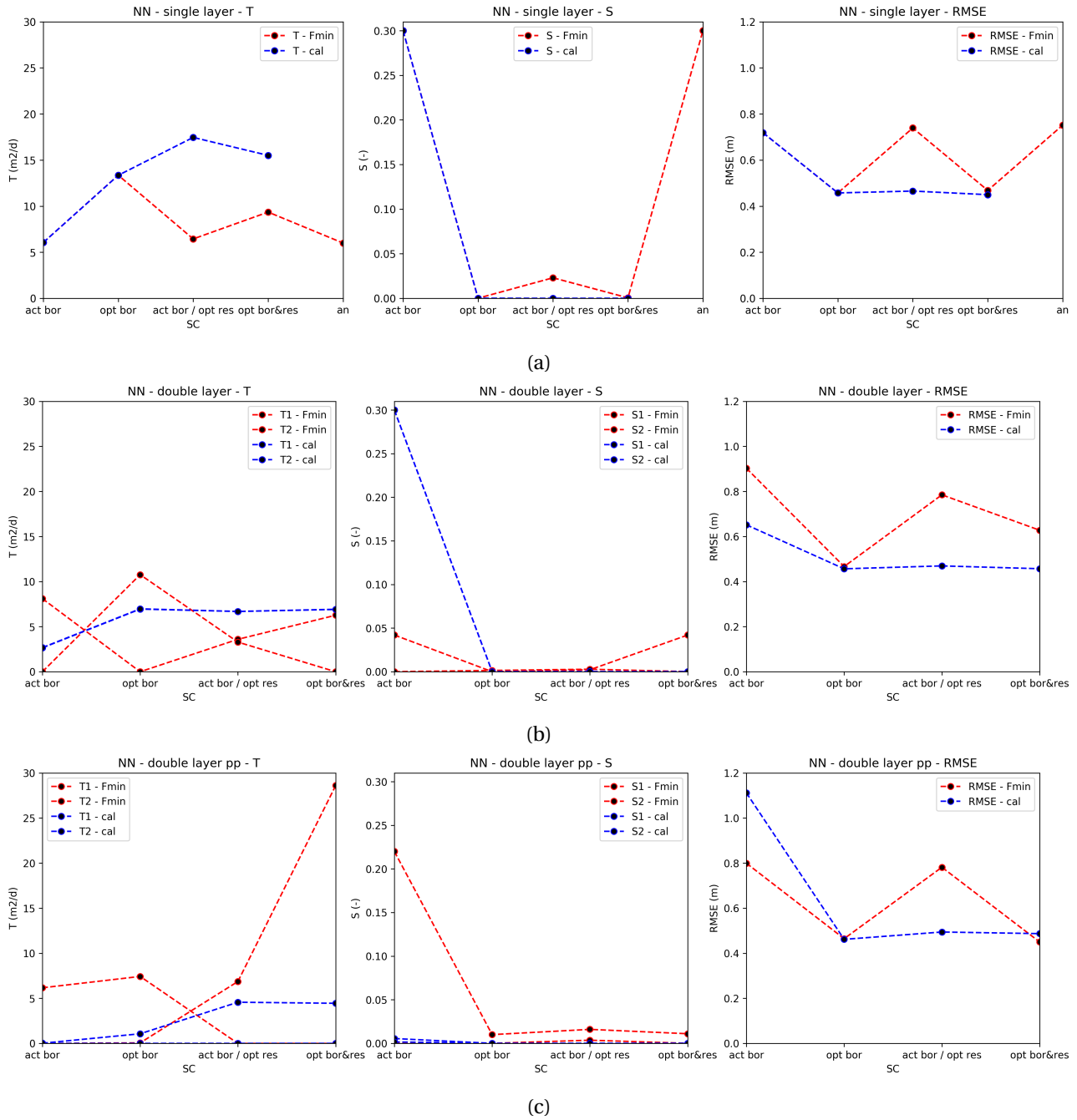


Figure C.8: Nyong Nayili - overview determined (Fmin and Cal) optimal parameter values of (??) a single layer system, (??) a double layer system, and (??) a system with two layers and partial penetration of the well

1339 C.4. Janga (1/2) - overview

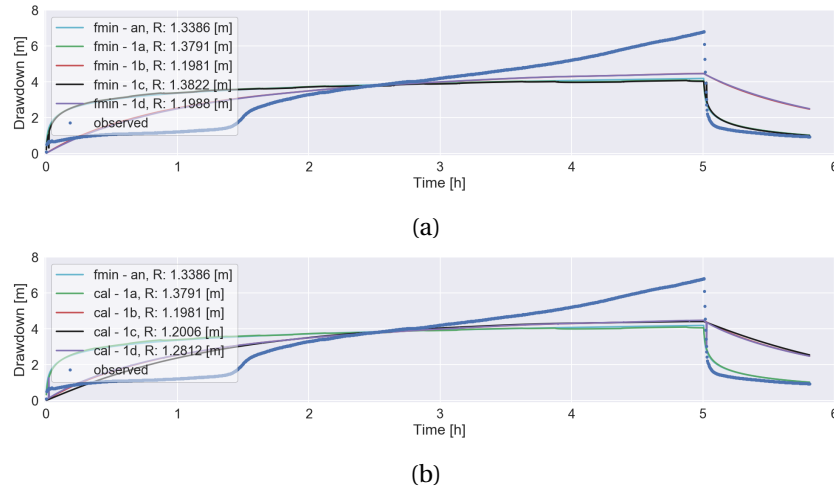


Figure C.9: Janga first attempt single layer fieldwork data analysis by the optimization (a) fmin-RMSE method and (b) TTIm calibration method

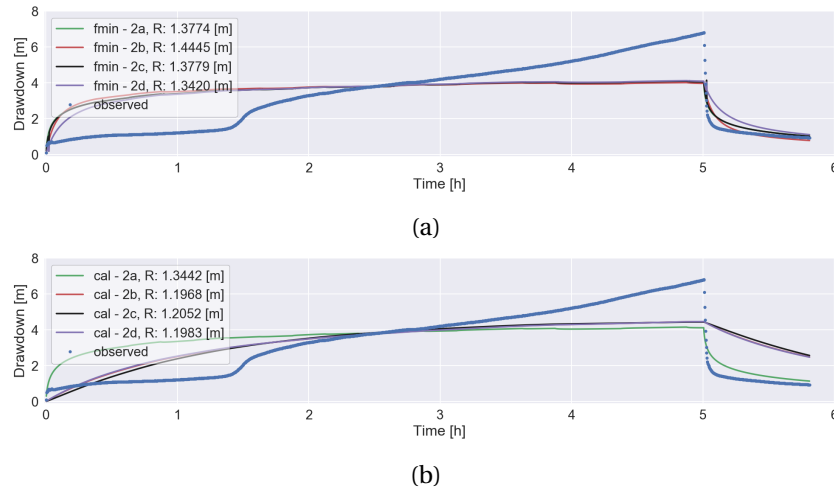


Figure C.10: Janga first attempt double layer fieldwork data analysis by the optimization (a) fmin-RMSE method and (b) TTIm calibration method

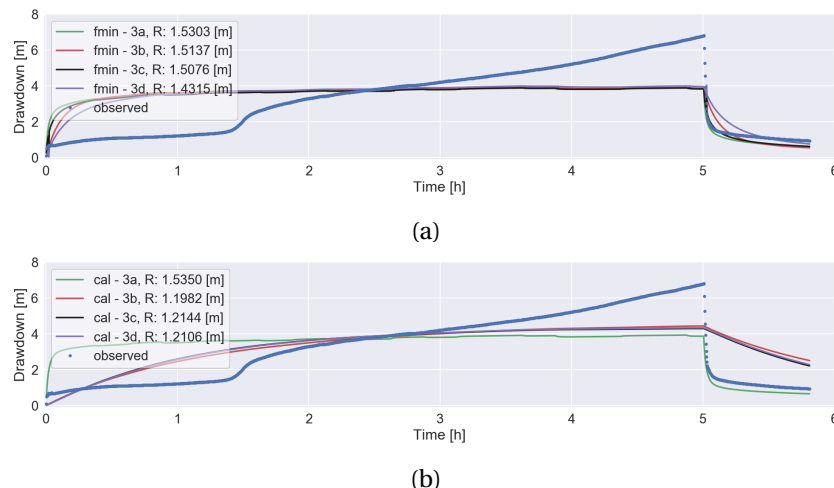


Figure C.11: Janga first attempt partially penetrating double layer fieldwork data analysis by the optimization (a) fmin-RMSE method and (b) TTIm calibration method

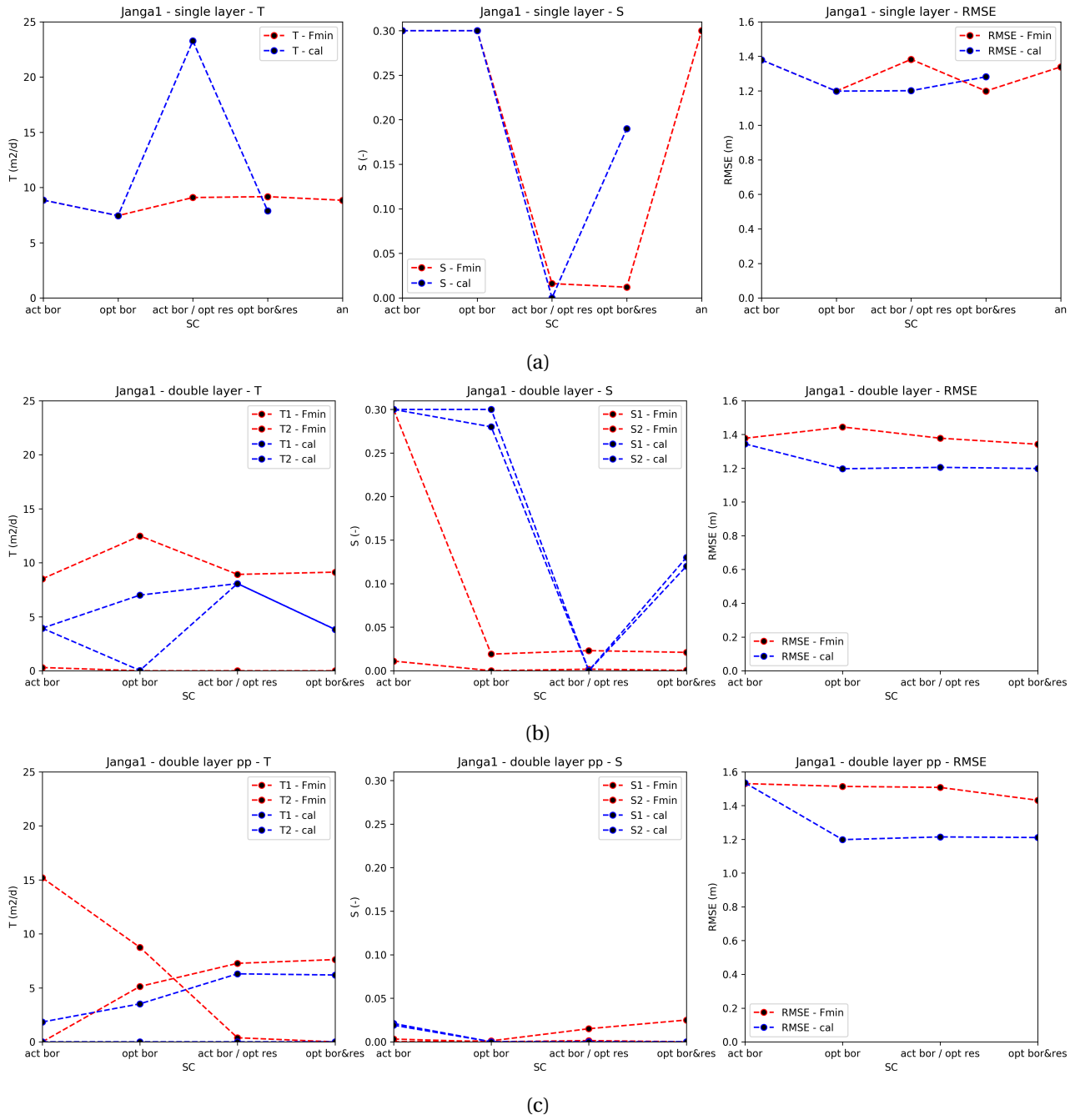


Figure C.12: Janga first attempt - overview determined (Fmin and Cal) optimal parameter values of (??) a single layer system, (??) a double layer system, and (??) a system with two layers and partial penetration of the well

1340 C.5. Janga (2/2) - overview

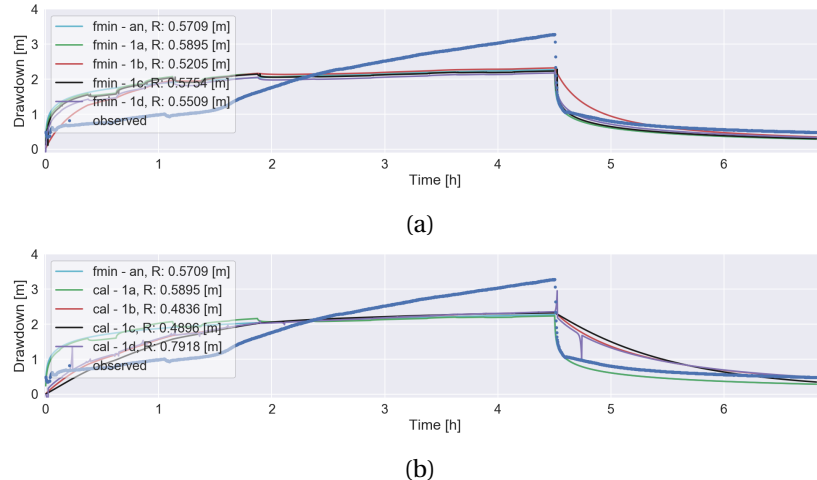


Figure C.13: Janga second attempt single layer fieldwork data analysis by the optimization (a) fmin-RMSE method and (b) TTIm calibration method

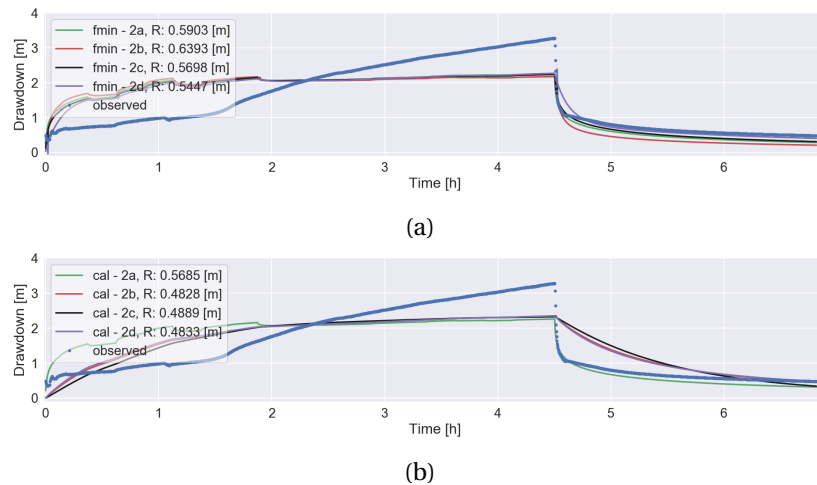


Figure C.14: Janga second attempt double layer fieldwork data analysis by the optimization (a) fmin-RMSE method and (b) TTIm calibration method

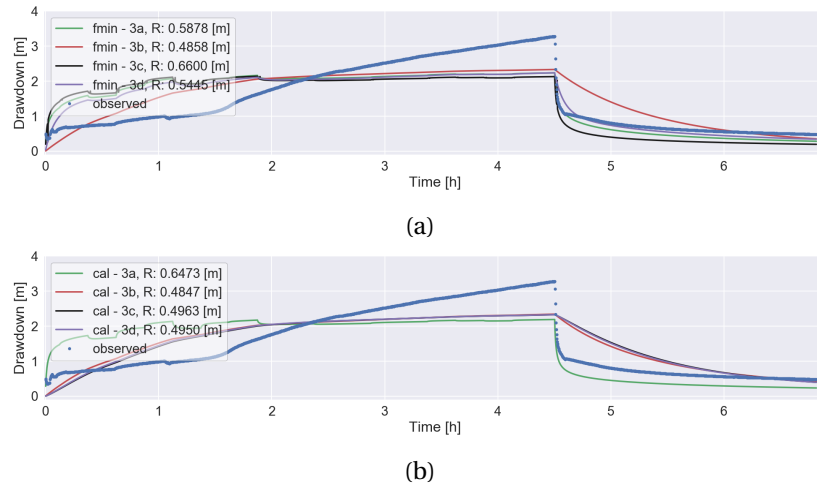


Figure C.15: Janga second attempt partially penetrating double layer fieldwork data analysis by the optimization (a) fmin-RMSE method and (b) TTIm calibration method

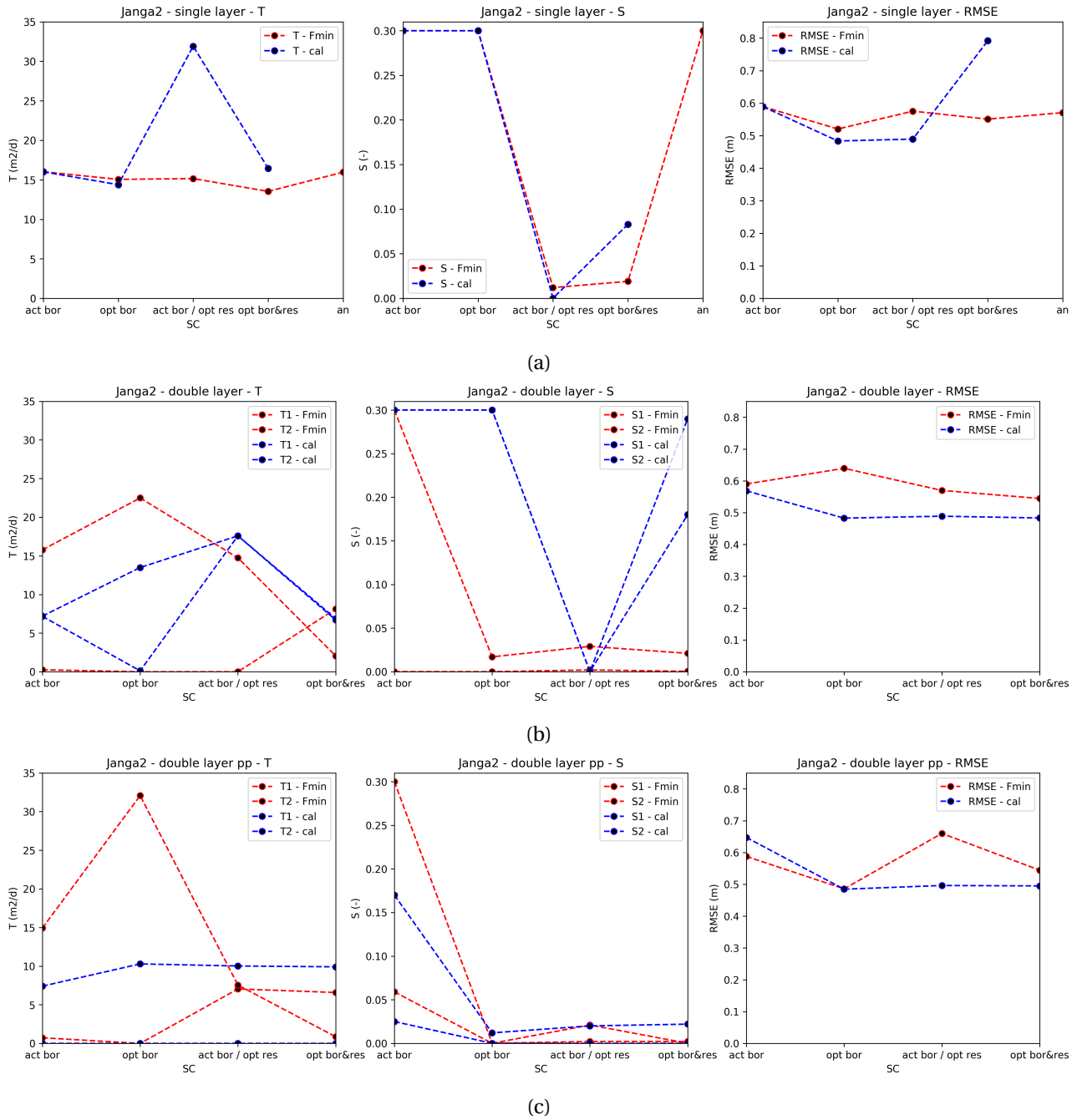


Figure C.16: Janga second attempt - overview determined (Fmin and Cal) optimal parameter values of (??) a single layer system, (??) a double layer system, and (??) a system with two layers and partial penetration of the well

1341 C.6. Ziong - overview

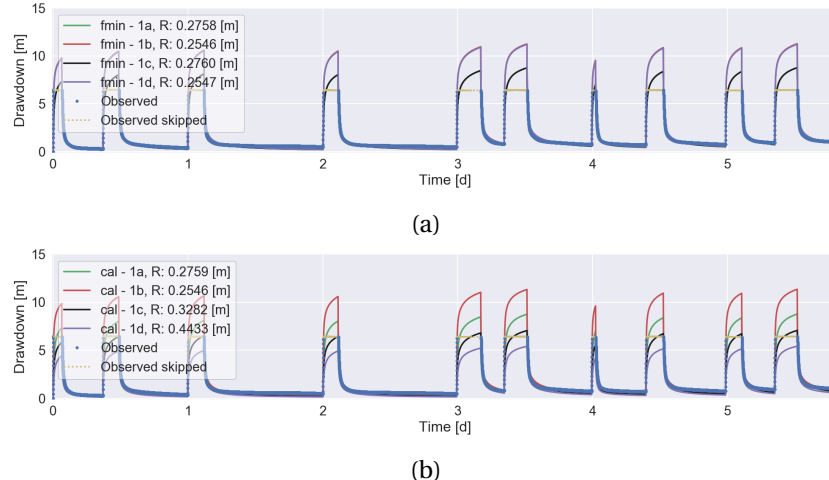


Figure C.17: Ziong single layer fieldwork data analysis by the optimization (a) fmin-RMSE method and (b) TTIm calibration method

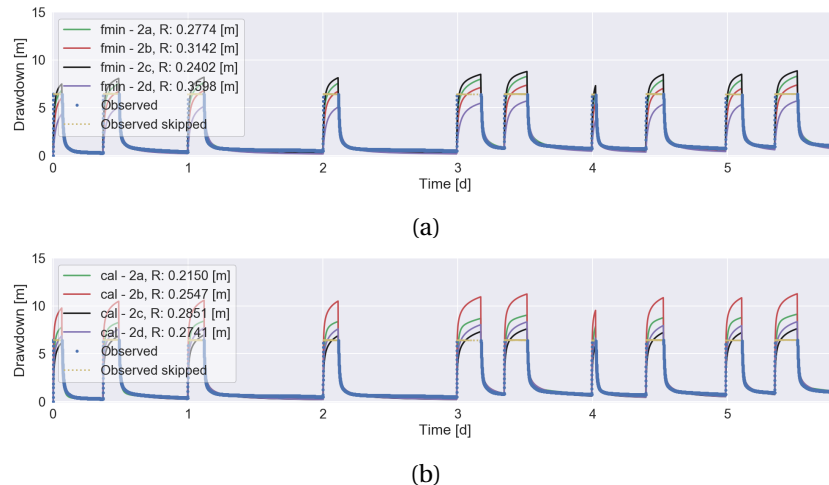


Figure C.18: Ziong double layer fieldwork data analysis by the optimization (a) fmin-RMSE method and (b) TTIm calibration method

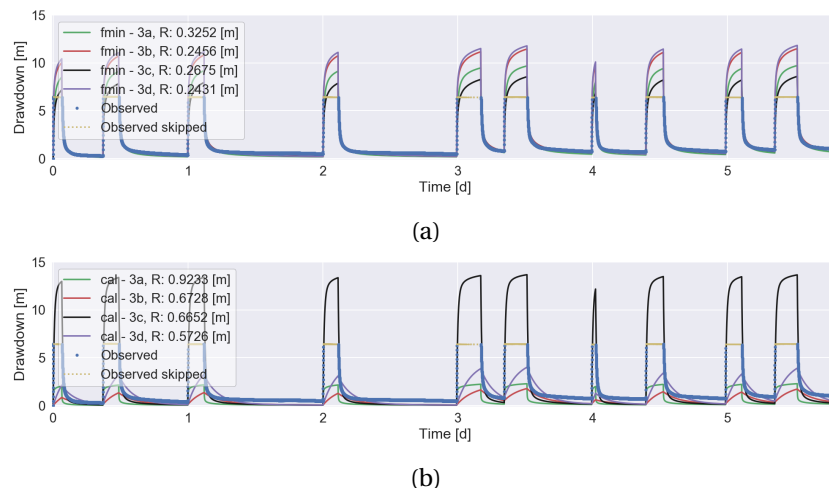


Figure C.19: Ziong partially penetrating double layer fieldwork data analysis by the optimization (a) fmin-RMSE method and (b) TTIm calibration method

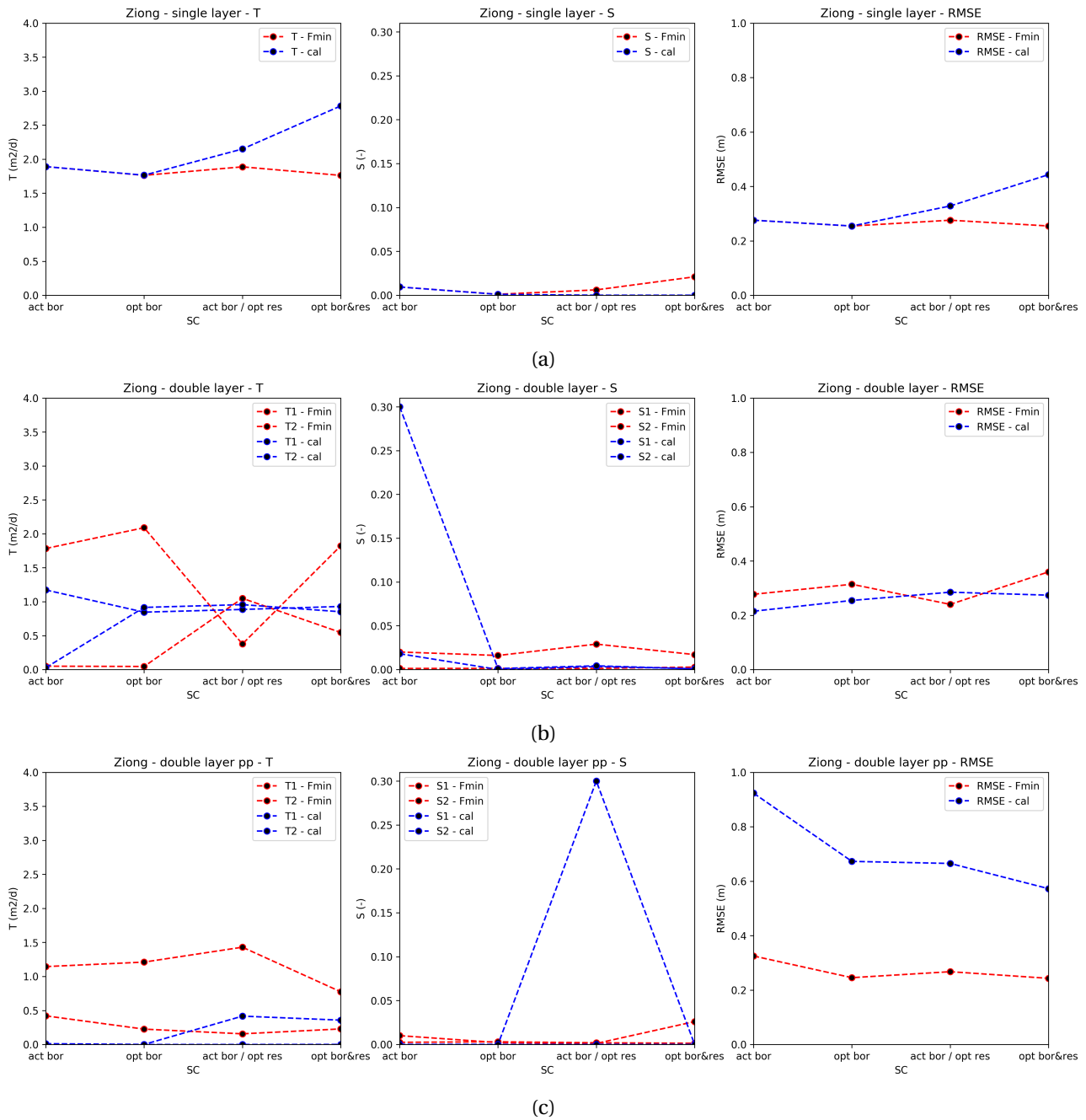


Figure C.20: Zions - overview determined (Fmin and Cal) optimal parameter values of (??) a single layer system, (??) a double layer system, and (??) a system with two layers and partial penetration of the well

D

1342

MODFLOW radial conversion

Introduction

The general thesis topic is pointed at the groundwater flow around a well. Due to seasonal circumstances the same well acts both as extraction and injection well. Direction of groundwater flow is alternately pointed towards and away from the well. This phenomenon can be simulated straightforward by the use of the USGS's modular hydrologic model MODFLOW. To generate adequate results in groundwater fluctuations high model accuracies are desirable, especially close to the well. The model preferably accommodates a fine-meshed grid by the implementation of a multitude of rows and columns. As a consequence model run times will last long.

However, groundwater flow around a well can (under specific conditions) be approached as a phenomenon of radial symmetry. Minor radial parameter conversions can reduce the number of dimensions in the MODFLOW model. A modification that reduces model run times substantially (Langevin, 2008). The section below contains a detailed description of the required radial scaling of parameters, as applied in this thesis. In addition, three examples are included to test and compare the radial scaled model performance.

Theoretical method

MODFLOW is naturally based on rectangular geometry. Without the inclusion of specific adjustments this results in (multi layered) rectangular models. Model shapes not by definition necessary in the case of a well simulation. Under the assumption of subsurface conditions to be homogeneous and the absence of elements disturbing the regional hydraulic gradient it is possible to interpret the groundwater flow around a well as a phenomenon strictly cylindrical. Assumptions on which one would approach well flow model simulation as being axially symmetric (Figure D.1).

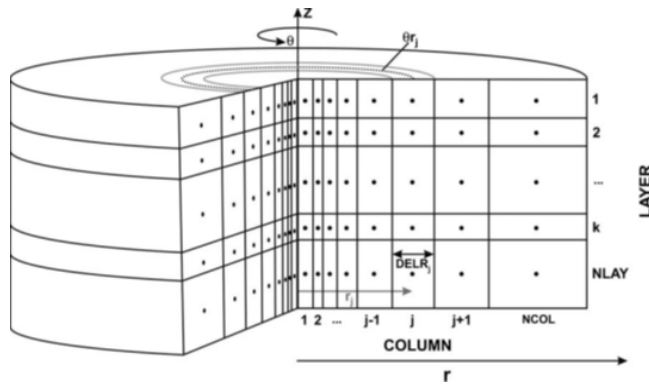


Figure D.1: Schematic of an axially symmetric model (Langevin, 2008)

1363

The in figure D.1 displayed cylindrical approach of a well model can be simulated by an MODFLOW model (rectangular geometry) which accommodates one or more layer(s), one row only and multiple columns. In this single row model it is assumed the well is included in the first column. Moreover, the single row should

act as the representation of a subsurface slice. This is achieved by the radial modification of multiple parameters. Radial parameter scaling guarantees the conversion of a rectangular (single row) MODFLOW model into a fictive radial model. Elaborating on the explanation of Langevin (2008) the following parameters become radial dependent:

$$K_h \rightarrow K_{h,j}^* = K_{h,j} \theta r_j \quad (\text{D.1})$$

$$K_v \rightarrow K_{v,j}^* = K_{v,j} \theta r_j \quad (\text{D.2})$$

$$S_s \rightarrow Ss_j^* = Ss_j \theta r_j \quad (\text{D.3})$$

$$S_y \rightarrow Sy_j^* = Sy_j \theta r_j \quad (\text{D.4})$$

$$n \rightarrow n_j^* = n_j \theta r_j \quad (\text{D.5})$$

Where K_h and K_v represent the horizontal and vertical hydraulic conductivity, S_s is the specific storage, S_y is the specific yield (phreatic storage) and n is the porosity. Scaled parameters modification is highlighted by the introduction of the superscript *. As visible by the subscript j the parameters hereby become column (radial) dependent. r_j is the radial distance between column j and the well (column 1) and θ is the angle of the representing slice. For the purpose of radial scaling θ covers a complete ring; $\theta == 2\pi$.

Main advantage of the implementation of the radial parameter conversion is the reduction in model dimensions. At local scale (close to well) the model can contain a detailed meshed-grid without the emergence of excessive model run times. Moreover the parameter is applied within the common modelling program MODFLOW itself, no specialized programs are required. However, it has to be mentioned the circular model approach can only be applied under the specific assumptions of radial symmetry (Langevin, 2008).

Test application

To validate the radial scaled model performance, a total of three fictive test exercises are applied. In these exercises a comparison is made between the radial scaled model (Figure D.2c) and two natural rectangular based MODFLOW models (Figure D.2a and Figure D.2b). The rectangular MODFLOW model is the most straightforward. Due to the squared shape deviations in model outcome are expected. Whereas the rectangular round MODFLOW model is manually circularized. This model accommodates the gradual increase in flow area in the radial direction. Based on Langevin (2008) it is expected the rectangular round model should approximate radial model outcomes.

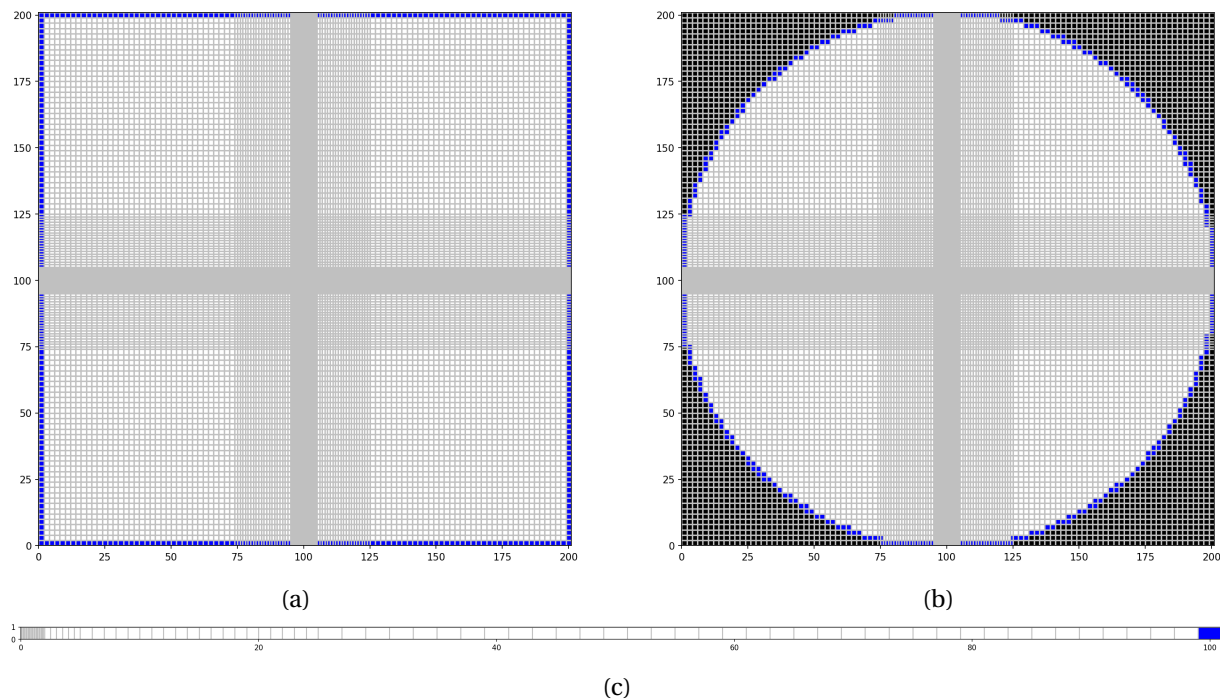


Figure D.2: MODFLOW topview schematisation of a: (a) Rectangular model, (b) Rectangular round model and (c) Single row model
 (grey = cell boundary, red = well position, blue = boundary condition, black = inactive cell)

1390 The exercises applied deliberately show strong similarities with the first two test problem cases described
 1391 by Langevin (2008). In terms of content the exercises are designed with the same set of parameters, making
 1392 it possible to validate the results in general. As an exception a small deviation is applied in terms of grid def-
 1393 inition. In these exercises the cell sizes increase (grouped) stepwise based on an increasing (radial) distance
 1394 from the well. By the use of the cell sizes 0.1 (20x), 0.5 (6x), 1.0 (20x) and 2.0 m (38x) a total model length
 1395 (radial length) of 101 m is simulated. This grid structure is applicable on the single row (radial) model. The
 1396 rectangular and rectangular round model accommodate a same and corresponding grid structure, as visible
 1397 in the model top views of figure D.2.

D.1. Test 1: Steady flow to a fully penetrating well in confined aquifer

The steady state solution of a confined aquifer fully penetrated by a well is applied as a first MODFLOW model performance test. The exercise schematic configuration is depicted in the overview of figure D.3. The case is characterized by its simplicity, making it an exercise ideally suitable for the comparison against the analytical solution. Thiem's method (Equation D.6) is applied as the analytical drawdown solution for radial well flow in a confined aquifer (Kruseman and de Ridder, 2000):

$$S_j = \frac{Q \ln(\frac{r_2}{r_j})}{2\pi K_{(h)} H} \quad (\text{D.6})$$

Where S_j is the drawdown in column j , Q is the discharge, $r_2 = 100$ m (constant head at a distance of in this case 100 m from the well), r_j is the radial distance between column j and the well (column 1), $K_{(h)}$ is the horizontal hydraulic conductivity and H is the aquifer thickness.

Decline in groundwater head due to well behaviour can also be expressed directly by the use of the analytical discharge potential (ϕ), as depicted in (Equation D.7). Applied on confined conditions it is assumed: $H = h_0$ (Bakker and Anderson, 2011; Strack, 1989). As a result confined heads can be determined by the application of equation D.9. Head values determined are in complete correspondence with the drawdown calculated by Thiem's method.

$$\phi_j = \frac{Q}{2\pi} \ln\left(\frac{r_j}{R}\right) + \phi_0 \quad (\text{D.7})$$

$$h_j = \frac{\phi_j}{k_h H} \quad (\text{D.8})$$

$$h_j = \frac{\phi_j}{k_h H} \quad (\text{D.9})$$

Where ϕ_j is the discharge potential at column j , Q is the discharge, $R = 100$ m (constant head (h_0) at a distance of in this case 100 m from the well), r_j is the radial distance between column j and the well (column 1), $K_{(h)}$ is the horizontal hydraulic conductivity and H is the aquifer thickness.

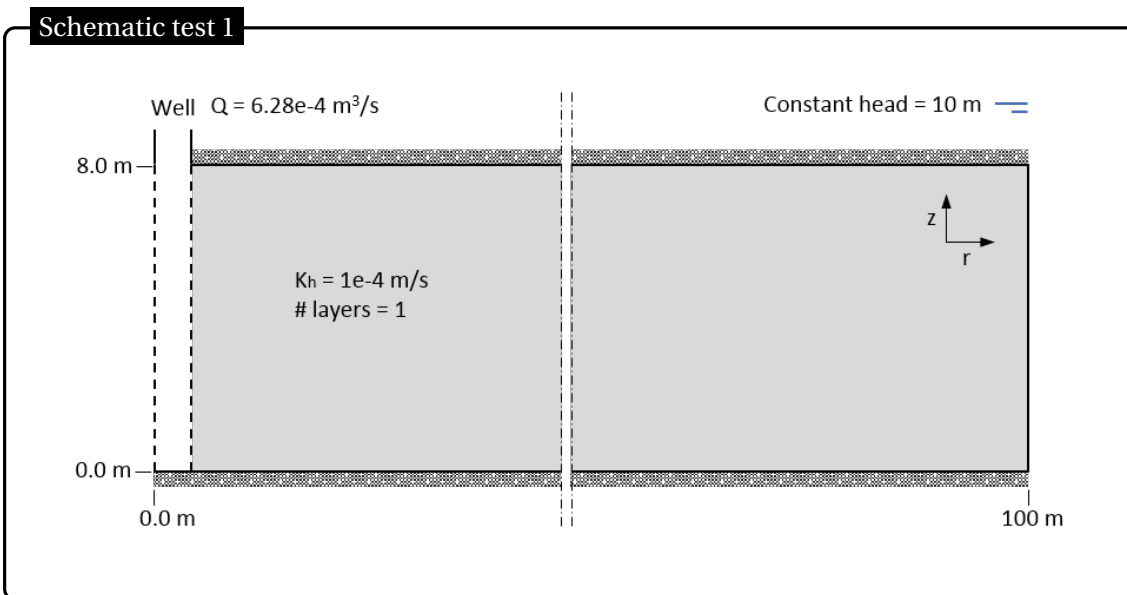


Figure D.3: Schematic test 1

The rectangular MODFLOW model overestimates drawdown (modelled heads are slightly lower) compared to the analytical solution. This difference can be explained by the rectangular shape of the model; imposed boundary condition along the model edge (especially the corners) are positioned 'outside' the defined radial

boundary of 100 m from the well. The rectangular round model works around this inconvenience, and already shows more similarities with the analytical solution. Some deviation in the first meter(s) around the well still exist, which can potentially be attributed to the cell structure. These minor deviations are no longer present by the application of the radial scaled (single row) model. Regardless the (radial) position, modelled heads and drawdown are identical to the analytical solution. A first indication the radial scaled MODFLOW model is preferential applicable on this thesis purposes.

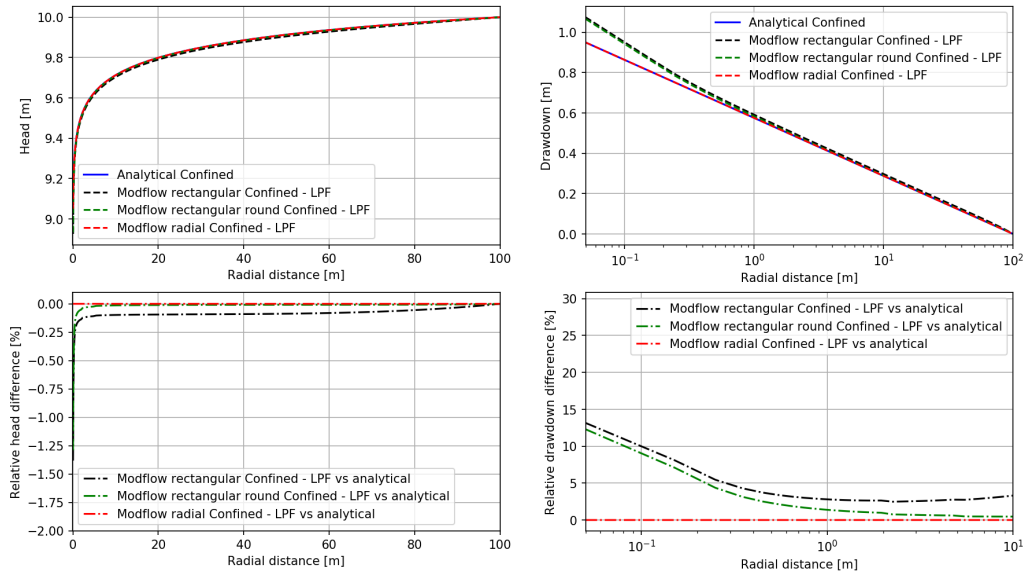


Figure D.4: Results test 1

D.2. Test 2: Steady flow to a fully penetrating well in unconfined aquifer

Example exercise two (Figure D.5) accommodates the same test problem as depicted in test 1, only exception is the transition towards unconfined aquifer conditions. In this example the analytical drawdown solution presented by the Thiem-Dupuit's method for steady-state flow to a fully penetrating well in an unconfined aquifer is used as a reference(Kruseman and de Ridder, 2000):

$$S'_j = \frac{Q \ln(\frac{r_2}{r_j})}{2\pi K_{(h)} D} \quad (\text{D.10})$$

$$S'_j = S_j - \frac{S_j}{2D} \quad (\text{D.11})$$

Where S'_j is the uncorrected drawdown in column j, S_j is the iteratively corrected drawdown in column j, Q is the discharge, $r_2 = 100$ m (constant head at a distance of 100 m from the well), r_j is the radial distance between column j and the well (column 0), $K_{(h)}$ is the horizontal hydraulic conductivity and D is the thickness between aquifer bottom and constant head. For the purposes of this exercise the analytical drawdowns are iteratively determined with a precision of 1e-6.

Also under unconfined conditions the analytical discharge potential (Equation D.12) can be applied (Bakker and Anderson, 2011; Strack, 1989). Only exception, compared to the confined conditions, is the minor change in head derivation, visualised in D.14. Major advantage, with respect to the analytical Thiem-Dupuit's method, is the absence of the iterative head derivation process. Result is a fast and accurate analytical calculation of heads by the application of the discharge potential.

$$\phi_j = \frac{Q}{2\pi} \ln\left(\frac{r_j}{R}\right) + \phi_0 \quad (\text{D.12})$$

$$\phi_0 = \frac{1}{2} k_h h_0^2 \quad (\text{D.13})$$

$$h_j = \sqrt{\frac{2\phi_j}{k_h}} \quad (\text{D.14})$$

Where ϕ_j is the discharge potential at column j, Q is the discharge, $R = 100$ m (constant head (h_0) at a distance of in this case 100 m from the well), r_j is the radial distance between column j and the well (column 1), $K_{(h)}$ is the horizontal hydraulic conductivity and H is the aquifer thickness.

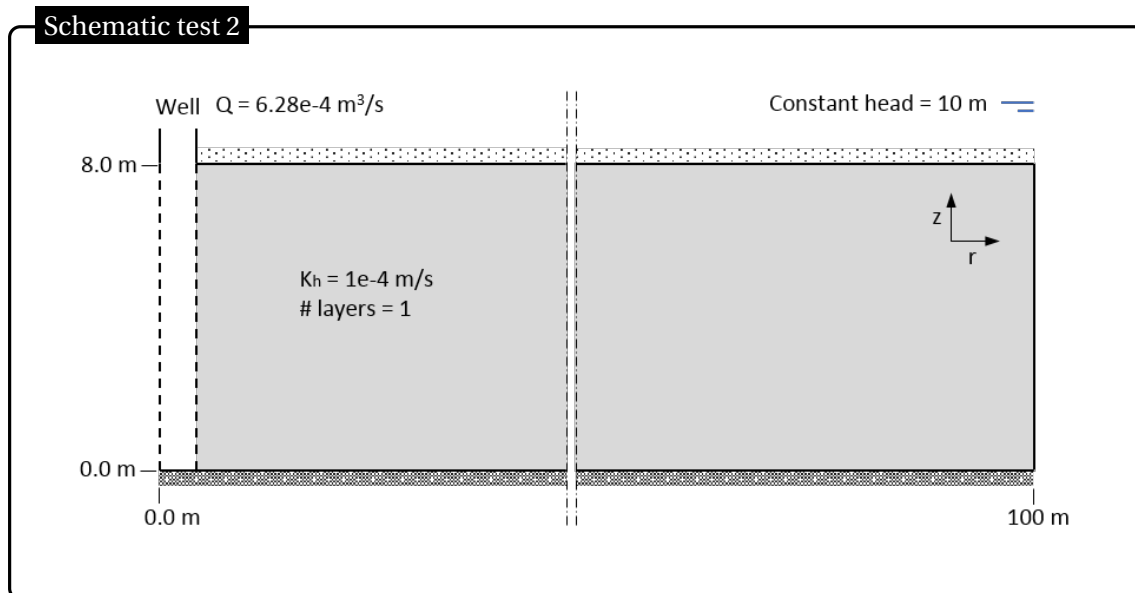


Figure D.5: Schematic test 2

1446 Due to a 10 m constant head boundary the aquifer area of flow is fictive enlarged in the unconfined case
 1447 (compared to the 8 m aquifer height under confined conditions). In accordance with the solutions in
 1448 Langevin (2008), overall drawdowns in the unconfined conditions are slightly lower with respect to the con-
 1449 fined situation. Model performances of the unconfined example exercise show similar behaviour as the
 1450 confined example exercise. Differences in modelled and analytical determined heads and drawdowns are
 1451 minuscule in general. As expected largest deviations from the analytical solution are present in the MOD-
 1452 FLOW rectangular model. The differences in outcome of this model do persist over almost the entire radial
 1453 distance from the well, regardless the use of the BCF or LPF package. Although it is only slightly, the use of the
 1454 LPF package shows slightly better performance. For the purposes of this thesis the LPF package is assumed
 1455 to be preferential in setting the aquifer properties. Application of this package in the MODFLOW round rect-
 1456 angular model results in improved model results, however deviations do continue to exist. In contrast with
 1457 the confined exercise (D.1) application of the radial scaled MODFLOW model under unconfined aquifer
 1458 conditions deviations from the analytical solution are still present. Modelled drawdowns show strong sim-
 1459 ilarities with the uncorrected analytical solution. Moreover, relative to the analytical solution the absolute
 1460 radial scaled MODFLOW model outcomes performs most accurately. Making the radial scaled (single row)
 1461 MODFLOW model suitable for the unconfined aquifer conditions of this thesis.

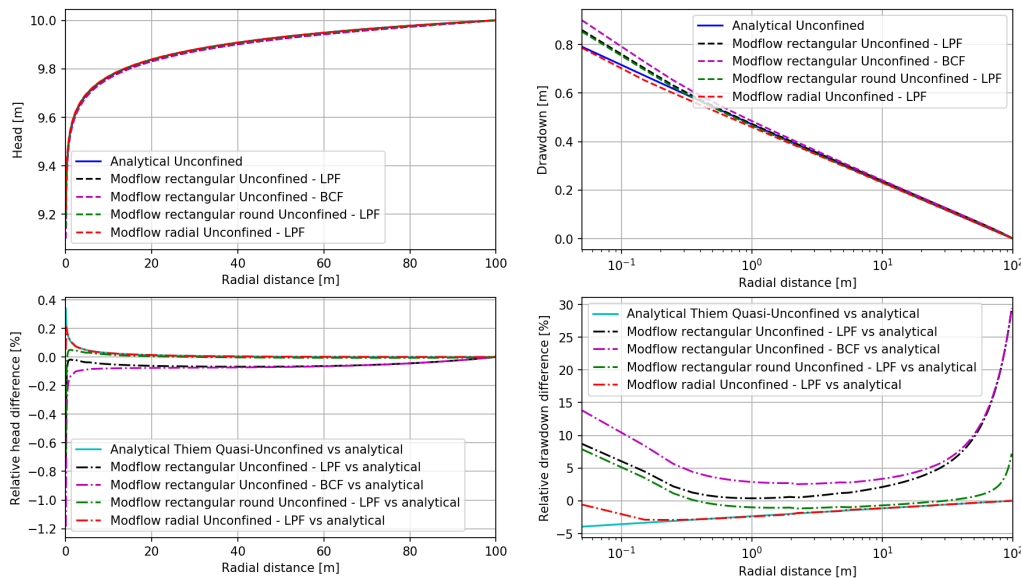


Figure D.6: Results test 2

D.3. Test 3: Unsteady flow to a partially penetrating well in unconfined aquifer

As a final exercise the different MODFLOW models are subjected to a more complicated case (Figure D.7). This specific exercise includes all model parameters dependent on radial scaling to test the overall radial model performance. This case accommodates a well which is partially penetrating the aquifer, making it a multi-layered problem. Sum up of the fractional discharges of the penetrating layers (48-72) results in the total well discharge. Moreover the exercise is time dependent. In this case all results are obtained after one day of groundwater withdrawal.

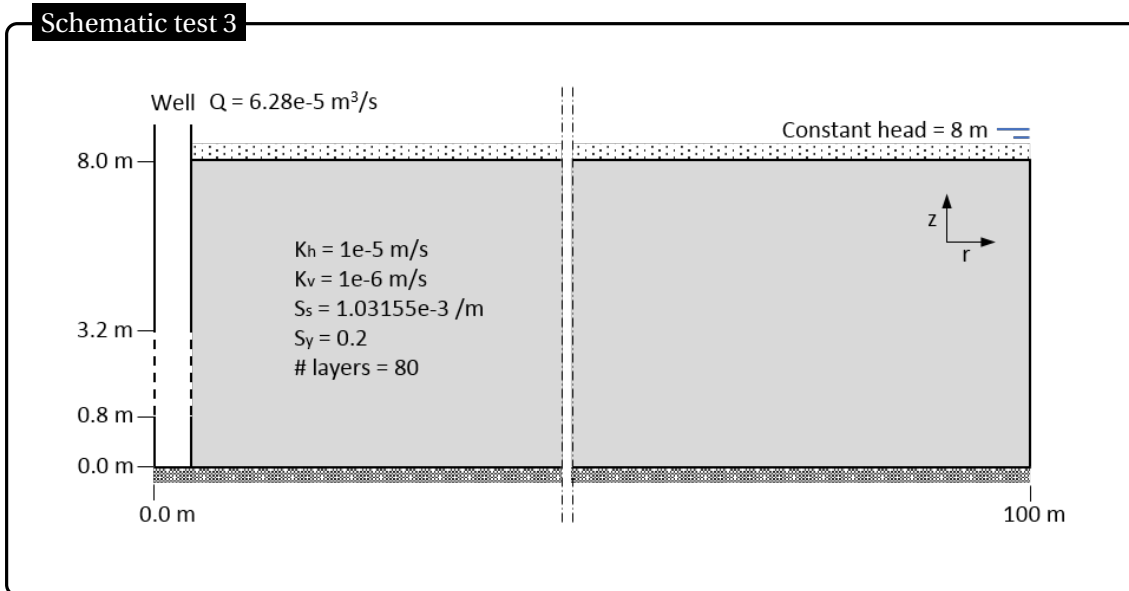


Figure D.7: Schematic test 3

Performance of the radial scaled (single row) MODFLOW model is visualized by the head contour plot in figure D.8. From the perspective of proper comparison results of the different models are in this case shown at an height of 2.0 m (relative to aquifer bottom) along the entire aquifer (Figure D.9). Outcome of the comparative study is a scaled (single row) radial model which performs as expected. With the exception of the first meter(s) around the well differences between the rectangular round and the radial MODFLOW models are negligible small. Deviations at close range to the well can be attributed to the chosen grid structure. Based on the test exercises 1 and 2 it can be assumed the results of the radial model simulates the natural well behaviour properly. Application of the radial scaled (single row) MODFLOW model with the use of the LPF package is a relative fast and suitable model for this thesis purposes.

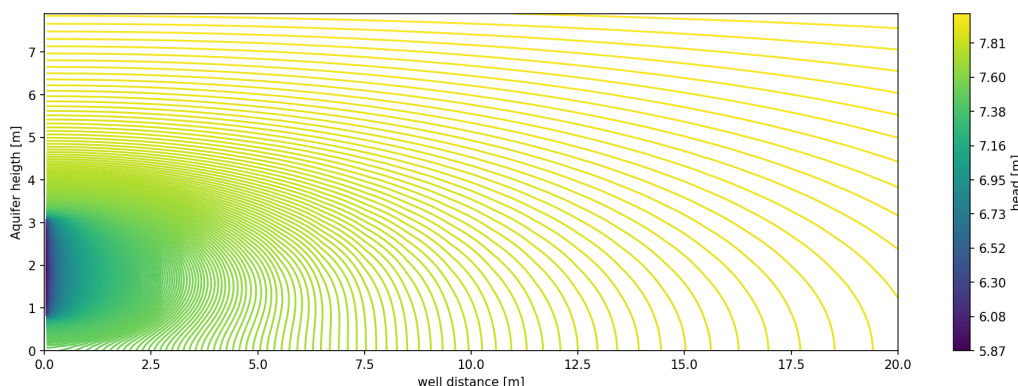


Figure D.8: Results test 3: Cross-section head contour after 1 day of pumping

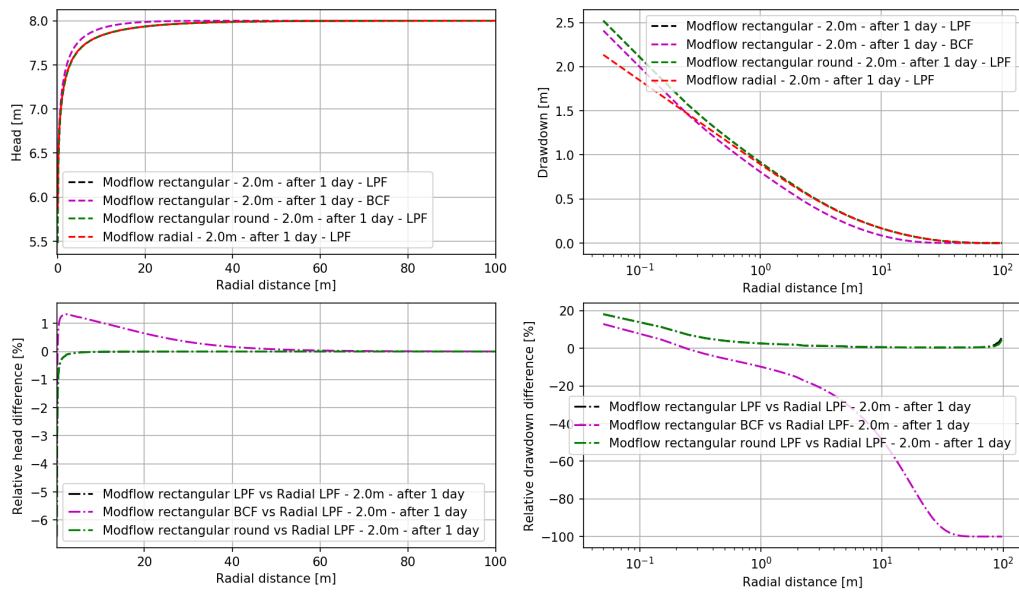
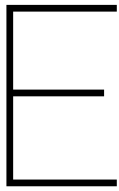


Figure D.9: Results test 3: Head after 1 day of pumping at 2.0m (relative to aquifer bottom)



1478

1479 Extense report - MODFLOW model definition

1480 E.1. Leakage factor λ

1481 MODFLOW model extent is based on the double layer leakage factor. The analytical solution for the leakage
1482 factor (λ) is depicted in equation E.1 (bron geo1 lecture notes week3).

$$\lambda = \sqrt{\frac{c * T_0 * T_1}{T_0 + T_1}} \quad (E.1)$$

1483 where λ is the leakage factor (m), c (d) is the resistance of the leaky layer between aquifer one and two and
1484 T_0 and T_1 are the transmissivities of respectively aquifer one and two.

1485
1486 As a source of input the optimal values (T_0 and T_1) determined by fieldwork analysis TTIm (Fmin); dou-
1487 ble layer system and the system with a double layer and partial penetration of the well are used. In TTIm
1488 Model3D soil stratification is not characterized by a regular sequence of alternately aquifers and leaky layers.
1489 TTIm Model3D houses an accumulation of aquifers. Resistance of the fictive leaky layer is computed from
1490 the middle of first layer to the middle of the second layer (Bakker, 2013a,b). For the determination of the
1491 leakage factor an vertical anisotropy of 0.25 (-) is assumed. An overview of all generate leakage factors can
1492 be found in Table E.1.

1493

Table E.1: Lambda (m) overview per location

SC	Bingo 2lay	Bingo 2lay pp	Nyong Nayili 2lay	Nyong Nayili 2lay pp	Janga (1/2) 2lay	Janga (1/2) 2lay pp	Janga (2/2) 2lay	Janga (2/2) 2lay pp	Ziong 2lay	Ziong 2lay pp
a	31.11	31.11	33.94	33.94	51.51	17.01	51.95	20.10	35.25	32.31
b	31.27	31.11	36.77	33.96	52.33	34.56	52.33	17.01	35.27	31.82
c	31.38	31.25	35.32	36.77	52.33	51.15	52.33	38.37	32.29	31.56
d	31.21	31.20	33.94	36.77	52.33	52.33	27.97	49.54	34.42	32.13

1494 A model extent of 3 to 4 times the leakage factor (characteristic length) is desirable. By meeting this require-
1495 ment it can be expected that 95-99% of the actual water flow is taken into account by the model. Moreover,
1496 the head at the model tail is by approximation no longer affected by the (centrally positioned) well be-
1497 haviour. The assumption of a constant head at model tail becomes valid (bron geo1 lecture notes week3).
1498 The majority of the leakage factors are in close range of the 36.74 m average leakage factor of obtained. To
1499 comply the above mentioned requirement a total model extent (radius) of 150 m is implemented.

F

1500

1501

1502

Pedrollo - 4" submersible pump - Product specifications

1503 Available pump: Type 4SR4/18

4SR

4" submersible pumps



- Clean water (Maximum sand content 150 g/m³)
- Domestic use
- Civil use
- Industrial use

PERFORMANCE RANGE

- Flow rate up to **340 l/min** (20.4 m³/h)
- Head up to **405 m**

APPLICATION LIMITS

- Maximum liquid temperature +35 °C
- Maximum sand content **150 g/m³**
- **100 m** immersion limit
- Installation:
 - vertical
 - horizontal, with the following limits:
4SR1 - 4SR1.5 - 4SR2 - 4SR4 up to **27 stages**
4SR6 - 4SR8 up to **17 stages**
4SR10 - 4SR12 - 4SR15 up to **12 stages**
 - Starts/hour: **20** at regular intervals
 - Minimum flow rate for motor cooling **8 cm/s**
 - Continuous service **S1**

CONSTRUCTION AND SAFETY STANDARDS

ELECTRIC MOTOR

- Single-phase 230 V - 50 Hz
- Three-phase 400 V - 50 Hz

Length of power cable:

- for P2 from 0.37 to 3 kW: **1.7 m** 4SR-PD, **2.0 m** 4SR-PS
- for P2 from 4 to 7.5 kW: **2.7 m** 4SR-PD, **3.0 m** 4SR-PS
- ⇒ The **4SR-PD** and **4SR-PS** single-phase versions supplied with a capacitor included in the packaging.

EN 60335-1
IEC 60335-1
CEI 61-150

EN 60034-1
IEC 60034-1
CEI 2-3



EU REGULATION N. 547/2012

CERTIFICATIONS

Company with management system certified DNV
ISO 9001: QUALITY
ISO 14001: ENVIRONMENT



INSTALLATION AND USE

Suitable for use with clean water with a sand content of no more than **150 g/m³**. Because of their high efficiency and reliability, they are suitable for use in domestic, civil and industrial applications such as for the distribution of water in combination with pressure tanks, for irrigation, for washing plants and for pressure boosting in fire-fighting sets, etc.

PATENTS - TRADE MARKS - MODELS

- Patent n. EP2419642

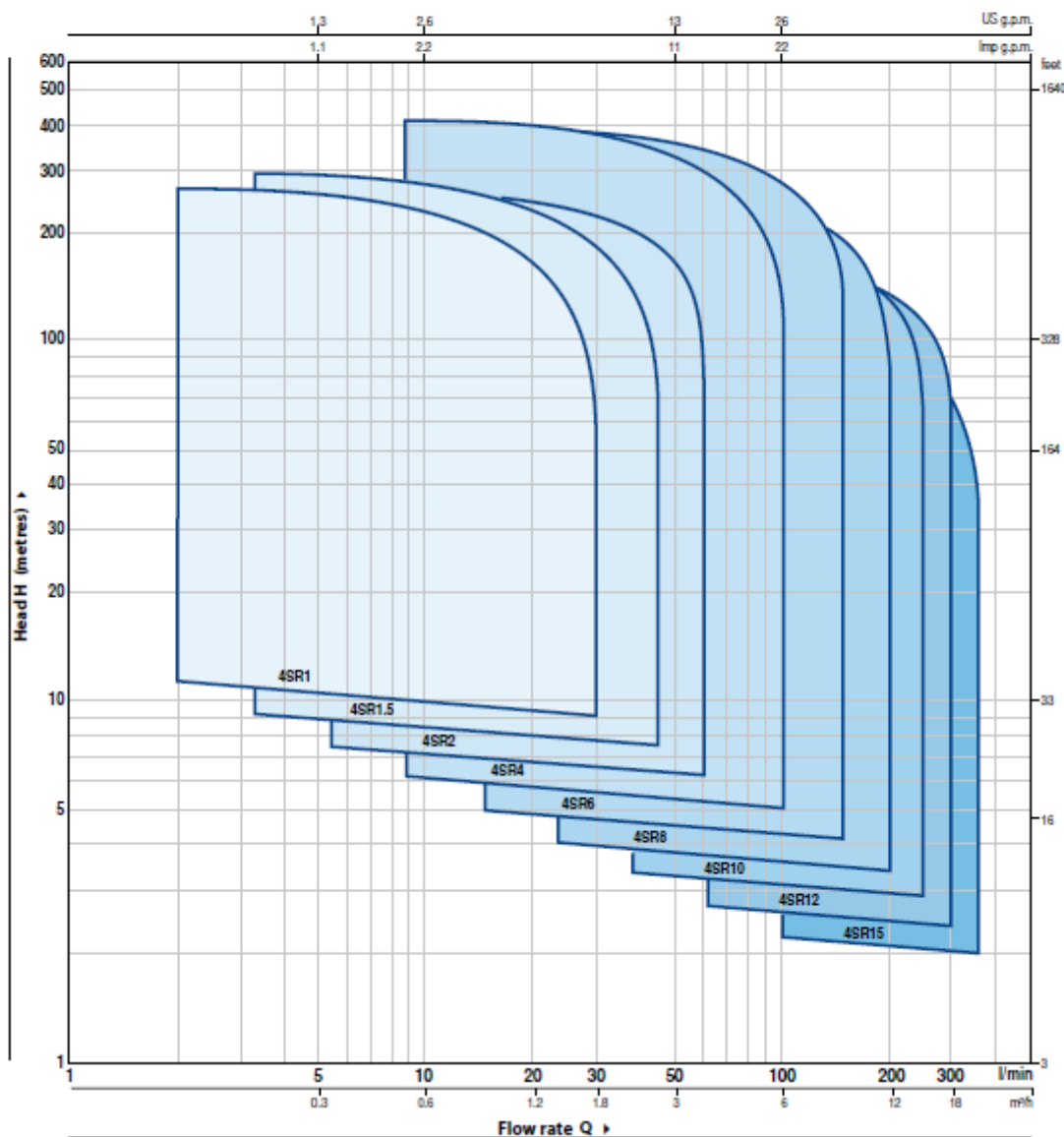
OPTIONS AVAILABLE ON REQUEST

- Other voltages or 60 Hz frequency
- Kit of cooling jacket complete with filter and supports



PERFORMANCE RANGE

50 Hz n = 2900 rpm



NOMENCLATURE

4 SR 1 m / 13 - PD or PS or HYD

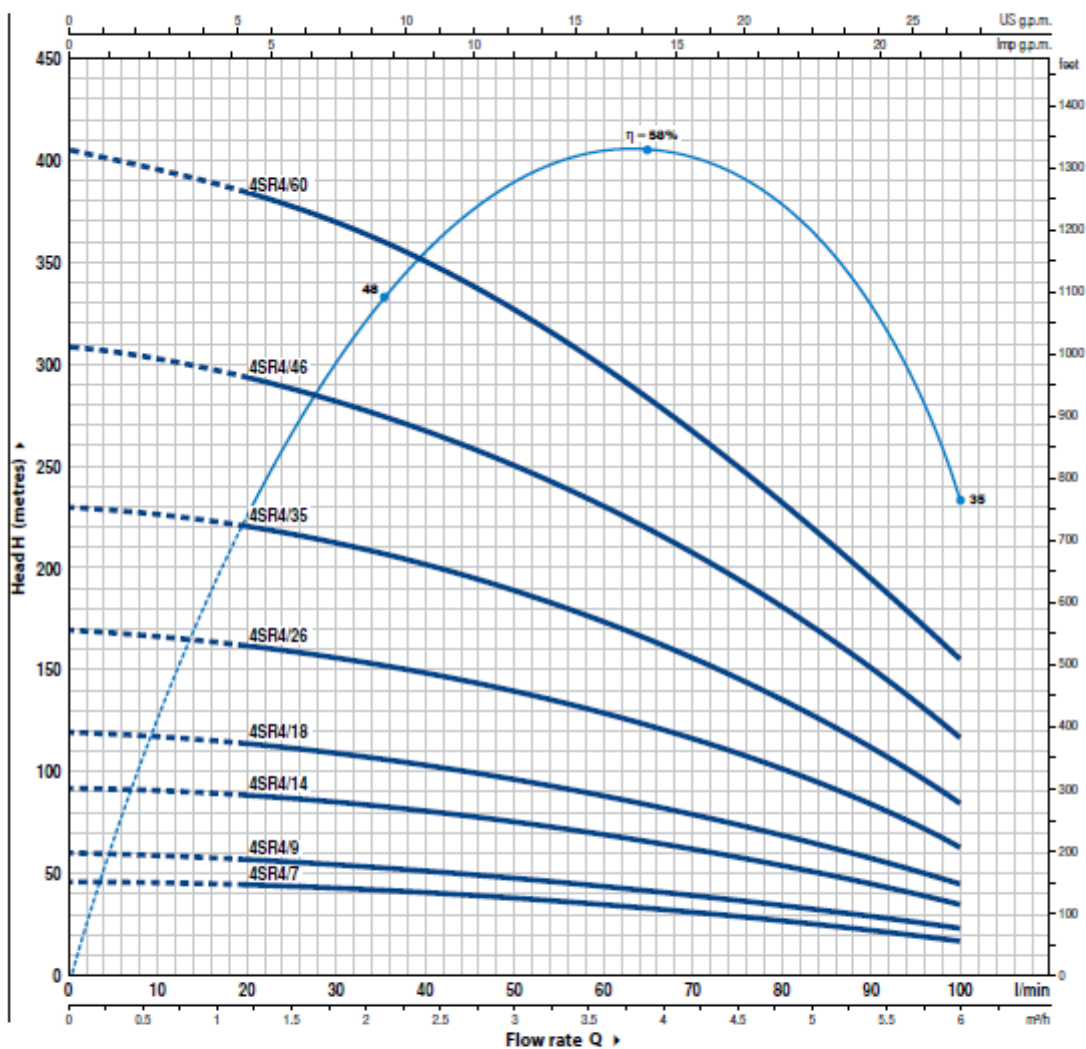
- Borehole diameter in inches _____
- Series _____
- Flow rate in m³/h at the point of highest efficiency _____
- Single-phase motor _____
- Number of stages _____
- PD: pump with "4PD PEDROLLO" motor _____
- PS: pump with "4PS PEDROLLO" motor _____
- HYD: pump without motor _____

4SR4

PEDROLLO
the spring of life

CHARACTERISTIC CURVES AND PERFORMANCE DATA

50 Hz n = 2900 rpm



MODEL		POWER (P_2)		Q m ³ /h l/min	0	1.2	1.8	2.4	3.0	3.6	4.2	4.8	5.4	6.0
Single-phase	Three-phase	kW	HP		46	44	42	40	38	35	32	28	23	17
4SR4m/7	4SR4/7	0.55	0.75	46	44	42	40	38	35	32	28	23	17	
4SR4m/9	4SR4/9	0.75	1	60	56	55	52	49	45	40	35	29	23	
4SR4m/14	4SR4/14	1.1	1.5	92	88	85	81	76	70	63	55	45	35	
4SR4m/18	4SR4/18	1.5	2	120	112	109	104	98	90	81	70	58	45	
4SR4m/26	4SR4/26	2.2	3	170	162	157	150	141	130	116	101	84	63	
-	4SR4/35	3	4	230	220	211	202	190	175	157	137	113	85	
-	4SR4/46	4	5.5	308	293	280	269	249	230	205	181	151	117	
-	4SR4/60	5.5	7.5	405	385	370	350	325	300	270	235	195	155	

Q = Flow rate H = Total manometric head

Tolerance of characteristic curves in compliance with EN ISO 9906 Grade 3B.